Ion Composition of Geomagnetic Storm-Time Events

Patrick Joseph Dixon

Department of Physics

Aberystwyth University

Supervision:

Professor Manuel Grande and Professor Eleri Pryse

Thesis submitted for the degree of Master of Philosophy.

31 October 2018

CONTENTS

ACKNOWLEDGEMENTS

This PhD was fully funded by the United Kingdom Science and Technology Facilities Council.

I would first like to thank Professor Manuel Grande and Professor Eleri Pryse for their supervision, advice and patience during the course of my PhD. I would also like the thank the staff of Aberystwyth Physics department, all of whom have been fantastic throughout my many years there but most notably Professor Andy Evans and Dr. Huw Morgan for their support and wise words.

I would like thank Dr. Elizabeth MacDonald for all the help and collaboration, greatly improving my understanding of lobe encounters and without which, much of this work would not have been possible. Also many thanks to the rest of the Van Allen Probes team, especially Geoff Reeves, Harlan Spence and Michelle Thomsen for giving me the opportunity to get involved with an exciting mission which formed the basis of my PhD.

To Hannah, without whom I would never have made it this far, thank you for your love, understanding and infinite patience.

And to all my fellow PhD students who have come and gone over the years; thank you for distraction, procrastination, friendship and that feeling that you are not alone in this.

ABSTRACT

This work focuses on the study of geomagnetic lobe encounters, where a spacecraft orbiting within the Earth's magnetosphere crosses the open/closed field line boundary into the tail lobes and back again.

A case study is performed on a series of flank lobe encounters observed by the twin Van Allen Probes between 0200 and 0515 on November 14th 2012. Observations by LANL GEO spacecraft at geosynchronous orbit also show lobe encounters in the northern hemisphere and on the dusk flank, providing evidence for a global phenomenon driving the events. Using the twenty-one total events observed by the Van Allen Probes and LANL GEO spacecraft, the global magnetic field topology is examined, as well as smaller scale spatial and temporal characteristics of the open/closed field line boundary, allowing the position and motion of the boundary to be constrained. A novel method is used to compare the observed behaviour of the OCB to that predicted by the BATS-R-US global MHD model. The model appears to simulate the dynamic processes that cause the spacecraft to repeatedly cross the OCB but incorrectly maps the overall topology of the boundary during these extreme conditions, overestimating the distance to it by as much as 3 R_E.

A survey of Van Allen Probe data was performed over a two year period from October 2012 – October 2014, where the spacecraft sampled the magnetosphere at near geosynchronous orbit for all MLTs and in both the northern and southern hemispheres. This allows a survey to examine the distribution of magnetospheric lobe encounters spatially, in MLT and magnetic latitude, as well as comparing their frequency to factors such as IMF conditions and substorm occurrences.

This survey highlighted how unusual it was to see a strong series of flank events - like that seen for November 14th 2012 - at a relatively low apogee (5.8 R_E) compared to previous studies. The predominance of substorm associated near-midnight encounters implies that these events are able to bring the lobe closer in to the Earth, making it more likely for spacecraft with lower orbits to encounter them.

Analysis of the Interplanetary Magnetic Field drivers of these events shows strong IMF B_Y and B_Z in the day preceding the event. Negative IMF By, was shown to prefer the south/dawn region of the magnetosphere, in agreement with *Moldwin et al*. [1995]. In-situ magnetometer data was analyzed and showed the spacecraft encountering a highly stretched field typical of the lobe, as well as a strong dipolarization of the field prior to exiting the lobe, which can be associated with a substorm injection.

1. INTRODUCTION

The Earth's magnetosphere is a highly dynamic, structured system with a variety of distinct regions and varied mechanism that govern the movement of particle populations, the flow of energy and the magnetic topology within it. The existence of this structure was first discovered when Explorer 1 observed high levels of charged particles far above the Earth's surface, now known to be the Van Allen Radiation Belts [*Van Allen et al.* 1958].

Since then numerous missions have been launched into the Earth's magnetic environment, most notably the CRRES (Combined Release and Radiation Effects Satellite) which launched in July 1990 and despite only lasting for one year of its three year planned mission, collected valuable data on the energetic particle composition and mechanisms of the magnetosphere [Johmson et al. 1992]. With an orbital period of 9 hours and 50 minutes, an inclination of 18.1˚ and apogee between 6 and 7 R_E, CRRES was able to sample a variety of magnetospheric regions and provided valuable data on the magnetospheric lobes, the focus of this work. Multiple studies of magnetospheric lobe encounters [*E.g.Thomsen et al., 1994; Moldwin et al., 199;, Fennell et al., 1996*] were undertaken in this era, combining data from CRRES and the geosynchronous GOES satellite to examine their frequency, distribution, drivers and characteristics.

After CRRES other missions such as Cluster and THEMIS were launched but with different orbits and goals to the CRRES mission, which lead to them being less suitable for examining geosynchronous lobe encounters. The spiritual and scientific successor to the CRRES mission were the Van Allen Probes, a set of two spacecraft whose orbit, payload and goals were similar those of CRRES but with the twin craft able to study the dynamics of the magnetosphere, sampling the same space with varying delays in time, as one spacecraft orbited behind the other.

The focus of this work is to utilise the energetic particle and magnetic field instruments aboard the Van Allen Probes to perform a survey of lobe encounters observed by the Van Allen Probes over a two year period and also to examine a unique and fascinating series of lobe encounters that occurred on November 14th 2012. Supporting data is also used from the LANL geosynchronous

spacecraft and results from the CRCM + BATS-R-US coupled global MHD and ring current model implemented in *Glocer et al.* [2013].

1.1 THE MAGNETOSPHERIC LOBES

The magnetospheric lobes are two regions of the magnetotail which contain field lines connected to the polar regions at one end and the interplanetary magnetic field (IMF) at the other. The north lobe (mapped to the northern polar region) contains field lines directed towards the Earth, whereas the south lobe (mapped to the southern polar region) contains field lines directed down-tail, away from the Earth. Separating these two regions is a current sheet surrounded by a layer of hot plasma known as the plasma sheet. [first tail obvs, Ness 1987 review]. The open field lines of the lobe are unable to trap energetic particles, leading to very low plasma density (n ~10^{-2} cm^{-3}) and temperature (T ~ 20 eV) [Sharp et al 1998]

The lobes are separated from the closed field lines of the inner magnetosphere by the open-closed field line boundary (OCB), a result of the frozen in theory which prevents the populations travelling on the two types of field line from mixing. The position of this boundary is not fixed and can vary greatly as the topology of the magnetosphere is perturbed by both solar wind drivers and internal mechanisms. The behavior of the OCB is critical to numerous topics in space physics, including the mechanisms and mapping of MHD models, planetary magnetosphere, and magnetosphere-ionosphere coupling.

1.3 SOLAR WIND DRIVERS, GEOMAGNETIC STORMS

The solar wind is a continuous flow of energetic plasma travelling outwards from the Sun at a typical velocity of roughly 400 km/s, but with high speed wind reaching velocities up to 800 km/s. The solar magnetic field is embedded in this flow of plasma, forming the interplanetary magnetic field which interacts with Earth's magnetic environment, defining the topology and dynamics of Earth's

magnetosphere. Its charged particles and frozen in magnetic field input plasma and magnetic flux into system, driving dynamic processes on various scales. During certain conditions the solar wind is responsible for causing geomagnetic storms, responsible for many of the phenomena observed by magnetospheric spacecraft.

1.4 MAGNETOSPHERIC LOBE ENCOUNTERS

During certain conditions it is possible for spacecraft at or near geosynchronous orbit to move between regions of open and closed field lines, crossing the open/closed field line boundary (OCB). These regions are usually easy to discern using in-situ energetic particle and magnetometer measurements as they typically have vastly different particle compositions and magnetic field topologies. This allows geosynchronous spacecraft to study the lobe environment and also the behaviour of the OCB itself.

Studies of spacecraft near geosynchronous altitudes moving between regions of open and closed field lines have been shown to be either magnetopause crossings [*Wrenn, et al.* 1981; *McComas et al.*, 1994] or tail-lobe entries [e.g. *Sauvaud and Winckler*, 1980; *Thomsen et al*., 1994]. Magnetopause crossings are only observed at geosynchronous orbit on the dayside of the magnetosphere, whereas lobe encounters have been observed at most local times [*Moldwin et al.*, 1995]. Lobe encounters are characterized by a rapid decrease of particle fluxes to background levels at energies from 1 eV to 40 keV [*McComas et al*., 1993], followed by a rapid recovery to previous levels. A strong, stretched and tail-like field is also seen when crossing into the lobes [*Fennell et al*., 1996], especially during times of increased geomagnetic activity and southward IMF [*Kopanyi & Korth*, 1995].

Moldwin et al. [1995] defined tail-lobe entry events as fitting into two distinct classes, those that occurred around local midnight and those that occur on the flanks of the magnetosphere. The former are associated with stretching of the near-Earth field, leading to thinning of the plasma sheet, during a substorm growth phase, and the latter with large scale reconfigurations caused by unusual IMF strength and orientation, i.e. very strong B_y or B_z. Flank lobe encounters have been observed by

spacecraft as low as ~3° south in magnetic latitude at 6.6 R_E [*Kopanyi & Korth*, 1995] and above 10° both north and south of the magnetic equator [*Fennel et al.*, 1996]. Lobe encounters have a tendency to occur in groups, with one statistical survey finding two thirds of lobe entry events occurring within 24 hours of another over a period of four years [*Moldwin et al*., 1995]. Multiple studies [e.g. *Thomsen et al*. 1994; *Moldwin et al*., 1995; *McComas et al*., 1994] have shown a preference for lobe encounters to occur in the morning sector of the magnetosphere, with suggested causes being an asymmetry in the rate of reconnection [*Thomsen et al*., 1994] or an unbalanced inflation of the magnetosphere on the dusk side, caused by an asymmetry in the storm time ring current [*McComas et al*., 1994].

Encounters with the lobe at or near geosynchronous orbit have been found to coincide with periods of strong disturbance caused by extreme IMF conditions, which lead to large scale reconfigurations of magnetosphere geometries [*Thomsen et al*., 1994]. The occurrence of these events during very strong IMF By has been previously simulated [*Moldwin et al*., 1995] by modifying the Tsyganenko T87 model, to show what the expected magnetic field topology should be during these conditions. An asymmetry was found in the magnetic field configuration which predicts that regions of open field lines should be brought closer to geosynchronous orbit for southern dawn and northern dusk sectors for negative B_y and the reverse for positive B_y. These magnetospheric reconfigurations, combined with a large geomagnetic storm are proposed as the cause of the majority of flank lobe encounters. However, a subsequent statistical study of numerous events did not show this B_y pattern unequivocally [*M. Thomsen, pers. comm*, 2013].

2. SPACECRAFT AND INSTRUMENTATION

2.1 THE VAN ALLEN PROBES

The Van Allen Probes mission, formerly known as the Radiation Belt Storm Probes (RBSP) mission [*Kessel et al*., 2013; *Mauk et al*., 2013] consists of two spacecraft, beginning operations September 2012. The two probes have similar nine hour low inclination (10°) orbits, with apogee at 5.8 Re and perigee at 1.1 Re, with one spacecraft lagging behind the other, lapping each other every 75 days. The spacecraft are spin stabilised, with a nominal spin period of ~12 seconds The apogee of the spacecraft precess in MLT, as well as switching between sampling the northern and southern hemispheres.

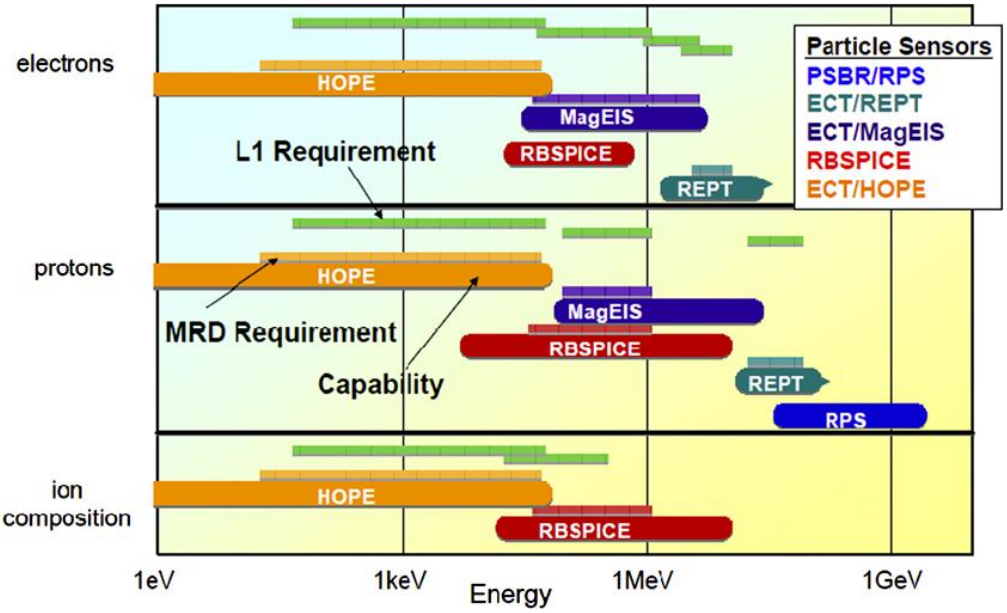

Figure 1: Van Allen Probes particle measurement capability [*Mauk et al*., 2013].

The Van Allen Probes mission, formerly known as the Radiation Belt Storm Probes (RBSP) mission [*Kessel et al*., 2013; *Mauk et al*., 2013] is designed to study the energetic particle composition and magnetic field structure of the magnetosphere. The two spacecraft, launched together in 2012, have similar nine hour low inclination (10°) orbits and lap each other every 75 days. Their apogee is 5.8 Re and their perigee is 1.1 Re. The Van Allen Probes carry an identical and comprehensive suite

of instruments designed to measure all waves and particles of interest in the harsh background of the radiation belt environment with higher sensitivity than any previous mission. The particle instruments aboard are: HOPE (Helium Oxygen Proton Electron Mass Spectrometer), MagEIS (Magnetic Electron Ion Spectrometer), REPT (Relativistic Electron-Proton Instrument), RBSPICE (Radiation Belt Storm Probes Ion Composition Experiment) and RPS (Relativistic Proton Spectrometer) instruments. The energy ranges measured by each instrument are shown in Figure #. Also aboard are EMFISIS (Electric and Magnetic Field Instrument Suite Integrated Science) and EFW (Electric Field and Waves Instrument), which measure electric and magnetic fields and waves over a range of frequencies shown in Figure X. The three instruments used in this work are the low energy particle instrument HOPE [*Spence et al.*, 2013], the medium energy particle instrument MagEIS and the electric and magnetic field instrument EMFISIS [*Kletzing et al.*, 2013], which will be discussed in more detail.

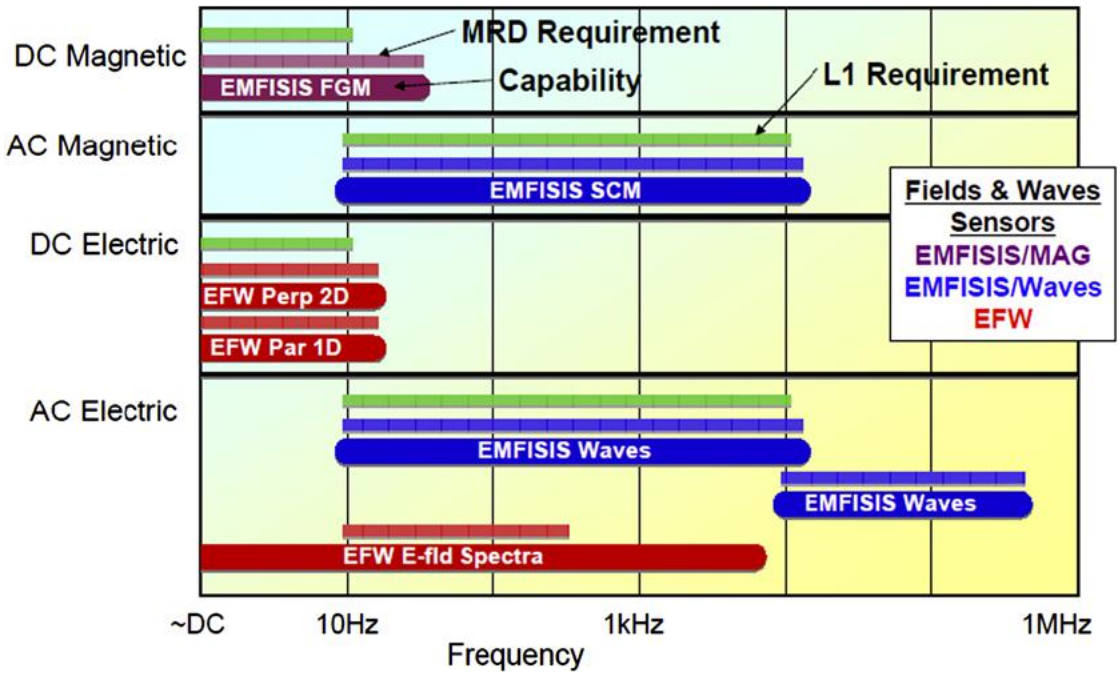

Figure 2: Van Allen Probes fields measurement capability [*Mauk et al.*, 2013].

The HOPE spectrometer was designed and built at Los Alamos National Laboratory and aimed to study the structure and dynamics of the radiation belts, specifically loss and acceleration mechanisms. These observations could then also be used to develop both empirical and physical magnetospheric models. The instrument uses a top-hat electrostatic analyzer to measure both positive and negative species from 1 eV – 50 keV [*Funsten et al.*, 2013]. Ten channel electron multipliers

(CEMs) are used as start and stop detectors and the coincidence and time-of-flight is recorded to reduce the background rate from penetrating radiation and to provide species identification.

The MagEIS instrument consists of four spectrometers, with a low (20- 240 keV), medium (80 – 1200 keV) and high (55 keV – 20 MeV) energy spectrometer orientated with a view direction out the side of the spacecraft at an angle of 75 degrees to the satellite spin axis. The fourth spectrometer also samples medium energies and is arranged to view out the bottom of the spacecraft at an angle of 35 degrees to the spin axis

The EMFISIS suite aboard the Van Allen Probes is primarily designed to study radiation belt acceleration, acceleration loss and transport mechanisms by examining electric and magnetic fields in the magnetosphere. The instrument used in this work is the fluxgate magnetometer (MAG) which is capable of measuring 3D vector magnetic fields, as well as ULF waves that are responsible for various particle transport and acceleration mechanisms. The instrument is capable of sampling magnetic field vectors in a range of -65536 nT to 65536 nT at a resolution of 2nT and accuracy of 0.1 nT. Greater resolutions are available for smaller measurement ranges but are unimportant for the larger scale magnetic field changes analysed in this work [*Kleitzing et al.*, 2013]

2.2 ACE (ADVANCED COMPOSITION EXPLORER)

To better understand the processes observed by spacecraft within the magnetosphere we have to try and find what drives them. One of the most important factors governing the topology and dynamics of the magnetosphere is the behaviour of the solar wind; its speed, composition and magnetic field orientation. The Advanced Composition Explorer (ACE) was launched in August 1997, sitting at the L1 point and providing us with the best in-situ measurements of the Earth-bound solar wind and the interplanetary magnetic field.

ACE carries six high resolution spectrometers capable of measuring charge state and composition of particles with masses as high as Nickel (Z=28), and of energies from ~1 kev to ~500 MeV. Data from the Solar Wind Electron, Proton and Alpha Monitor (SWEPAM) instrument is used in this work, capable of observing ions with energies between ~0.26 and 36 keV, and electrons between 1 and 1350 eV [*McComas et al.*, 1998]. ACE also carries two magnetometers, mounted on separate booms on either side of the spacecraft to avoid interference from the main body and other on-board instruments, allowing the spacecraft to measure the magnitude and direction of the interplanetary magnetic field thirty times per second with a range of 0.004 – 65536 nT.

2.3 LANL (LOS ALAMOS NATIONAL LABORATORY) GEO

Data is also utilized from the Los Alamos National Laboratory geosynchronous spacecraft energetic particle instrument Synchronous Orbit Particle Analyzer (SOPA).The satellites operate at geosynchronous orbit (6.6 Re) at the geographic equator with a 24-hour orbital period, giving a fixed longitude and a nominal magnetic latitude of up to 11 degrees. The spacecraft have a spin period of 10.24 seconds with the spin axis actively controlled to point toward the centre of the Earth. The SOPA instrument measures electrons from 50 keV to 26 MeV over 16 energy channels and protons from 50 keV to >50 MeV over 15 energy channels [*Belian et al.*, 1992].

3. THE NOVEMBER 14TH 2012 CASE STUDY

3.1 INTRODUCTION

Previous observations of spacecraft near geosynchronous altitudes moving between regions of open and closed field lines have been shown to be either magnetopause crossings [*Wrenn, et al.* 1981; *McComas et al.*, 1994] or tail-lobe entries [e.g. *Sauvaud and Winckler*, 1980; *Thomsen et al*., 1994]. Magnetopause crossings are only observed at geosynchronous orbit on the dayside of the magnetosphere, whereas lobe encounters have been observed at most local times [*Moldwin et al.*, 1995]. *Moldwin et al.* [1995] defined tail-lobe entry events as fitting into two distinct classes, those that occurred around local midnight and those that occur on the flanks of the magnetosphere, the former are associated with stretching of the near-Earth field, leading to thinning of the plasma sheet, during a substorm growth phase and the latter with large scale reconfigurations caused by unusual IMF strength and orientation, i.e. very strong B_y. Flank lobe encounters have been observed by spacecraft as low as ~3° south in magnetic latitude at 6.6 R_E [*Kopanyi & Korth*, 1995] and above 10° both north and south of the magnetic equator [Fennel et al. 1996]. Lobe encounters have a tendency to occur in groups, with one statistical survey finding two thirds of lobe entry events occurring within 24 hours of another over a period of four years [*Moldwin et al*., 1995]. Multiple studies [e.g. *Thomsen et al*. 1994; *Moldwin et al*., 1995; *McComas et al*., 1994] have shown a preference for lobe encounters to occur in the morning sector of the magnetosphere, with suggested causes being an asymmetry in the rate of reconnection [*Thomsen et al*., 1994] or an unbalanced inflation of the magnetosphere on the dusk side, caused by an asymmetry in the storm time ring current [*McComas et al*., 1994].

Lobe crossing events are characterized by a rapid decrease of particle fluxes to background levels at energies from 1 eV to 40 keV [*McComas et al*., 1993], followed by a rapid recovery to previous levels. A strong, stretched and tail-like field is also expected when crossing into the lobes [*Fennell et al*., 1996], especially during times of increased geomagnetic activity and southward IMF [*Kopanyi & Korth*, 1995].

Encounters with the lobe at or near geosynchronous orbit have been found to coincide with periods of strong disturbance caused by extreme IMF conditions, which lead to large scale reconfigurations of magnetosphere geometries [*Thomsen et al*., 1994]. The occurrence of these events during very strong IMF By has been previously simulated [*Moldwin et al*., 1995] by modifying the Tsyganenko T87 model, to show what the expected magnetic field topology should be during these conditions. An asymmetry was found in the magnetic field configuration which predicts that regions of open field lines should be brought closer to geosynchronous orbit for southern dawn and northern dusk sectors for negative B_y and the reverse for positive B_y. These magnetospheric reconfigurations combined with a large geomagnetic storm that are proposed as the cause of the majority of flank lobe encounters. However, a subsequent statistical study of numerous events did not show this B_y pattern unequivocally [*M. Thomsen, pers. comm*, 2013].

The open-closed field line boundary (OCB) is the separation between closed field lines having both footpoints in the Earth's ionosphere, and open field lines which have one footpoint in the solar wind The OCB is readily determined in physics-based magnetohydrodynamic models and can be compared to in situ observations [e.g. *Kabin et al*., 2004; *Aikio et al*. 2008; *Rae et al.* 2004]. A variety of techniques exist to probe the open-closed boundary remotely using radars, magnetometers, optical instrumentation, for instance [*Aikio et al*., 2006; *Amm et al*. 1997, *Amm et al*., 1998; *Chisham et al*., 2005; *Clausen et al*., 2013; *Urban et al*., 2011]. The OCB is critical to numerous topics in space physics, including the mechanisms and mapping of MHD models, planetary magnetosphere, and magnetosphere-ionosphere coupling. Magnetic mapping problems are of critical importance to magnetosphere-ionosphere coupling and geospace systems science. Global MHD models may represent the most self-consistent method of mapping [*Paschmann et al*., 2003] however mapping remains extremely challenging during storms and over long distances. This chapter will examine mapping issues during an active storm-time, at the flanks of the magnetosphere. Multipoint observations and global MHD models will be compared in situ to assess the spatial and temporal constraints on the boundary observed.

3.1.2 INSTRUMENTATION AND MODELS USED

In this chapter data from the HOPE energetic particle instrument and the EMFISIS magnetometer from the Van Allen Probes, described in Chapter 1. The two spacecraft have similar nine hour low inclination (10°) orbits and lap each other every 75 days. Their apogee is 5.8 Re and their perigee is 1.1 Re. During the period examined the spacecraft had their apogee in the dawn sector and were relatively close together, ideally located to observe extreme stretching during the November 14th 2012 geomagnetic storm.

Data is also utilized from the Los Alamos National Laboratory geosynchronous spacecraft energetic particle instrument Synchronous Orbit Particle Analyzer (SOPA) on board the spacecraft in operation at the time of the event: LANL-080, LANL-084, LANL-97A, LANL-01A, LANL-02A and LANL-04A. The satellites operate at geosynchronous orbit (6.6 Re) at the geographic equator with a 24-hour orbital period giving a fixed longitude and a nominal magnetic latitude of up to 11 degrees. The spacecraft have a spin period of 10.24 seconds with the spin axis actively controlled to point toward the centre of the Earth. The SOPA instrument measures electrons from 50 keV to 26 MeV over 16 energy channels and protons from 50 keV to >50 MeV over 15 energy channels [*Belian et al.*, 1992]. Though the Magnetospheric Plasma Analyzer (MPA) instrument has similar energies to the HOPE instrument, MPA flux data were not publicly available at the time of this writing; however the dropouts occur over a wide range of energies so this is not expected to impact the subsequent analysis.

Simulated magnetospheric data was obtained using the CRCM + BATS-R-US coupled global MHD and ring current model implemented in *Glocer et al*. [2013]. In this study the Block-Adaptive-Tree Solar-Wind Roe-Type Upwind Scheme (BATS-R-US) model is configured to solve ideal MHD equations, using a Cartesian grid. The domain of the modelled magnetosphere ranges from 32 R_E sunward to 224 R_E tailward and 64 R_E to sides of the Earth, with an inner boundary 2.5 R_E from the planet. The resolution of the simulation varies from 1/8 R_E in the inner magnetosphere to 4 R_E at the edges of its domain. The Comprehensive Ring Current Model (CRCM) simulates the ring current electrons and ions by solving the bounce averaged Boltzmann transport equation described in *Fok and*

Moore [1997]. The domain of the model is defined by the ionospheric foot point of its field lines and the distance of the last closed field line, extending no further than 15 R_E from the Earth. It is important to note that the ionospheric outflow model, such as PWOM [*Glocer et al.*, 2009], was not used in this simulation.

The two models are coupled together using the Space Weather Modelling Framework described by *De Zeeuw et al*. [2004]. Information from field lines whose footpoints are within the CRCM grid are extracted from BATS-R-US and passed to CRCM along with equatorial mass density and thermal pressure at the model boundary. CRCM then uses this data along with ionospheric potential obtained from a height-integrated conductance model and potential solver [*Ridley et al*., 2004] to calculate ring current fluxes, density and parallel and perpendicular pressure. These values are then fed back to BATS-R-US and used to nudge its values in the inner magnetosphere towards those provided by CRCM over a short period of time (typically 20 seconds). The present runs use a version of BATS-R-US that solves the anisotropic MHD equations. As such the coupling is able to account for pitch angle anisotropy in the coupling as described by *Meng et al*. [2013].

3.1.3 EVENT CONDITIONS

The period of interest (0100 – 0600 UT on 14 November 2012) occurs during the main phase of a moderate geomagnetic storm (minimum D_{st} = -108 nT) and during a period of highly disturbed interplanetary magnetic field (IMF) conditions observed by the ACE spacecraft at L1 (Figure 1). This was followed by a period of rapidly fluctuating IMF conditions before a period of very strong, persistent IMF B_y (+20 nT) and a rotation of IMF B_z from northward to southward beginning at approximately 0900 13 November 2012. IMF B_z becomes southward at 1700 and stays southward until 0900 the next day, after the period examined is over. Solar wind speed was nearly constant at ~380 km/h for twelve hours prior to the events. There was a large increase in proton density starting at 0212 UT and peaking at 21 particles/cm^3 at 0357 UT.

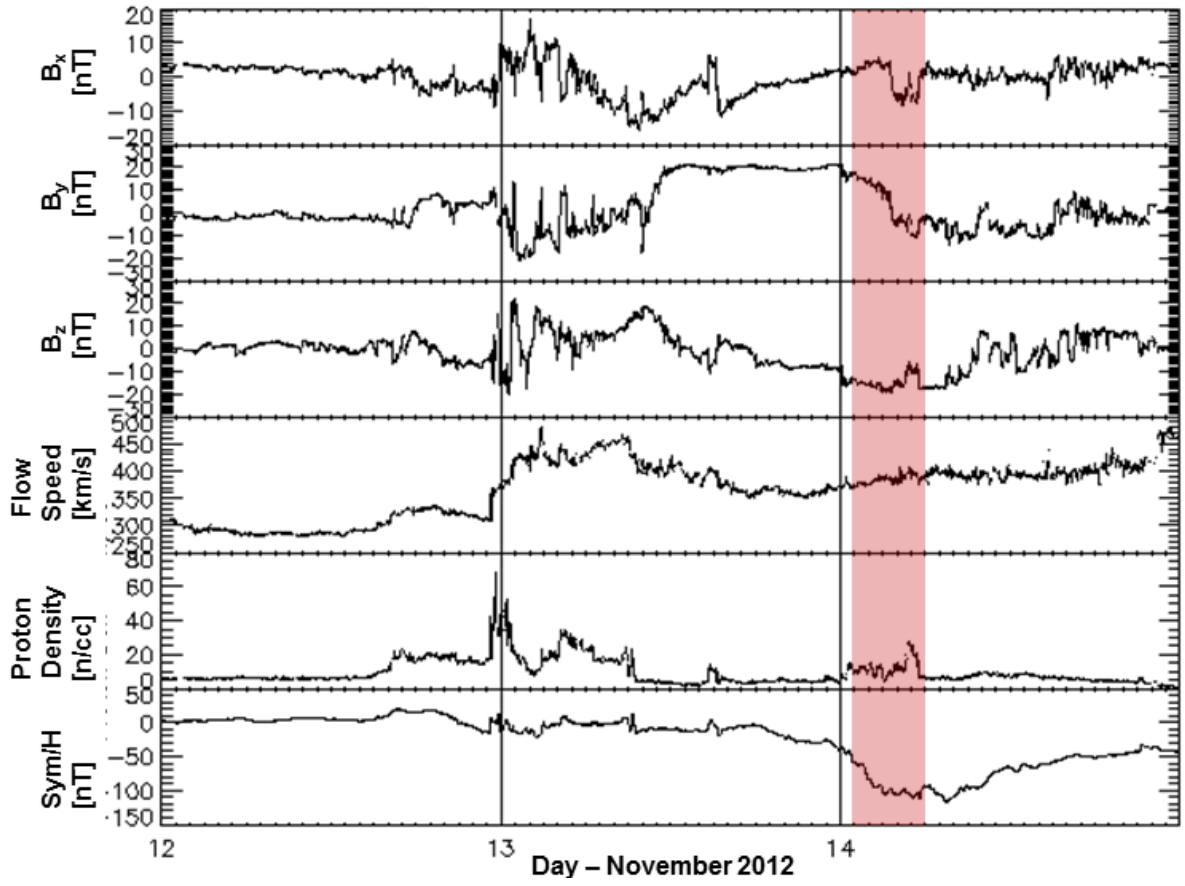

Figure 3: Solar wind data from the ACE spacecraft with times shifted to account for distance for L1 to the magnetosphere for the 12th-14th of November 2012. The period examined in this work, 0100 – 0600 November 14th 2012, is highlighted in red. At approximately 2300 November 12th 2012 a CME can be seen reaching the magnetosphere. Data obtained and plotted from the NASA OMNIWEB service.

Both the IMF B_y and B_z are unusually large, taking on their highest values in several months. These conditions, consistent with those seen in *Moldwin et al.* [1995] and *Thomsen et al.* [1994] would cause a build-up of flux in the lobes via reconnection and for the lobes to be highly skewed in the y-direction. There are no clear IMF signatures relating to the individual events for any of the solar wind parameters, though shortly after the onset of the events the IMF conditions change dramatically with B_x and B_y beginning to fluctuate.

Over a five hour period on 14 November 2012 the twin Van Allen Probes observed multiple rapid decreases and then recoveries of particle fluxes over almost the whole energy range of the HOPE instrument, from tens of eV to 50 keV. Figure 2 shows differential ion and electron fluxes from the HOPE instruments aboard RBSP-A and RBSP-B for the period of 0100 – 0600 UT on 14 November 2012. Events 1-5 are seen by RBSP-A shown in panels A, C, E and

G and events 2-6, seen by RBSP-B are shown in panels B, D, F, H. For each event the plasma fluxes for both positive and negative species sharply drop several orders of magnitude to background levels, before rapidly recovering to their previous state minutes later. There is some structure within each dropout, particularly for events 4 and 5, where the particle fluxes very briefly recover to levels seen outside the events. There is no overall change in particle fluxes after each event as compared to before, which is consistent with the spacecraft having moved between two different plasma populations. Figure 2 also shows large (Δ50 nT) increases and then decreases in magnetic field strength, observed by the magnetometer in the EMFISIS instrument suite between 0100 and 0600. Panel I shows EMFISIS data from RBSP-A and panel J shows EMFISIS data from RBSP-B. These observations coincide with the flux dropouts seen by the HOPE instrument, both for the start and end times of each event and also some of the finer structure within them. The magnetic field for this entire orbit is abnormally strong, highly stretched and not very dipolar. These particle and magnetic field signatures appear wholly consistent with those seen in previous investigations during the CRRES era of spacecraft near geosynchronous orbit crossing the open-closed field line boundary (OCB) and entering the lobe e.g. [*Moldwin et al*., 1995; *Thomsen et al*., 1994; *Fennell et al*., 1996].

TABLE 1: Lobe crossing times identified in the text. Events that overlap in time are given the same number.

	Start/End Times (UT)	Δt	Label
RBSP-A	02:00:27 - 02:04:17	3m 50s	1
	02:46:40 - 02:54:09	7m 29s	2
	03:36:07 - 03:45:45	9m 38s	3
	04:19:42 - 04:28:42	9m	4
	04:44:14 - 04:48:43	4m 29s	5
RBSP-B	02:45:19 - 02:50:45	5m 26s	2
	03:33:37 - 03:44:39	11m 2s	3
	04:15:19 - 04:23:33	8m 14s	4
	04:42:37 - 04:47:01	4m 24s	5
	05:06:45 - 05:09:19	2m 34s	6
LANL-97A	01:59:29 - 02:04:11	4m 42s	1
	03:35:53 - 03:42:11	6m 18s	3
	04:42:35 - 04:47:51	5m 16s	5
1991-080	02:09:15 - 02:59:59	50m 44s	8
	03:15:57 - 03:37:47	20m 50s	11
	03:54:52 - 04:20:43	25m 51s	13
	05:08:18 - 05:27:56	19m 38s	14
LANL-01A	03:47:04 - 03:56:07	9m 3s	9
	04:07:34 - 04:27:12	19m 38s	10
	04:53:46 - 05:29:27	35m 41s	12
LANL-04A	03:55:54 - 04:00:58	5m 4s	7

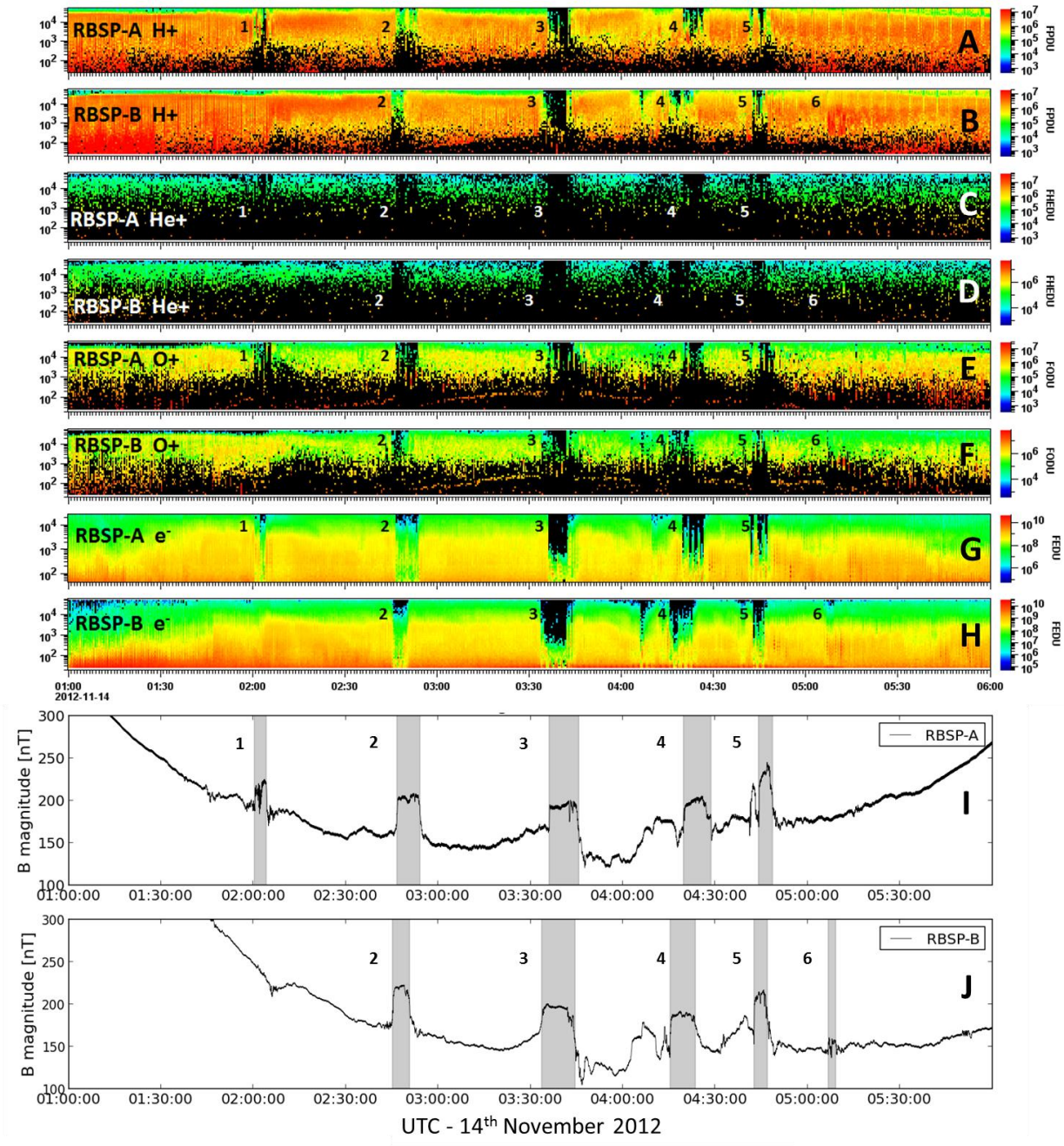

Figure 4: Van Allen Probes particle flux and magnetic field data showing multiple flux dropouts and magnetic field strength increases between 0100 and 0600 on November 14th 2012. Panels A-H show HOPE differential particle fluxes for RBSP-A and RBSP-B over an energy range of eV to 50 keV, with the events seen by each spacecraft numbered 1-6. Panels I and J show the magnetic field strength detected by the EMFISIS magnetometer over the same period. Each event is highlighted in grey and numbered similarly to the particle fluxes.

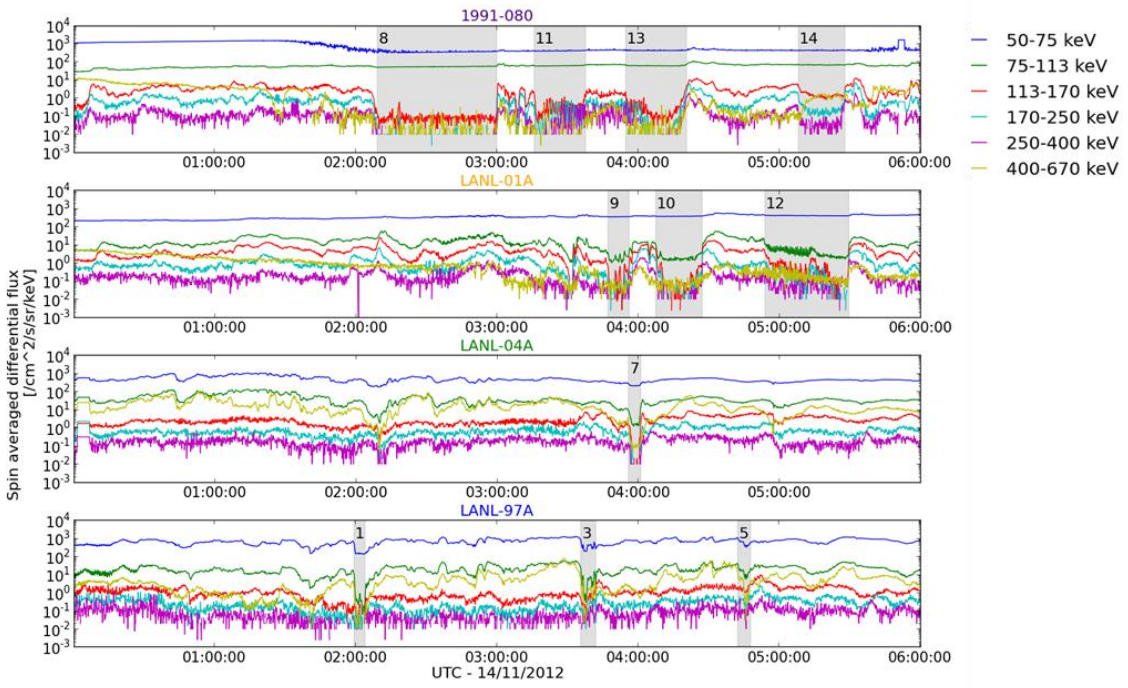

Figure 5: LANL-GEO spin averaged differential proton fluxes from the SOPA instrument. Six energy bands are shown from 50 – 670 keV. Grey shaded areas highlight lobe entries. 1991-080 and LANL-01A, situated in the dusk region of the magnetosphere, are shown in the top two panels. LANL-04A and LANL-97A situated in the dawn region are shown in the bottom two panels. 1994-084 and LANL-02A did not encounter the lobe and are not shown.

During this time period four of the six LANL geosynchronous satellites also observed dropouts of electron and proton fluxes consistent with lobe entries. Figure 3 shows proton flux data from the SOPA instrument aboard the four LANL-GEO spacecraft that saw flux dropouts between 0100 and 0600 UT. Fluxes from the six lowest energy channels with an overall range of 50 – 670 keV are used. This does not overlap with the energy range of HOPE (25 eV – 50 keV) but examination of higher energy ion and electron data from the RBSPICE [*Mitchell et al*., 2013] and MagEIS [*Blake et al*., 2013] instruments aboard the Van Allen Probes shows that the flux dropouts they observe extend up to energies similar to those seen by SOPA. Three lobe encounters seen by LANL-97A occurred at very similar times and magnetic local times to encounters 1, 3 and 5 seen by the Van Allen Probes; they have been given the same label. The rest of the LANL-GEO spacecraft lobe entries have been labelled in order of increasing magnetic local time (MLT).

In total there are twenty entries into the lobe seen over five spacecraft in the southern dawn (RBSP-A, RBSP-B), northern dawn (LANL-97A) and southern dusk (1991-080 & LANL-01A) sectors of the magnetosphere. These entries vary in duration from a few minutes to almost an hour, with the two spacecraft in the southern dusk sector seeing significantly longer entries than the others. The lobe entry times and durations are summarised in Table 1 and derived by the following method.

Each Van Allen Probes boundary crossing is identified by a sharp drop in particle flux (seen in all ions and the electrons) accompanied by a sharp increase in the magnetic field strength. As the magnetic field strength measurements consist of a sharper boundary, they are chosen to identify the start and end points of each event. For consistency the onset and recovery time of each event is defined as the time at which the magnetic field magnitude is halfway through its increase or decrease, e.g. if the magnetic field strength rose from 150 nT to 210 nT then the onset would be defined as the time at which it reached 180 nT.

Event 6, seen only by RBSP-B has a significantly smaller increase in magnetic field strength compared to the other events, with the drop in particle fluxes also being particularly small. The magnetic field observations for this event still show the sharp increase and then rapid decline seen for the other events and so it is included as a valid event, despite its relative weakness.

For the LANL-GEO spacecraft a slightly different approach was taken as they are not equipped with on-board magnetometers and the event times cannot be ascertained from changes in magnetic field strength. Instead the changes in proton flux in the 75-113, 113-170 and 170-250 keV channels of the SOPA instrument were examined. A similar procedure to that used above for the Van Allen Probes magnetometer data was implemented to identify the start and the end of each flux dropout. The mid-points of each sharp decrease and increase in flux are calculated and the mean times for the three energy channels found. This accounts for the small differences seen in start and end times of the dropouts for the different energy levels.

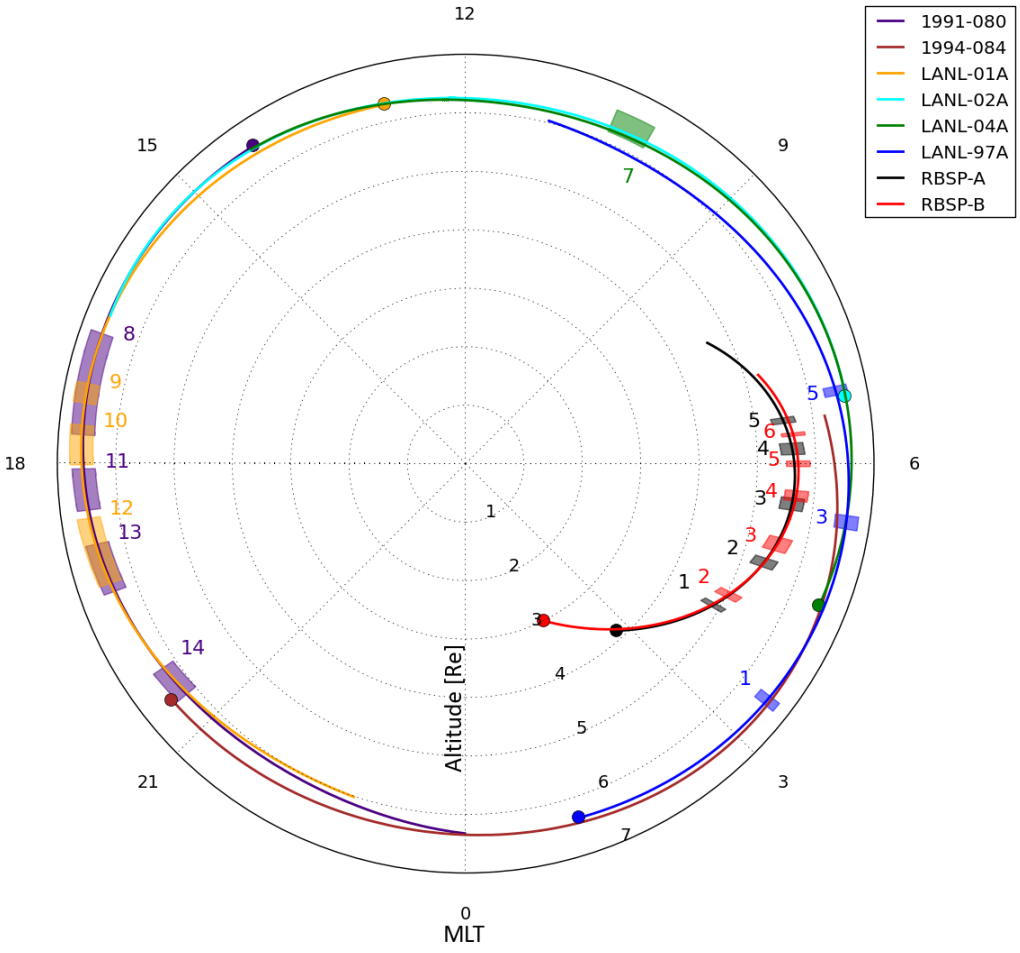

Figure 4: Polar plot of magnetic local time (MLT) and Altitude for the orbits of the Van Allen Probes and six LANL-GEO spacecraft. Spacecraft orbits shown for the period 0100-0600 with the times at which they entered the lobe marked by shaded boxes on their orbit line. All orbits are forward in MLT and the start of each is marked by a circle. Lobe encounter events are numbered in ascending MLT with full details in Table 1. Note that 1994-084, situated near midnight, and LANL-02A, situated near noon, did not encounter the lobe.

3.2 IN-SITU LOBE LOCATION ANALYSIS

Figure 4 shows a polar plot of magnetic local time (MLT) against altitude for all six of the LANL geosynchronous spacecraft and the twin Van Allen Probes. The coloured lines show the orbit of each spacecraft over a five hour period from 0100 to 0600 UT and the shaded boxes show the periods at which each spacecraft entered the lobe. The coloured circles mark the start time at each spacecraft's orbit. For lobe encounters 1, 3 and 5 it can be seen that LANL-97A is at a similar MLT to the Van Allen Probes when it encounters the lobe. For the dusk spacecraft, 1991-080 and LANL-04A, the lobe encounters mostly occur between 16.5 and 19.5 MLT. The overlap of the shaded boxes show that the lobe encounters happened in similar regions of space but at significantly different times e.g. event 9 happens about ninety minutes after event 8.

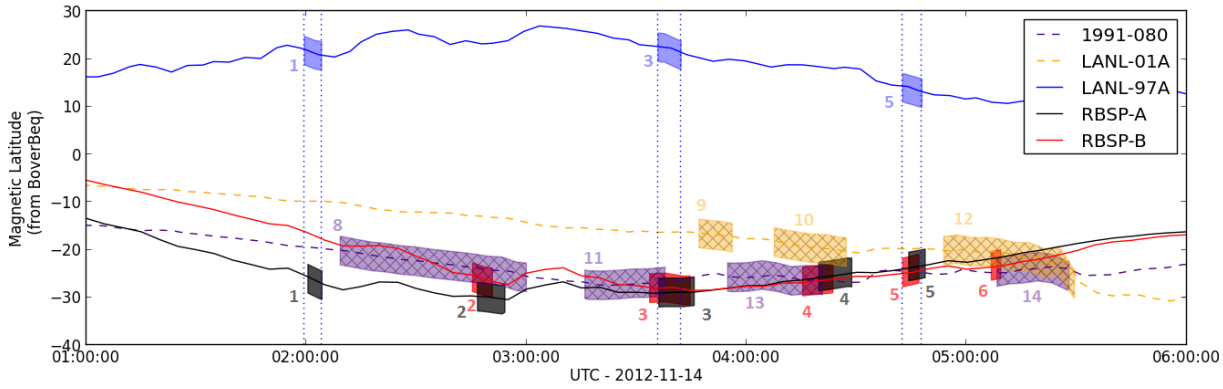

Figure 6: Magnetic latitudes estimated from Tsyganenko TSO4 magnetic field calculations. Shaded boxes show durations of lobe entries for each spacecraft. Dashed lines/hatched boxes mark the two spacecraft (1991-080 & LANL-01A) that are on the dusk side of the magnetosphere. The dotted vertical lines are used to highlight the similarity in time between the three events seen by LANL 97-A in the northern hemisphere and lobe encounters 1, 3 and 5 seen by the Van Allen Probes in the southern hemisphere.

These magnetic latitudes are determined from the RBSP SOC magnetic ephemeris files in the following way. The Tsygenanko 2004 (TS04) magnetic field model is used for the external field while the IGRF is used for the internal [*Tsyganenko and Sitnov*., 2005]. The TS04 model traces the field line connected to the spacecraft trajectory at each time step and determines the minimum magnetic field along that field line. From the ratio of the B field at the spacecraft to the minimum magnetic field the

magnetic latitude at the spacecraft is estimated. The shaded boxes show the times at which the spacecraft are inside the lobe and it should be noted that the height of each box does not represent an extent in magnetic latitude. The two spacecraft on the dusk side of the magnetosphere are differentiated by dashed lines and hashed boxes. The vertical, dotted, blue lines are used to highlight the strong correlation between the lobe encounters seen by LANL-97A and the 1st, 3rd and 5th encounters seen by the Van Allen Probes. There are also small reductions in flux seen by LANL-97A at the same time as the second and fourth events but these are difficult to discern and cannot reliably be defined as a lobe crossing.

It can be seen that the Van Allen Probes reach a greater absolute magnetic latitude (~ -30°) in the southern hemisphere than LANL-97A does in the northern hemisphere (~25°). Before 0400 RBSP-A is at a higher magnetic latitude than RBSP-B with the difference largest (~10°) for the first lobe encounter and gradually getting smaller as the spacecraft reach apogee. After apogee, RBSP-B is at slightly more northerly magnetic latitudes than RBSP-A.

The two spacecraft in the southern dusk region (1991-080 and LANL-01A) experienced the most prolonged and complete entries into the lobe, with 1991-080 measuring a drop in flux to background levels for a period of approximately fifty minutes. LANL-97A, situated in the northern-dawn region and at very similar MLT as the Van Allen Probes during the events, measures three clear flux dropouts nearly simultaneously with the first, third and fifth events seen by the RBSP spacecraft.

1991-084 and LANL-02A situated around midnight and late morning respectively did not experience any clear entries into the lobes, which is not unusual for spacecraft in those regions. LANL-04A does experience a dropout and recovery of flux at 0355 and ~10 MLT but its position near to noon means this flux dropout could be an encounter with the magnetopause rather than the lobe. The model of *Shue et al*. [1997] shows the magnetopause being compressed to ~7.5 Re at this time but only has a resolution of an hour.

Previous work by *Moldwin et al*. [1995] suggested there should be a preference for entries into the lobe at geosynchronous orbit in the southern dusk and northern dawn regions due to the

strong positive IMF B_y seen before the events. This is supported partly by the prolonged lobe entries seen in the southern dusk region but not by the events seen in the southern dawn and the relative weakness of those seen at northern dawn. These mixed results suggest that though the strength and orientation of IMF B_y may be a factor in where geosynchronous spacecraft can access the lobes, factors such as seasonal variations, solar wind conditions and storm-time dynamics also play a role.

These multiple encounters into the southern and northern lobes in both the dawn and dusk regions of the magnetosphere suggest that the movement of the OCB is a global phenomenon. Though there may be small scale local phenomena occurring near the spacecraft the expansion of the lobes which makes them more accessible to the spacecraft, occurs across most of the magnetosphere at very similar times. These spatial and temporal results can be compared with global boundaries obtained from modelling techniques. Here we will present results obtained using the CRCM + BATS-R-US global MHD model.

Figure 6 shows some example frames of the open-closed field line location data visualization obtained from CRCM + BATS-R-US. The model differentiates between regions of open and closed field lines, with the open field line of the northern and southern lobes coloured green and yellow, and the closed field lines of the equatorial region coloured red. A subset of the global magnetospheric data produced by the model is used here, with each data point situated on the surface of a sphere at 6.6 R_E. This figure shows 1991-080 and LANL-01A (situated at dusk) spacecraft, as well as portions of the orbits of 1994-084 (situated around midnight) and LANL-02A (situated around noon). The first frame, taken at approximately 0140 UT shows 1991-080 within the southern lobe and LANL-01A situated just outside it in a region of closed field lines. The second frame, taken at 0340 UT shows LANL-01A inside the lobe and 1991-080 having just crossed the OCB back onto closed field lines. Between the second and third frames there is a large retreat of the lobe to higher negative magnetic latitudes, greatly increasing the distance between the spacecraft and the OCB. These examples qualitatively show that for the dusk spacecraft the model predicts that the spacecraft would have access to the lobe at times during this period. They also highlight both the large scale motions of the

boundary e.g. the retreat of the southern lobe after 0340 UT and the smaller scale topological changes that can be seen along the boundary between each frame.

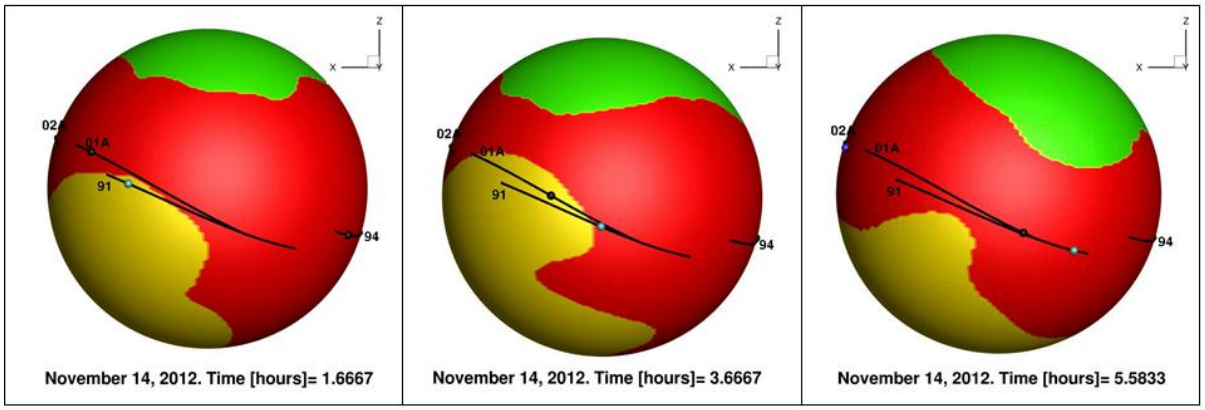

Figure 7: CRCM + BATS-R-US model data showing the locations of regions of open and closed field lines at 6.6 R_E. The red area represents the equatorial region of closed field lines, the green area the open field lines of the northern lobe and the yellow area the open field lines of the southern lobe. The snapshots are taken from a dusk perspective and show the orbits of the two spacecraft situated in this region, 1991-080 (abbreviated to "91" in the figure) and LANL-01A (abbreviated to "01A"). Partial orbits of LANL-02A ("02A"), situated around noon, and 1994-084 ("94"), situated around midnight, are also shown.

The multiple encounters with the magnetospheric lobe seen by the LANL geosynchronous spacecraft and the Van Allen Probes allow us to constrain the position of the open closed field line boundary and compare it to the predicted position obtained through simulation. The model temporal resolution of the output is five minutes, compared to 10.9 seconds for the HOPE instrument aboard the Van Allen Probes and 10 seconds for SOPA aboard the LANL-GEO spacecraft. This means the comparison can only be done at five minute intervals with each time frame in the model being matched to the spacecraft data point which is closest to it in time. Similarly the model only has a spatial resolution of about 0.1-0.2 R_E in this region of the magnetosphere so there may be some error due interpolation inside the coarse of the grid. At each time step of the spacecraft trajectory moving through the model, the region of space nearby is searched for the nearest lobe boundary. When the lobe boundary is found the magnitude of the vector between the spacecraft trajectory point and the lobe boundary is reported. For numerical efficiency the exact method to find the lobe boundary expands a series of spheres around each trajectory points. Field lines are traced starting at each point on the surface of a given sphere and the corresponding magnetic topology is determined. When the

spacecraft is on a closed (open) field, a very small sphere will only have closed (open) topologies present on the surface. As the sphere gradually increases in size it will eventually touch the surface defining the open-closed boundary and more than one topology type will be found on the sphere. The radius of the sphere then defines the distance from the spacecraft to the open-closed boundary. To make the calculation of the distance even more efficient, we use a bisection method rather than simply step radially outward with small steps.

Thus we derive, at the time of a boundary crossing how far away the MHD model says the lobe boundary is. When the model and the in situ data agree about being in the lobes this is reflected as a (nonphysical) separation of less than 0 Re and the nominal interpretation is that this good agreement represents accurate mapping of the open-closed boundary in the model. We present these results for each region, starting at dusk. Figure 7 shows the calculated distance to the OCB for the two spacecraft in the southern dusk region, 1991-080 (purple) and LANL-01A (yellow). The thick lines show the times at which the spacecraft data indicated they had passed into the lobe. Events 8 and 11 seen by LANL-080 and 9 seen by LANL-01A occur at times when the model predicts the spacecraft would be either very close to or inside the lobe. This represents the most consistent data-model comparison.

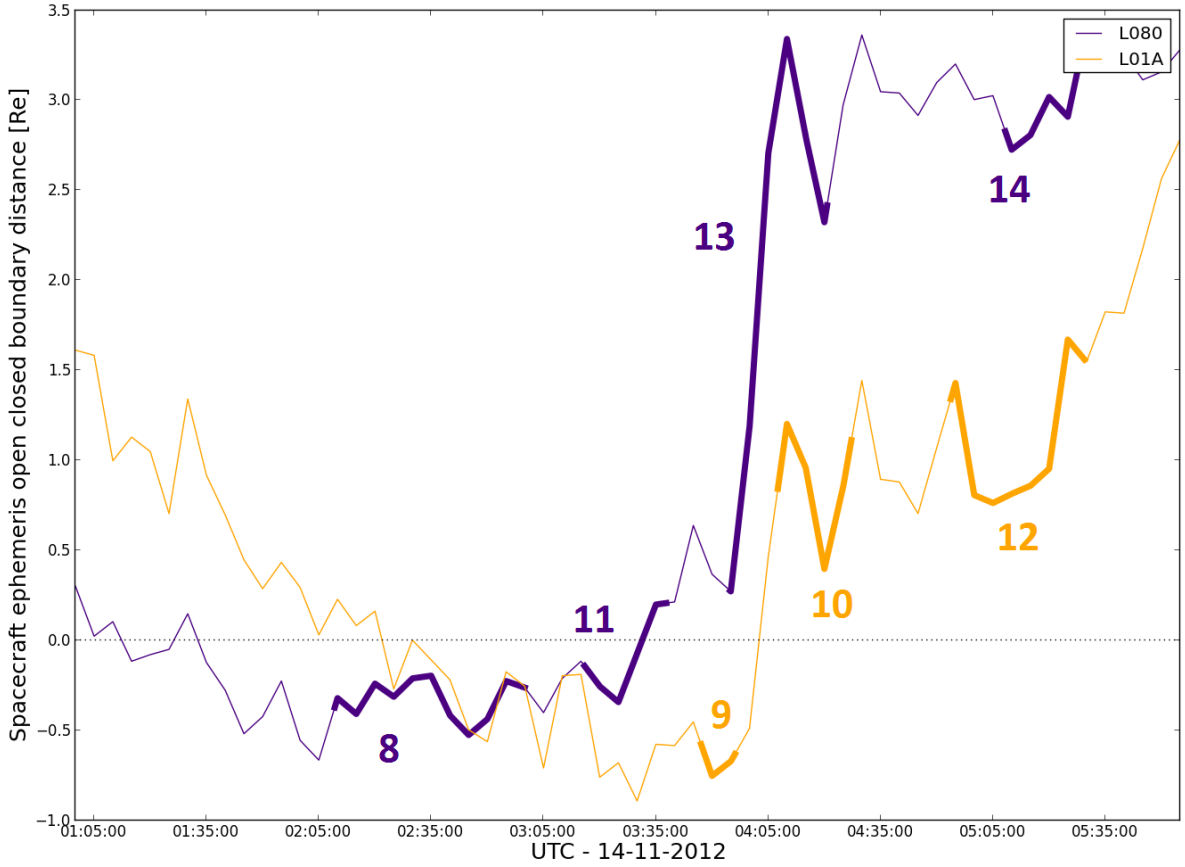

Figure 8: Calculated distances from 1991-080 (purple) and LANL-01A (gold) to the open-closed field line boundary position predicted by CRCM + BATS-R-US. Distances shown are in R_E with negative distance representing when the spacecraft has entered the lobe. Thicker lines show periods where the spacecraft data indicate that it has entered the lobe.

At around 0400 UT the model shows the southern lobe contracting back to higher latitudes, increasing the distance to the OCB to over 3 R_E and 1 R_E for 1991-080 and LANL-01A respectively. This large change in the topology of the magnetosphere coincides with the change in IMF B_y from positive to negative. Events 13 and 14 seen by 1991-080 occur after this movement of the OCB, when the model predicts the spacecraft should have had no access to the lobe. Events 10 and 12 seen by LANL-01A also occur after the OCB retreats, but due to LANL-01A being behind 1991-080 by approximately 90 minutes of MLT and the specific topology of the boundary, LANL-01A stays in closer proximity to the lobe. For both events there seems to be a movement of the boundary towards the spacecraft, with the model showing it being within 0.5 R_E of the spacecraft for event 10.

Figure 8 shows the calculated distance to the OCB for the three spacecraft in the dawn region with the two Van Allen Probes, RBSP-A (black) and RBSP-B, (red) in the southern hemisphere and LANL-97A (blue) in the northern hemisphere. The thick lines show the times at which the spacecraft data indicated they had passed into the lobe. No lobe encounters are predicted. Generally, the comparison is not as consistent at dawn, likely because the lobe encounters are shorter and more difficult to reproduce in the model.

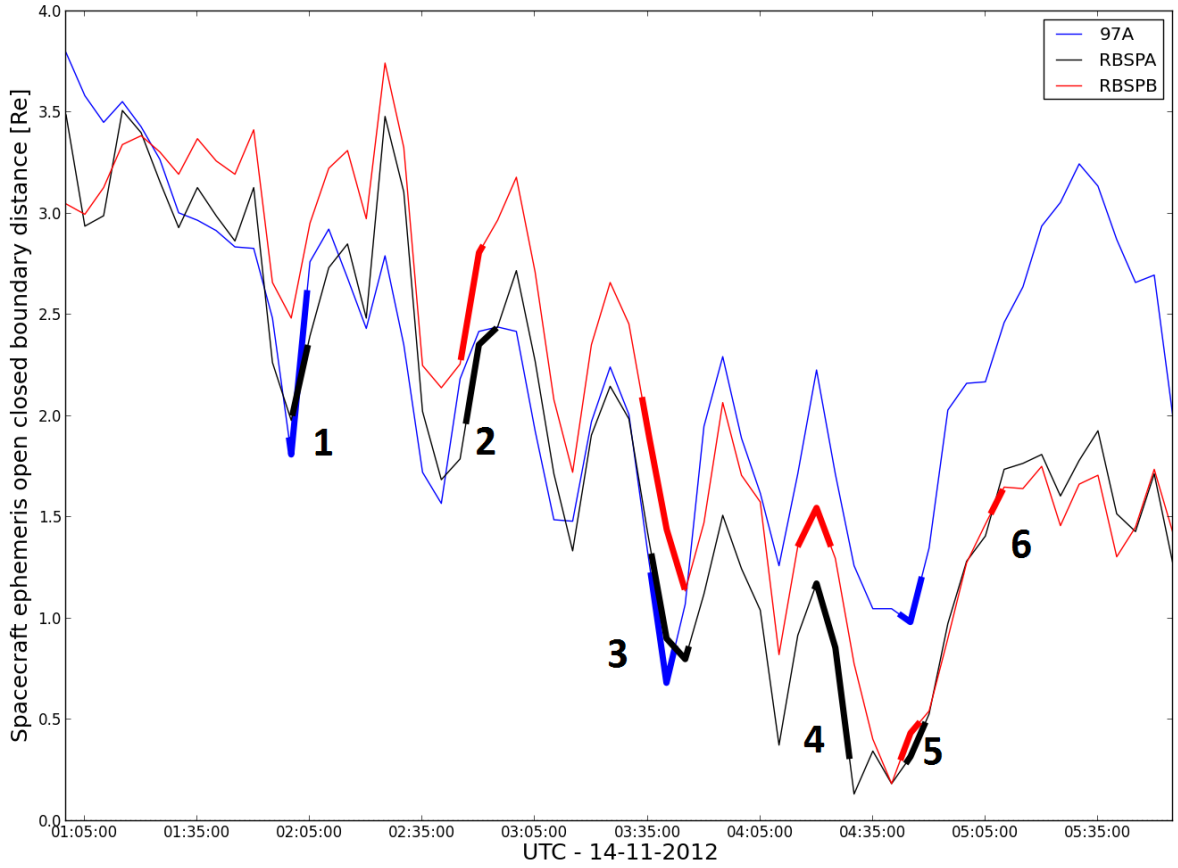

Figure 9: Calculated distances from the RBSP-A (black), RBSP-B (red) and LANL-97A (blue) to the open-closed field line boundary position predicted by CRCM + BATS-R-US. Distances shown are in R_E with negative distance representing when the spacecraft has entered the lobe. Thicker lines show periods where the spacecraft data indicate that it has entered the lobe.

For all three spacecraft the model shows both the northern and southern lobe advancing and retreating in a cyclical manner with a period of around half an hour. Events 1, 2, 3 and 5 coincide fairly well with the lobe expansions, occurring at least partially within the minima of the oscillations.

Event 4 occurs when the model shows the lobes to be in retreat and is not seen by LANL-97A in the northern hemisphere. Event 6, which is only seen by RBSP-B, occurs after the periodic expansion and contraction has ceased and the model predicts the OCB to be over 1.5 R_E from the spacecraft. There is a clear minimum between events 2 and 3 which does not coincide with a lobe crossing seen by any of the spacecraft.

As well as the periodic movement of the boundary there is also a steady decrease in the distance to the OCB until 0430 UT where the lobes contract again. This gradual expansion and then faster contraction of the lobes may coincide with a steady increase and then decrease in solar wind proton density.

To further understand the lobe encounters we next examine in more detail another critical aspect of their character, that of the magnetic field. It is advantageous to look at fluctuations from the background magnetic field to isolate the stretching that is associated with the lobe encounters. To isolate these fluctuations the expected magnetic field characteristics contained in the HOPE ephemeris data, derived from the TS04 model, are removed from the magnetometer measurements from EMFISIS. This effectively removes the large scale changes in the magnetic field and leaves only the signatures associated with the lobe encounters. We note that the TS04 model reproduces the large scale field for this orbit reasonably well; however as an average statistical model it does not come close to reproducing the lobe encounters nor should it.

Figure 9 shows the magnetic field fluctuation vectors relative to the nominal TS04 + IGRF from RBSP-A observations (thick lines) and as simulated at the spacecraft position by CRCM + BATS-R-US (thin lines). The top panel shows the magnetic field before the removal of the background and the bottom three after it is removed, with the grey shaded boxes indicating the lobe encounters.

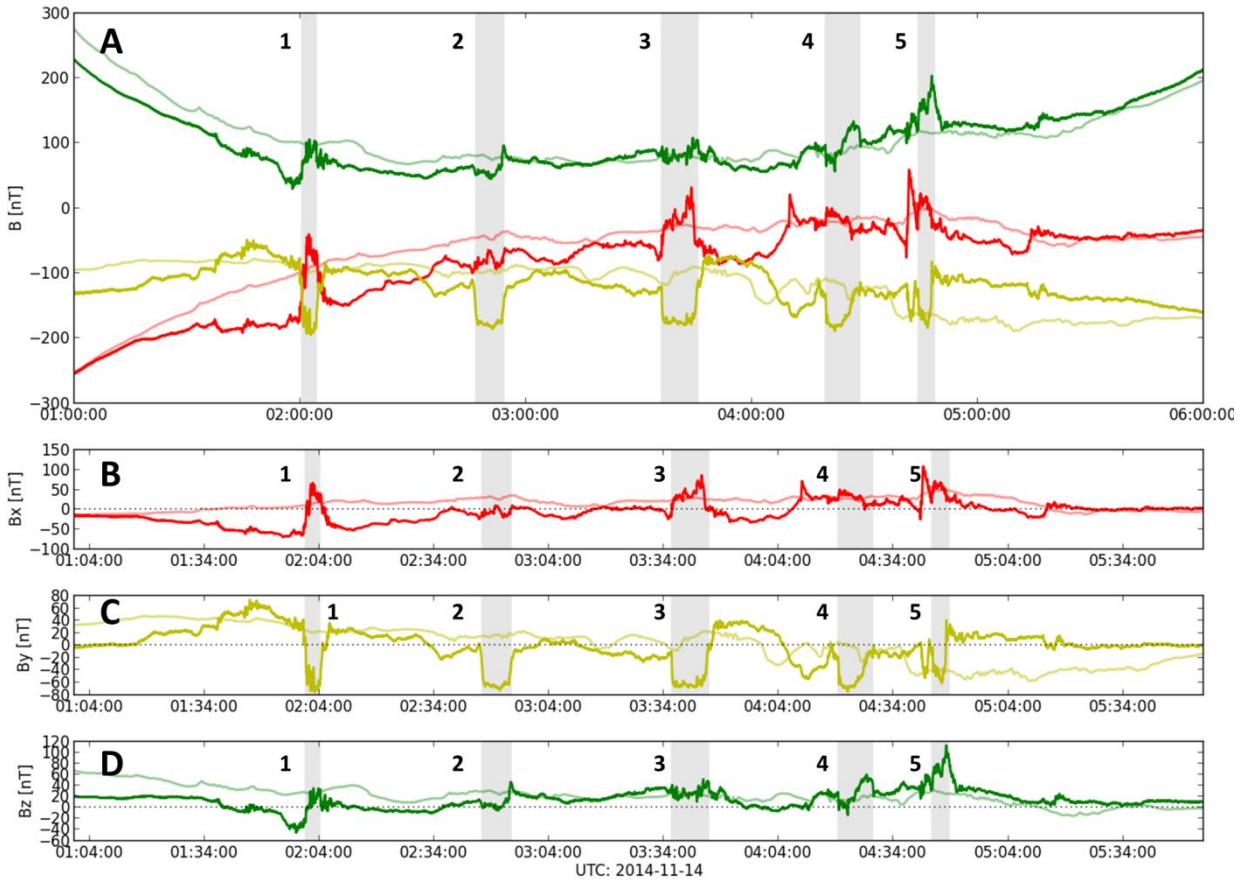

Figure 10: RBSP-A EMFISIS magnetometer data and CRCM + BATS-R-US simulated magnetic field for 0100 – 0600 14th November 2012. A) B_x (red), B_y (yellow) and B_z (green) shown. Bold lines show magnetometer data from EMFISIS and light lines show model magnetic field. B) B_x after removal of TSO4 predicted magnetic field. C) B_y after removal of TS04 predicted magnetic field. D) B_z after removal of TS04 predicted magnetic field. Grey shaded areas show periods when the spacecraft has entered the lobe.

The lobe encounters seen by RBSP-A are characterised by an increase in negative B_y (~ -60 to -80 nT) seen for all five of the events and an increase in B_x observed for all of the encounters apart from the second. There are changes in B_z during the events but these are not consistent. Event 1 shows a sharp change of B_z (-50 to 50 nT) at the start of the event, whereas event 2 shows a sharp increase in B_z at the end of the event. Event 3 shows little change, except for a small increase at the end. Event 4 changes from -20 to 50 nT but gradually over the duration of the event. Event 5 shows a large increase in B_z which persists for the duration of the vent and peaks at 100 nT. These changes seem to represent the spacecraft encountering a region of highly stretched magnetic field, flattened towards the x-y plane.

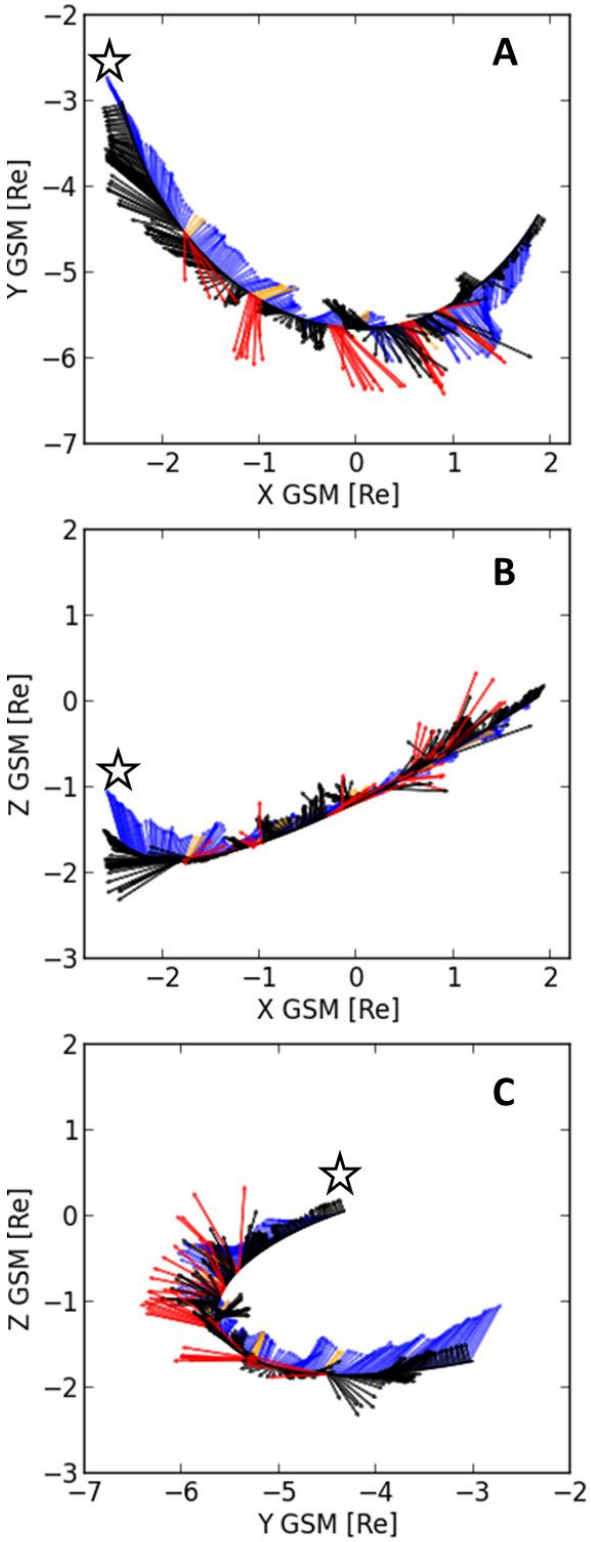

Figure 11: Magnetic field vectors derived from RBSP-A EMFISIS magnetometer data and BATS-R-US simulated magnetic field for the period 0100 – 0600 November 14th 2012. Arrows show the direction and relative strength of the magnetic field, plotted along the spacecraft orbit. Black arrows show the magnetic field configuration for RBSP-A EMFISIS with the red arrows marking times when the spacecraft has entered the lobe. The blue arrows show the model magnetic field configuration with the yellow arrows marking times when the spacecraft has entered the lobe. Panels A, B and C are in the X-Y GSM, X-Z GSM and Y-Z GSM plane respectively. Stars mark the beginning of each orbit.

The magnetic field predicted by the MHD model does not show these large scale changes. This lack of stretching in the MHD model is consistent with the OCB distance calculations that show the lobe to be greater than 0.5 R_E away for the majority of the events. Outside of the times when the spacecraft encounter the lobes there are other inconsistencies between the spacecraft and MHD model field topology. The model underestimates B_x and overestimates B_y and B_z, though there is a closer agreement around the later lobe encounters, which is consistent with the model predicting the OCB being very close to the spacecraft for these events.

The stretching of the magnetic field and the differences between the observations and the model field are visualized in Figure 10 for RBSP-A only where the magnetic field (with the background subtracted) is shown as a vector. The arrows show the direction and strength of the magnetic field taken at one minute intervals and plotted along the spacecraft orbit in GSM coordinates, using the same scale factor and same size of range for all panels. The three panels A, B, C show the X-Y, X-Z and Y-Z planes with the black/red arrows showing the field observed by RBSP-A and the blue/yellow arrows that produced by the model. The red and yellow arrows occur within a lobe crossing. This figure illustrates the amount of magnetic field stretching encountered by RBSP-A during each OCB crossing. In Panel A the magnetic field is strongly stretched in Y GSM and to a lesser extent in X GSM during each event. Panel B & C both show that for event 5 there is a large increase in B_z and although there is also a significant B_y component, this dominates the encountered magnetic field. The model field is significantly different to that observed by RBSP-A, both in general and during the lobe encounters. This is consistent with the model placing the spacecraft a significant distance from the lobe for the majority of the events. It can be seen in Panel B that the observed and modelled fields converge slightly towards the latter section of the orbit.

3.4 DISCUSSION

On 14 November 2012, the Van Allen Probes experienced a series of rapid dropouts and then recoveries of plasma ion and electron flux coinciding with the spacecraft encountering a strong,

highly stretched magnetic field. These flux dropouts are consistent with the spacecraft moving from the densely populated equatorial region of closed field lines to the tail lobes, which consist of open field lines and have a much sparser particle population.

Pitch angle binned data from the HOPE instrument aboard the Van Allen Probes is used to determine if the variations in pitch angle distribution during the flux dropouts seen is consistent with the spacecraft having encountered the open field lines of the tail lobe. Both protons and oxygen ions are shown in Figure 11 for the 18˚ (parallel) and 162˚ (anti-parallel) bins. Examination of pitch angle binned data from the HOPE instrument shows that for the parallel field aligned particles, travelling anti-sunward from the southern magnetic pole, there are ions of all species present during the flux dropouts. This is consistent with the spacecraft encountering the open field lines of the southern lobe and observing ions travelling from the ionosphere. The presence of oxygen in these ion populations seen during the dropouts is indicative of an ionospheric source. The flux of oxygen appears to exceed that of hydrogen as would be expected for outflow at these activity levels [*Cully et al.*, 2003].

Similar accelerated structures are encountered by both spacecraft at nearly the same time which indicates a spatially large or rapidly moving structure (the former being more likely) which threads both open and closed regions. Interestingly, there appears to be energy dispersion with the highest energy ionospheric ions detected during the lobe encounter and then lower energy ions being detected later while in the closed field line region. The gap corresponding to the newly open field line devoid of flux appears with a dispersed signature as well at low energies. This may be consistent with the relatively stationary spacecraft encountering the OCB sweeping past it, and then returning towards

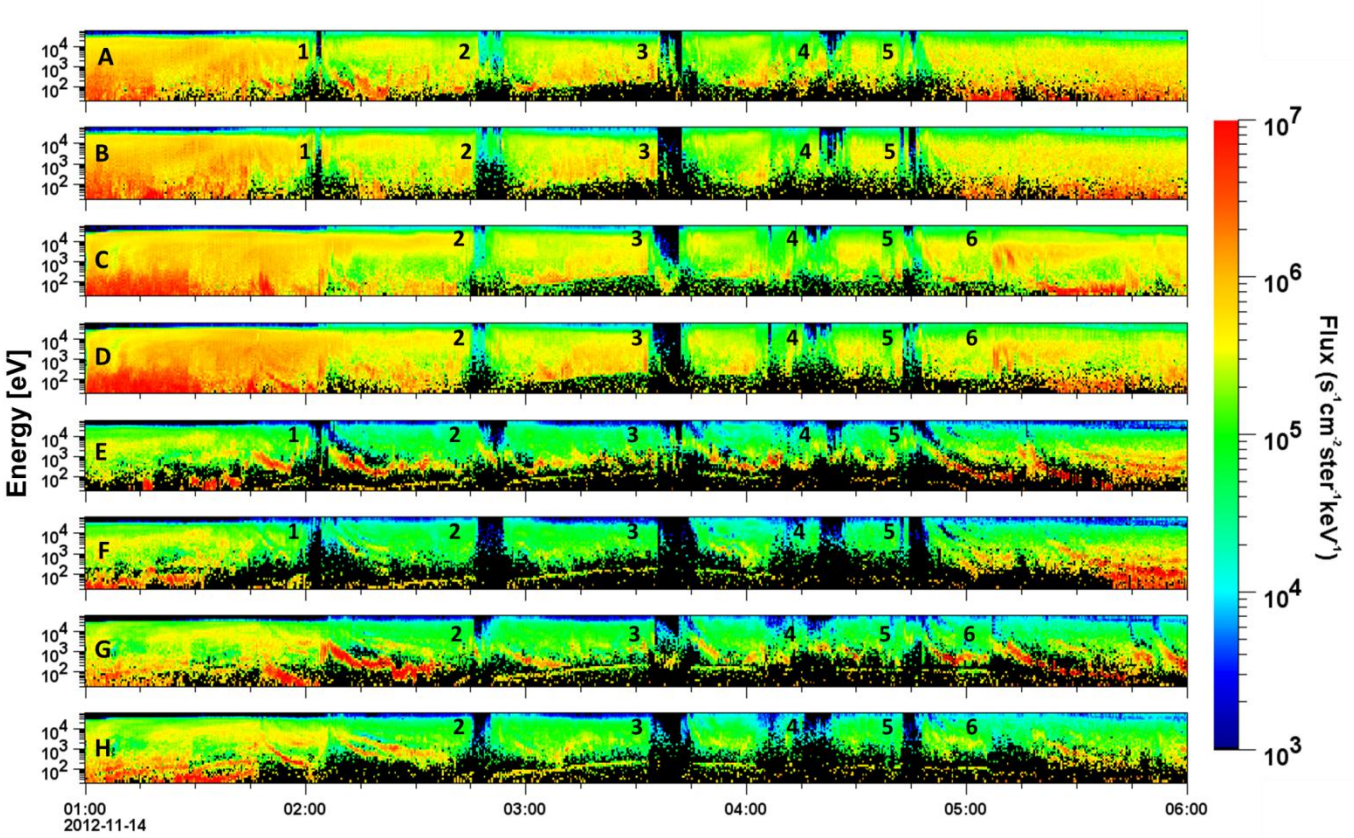

Figure 12: HOPE pitch angle binned differential particle fluxes for the Van Allen Probes between 0100 and 0600, November 14th 2012. . A) RBSP-A 18° pitch angle protons, travelling parallel to the magnetic field (outward from the southern pole). B) RBSP-A 162° pitch angle protons, travelling anti-parallel to the magnetic field (towards the southern pole). C) RBSP-B 18° pitch angle protons, travelling parallel to the magnetic field (outward from the southern pole). D) RBSP-B 162° pitch angle protons, travelling anti-parallel to the magnetic field (towards the southern pole). E) RBSP-A 18° pitch angle oxygen ions, travelling parallel to the magnetic field (outward from the southern pole) F). RBSP-A 162° pitch angle protons, travelling anti-parallel to the magnetic field (towards the southern pole). G) RBSP-B 18° pitch angle oxygen ions, travelling parallel to the magnetic field (outward from the southern pole) H). RBSP-B 162° pitch angle protons, travelling anti-parallel to the magnetic field (towards the southern pole)

the pitch angle structure these particles may be directly injected from the nightside ionosphere to the region near the spacecraft and then lost to the lobes.

There is a shortage of observations and understanding of such ions [e.g. *Walsh et al.*, 2014]. Some estimates indicate that only 10% of the estimated ion outflow is observed in the magnetosphere [*Seki et al.*, 2001]. There are also strong waves detected during the lobe encounters which are described by *Moya et al.* [2014]. The nature of the acceleration mechanism and the source of these dispersed ions are beyond the scope of this work. Conversely, the anti-parallel field aligned particles which are travelling sunward from down-tail to the ionosphere show comparatively reduced ion

populations during the dropouts, especially for the oxygen ions. Observations of both parallel and anti-parallel particles are highly indicative that the spacecraft are encountering the open field lines of the southern lobe.

Examination of the spatial and temporal characteristics of the OCB crossings can be used to give insight into the dynamics of the spacecraft encounters with the lobes and the topology of the boundary. The twin Van Allen probes follow near identical orbital paths, with RBSP-A lagging behind by approximately forty-five minutes during the November 14th event. For the four events (2-5) seen by both spacecraft the delay between the two spacecraft observing the lobe is 3-11 minutes, with RBSP-B encountering and leaving the lobe first each time. There are also two events (1 & 6) seen only by RBSP-A or RBSP-B respectively.

The near simultaneity of the lobe encounters seen by the two spacecraft clearly implies that it is the OCB that is expanding and then retreating over the spacecraft. The two events seen only by one spacecraft could be a result of the boundary only extending far enough to encounter one of them, smaller scale topological changes on the boundary causing only one spacecraft to encounter the lobe or most likely a combination of these two scenarios. This conclusion is also supported by the simulated results obtained from CRCM + BATS-R-US. The OCB distance calculations shown in Figure 8 show a periodic advance and retreat of the boundary which coincide fairly well with the spacecraft lobe encounters.

It is worth considering how the orbital positions for each spacecraft may determine whether and when they encounter the lobe for each event. The relative timings of the events for the two RBSP spacecraft and their spatial separation can be used to constrain the dynamics of the OCB. Three important spatial and temporal factors are: 1) RBSP-B is always at an earlier MLT than RBSP-A, as the direction of their orbits is from midnight to noon for the period examined and B's orbit lags behind A's. 2) For the first three events RBSP-A is closer to the southern lobe in magnetic latitude and at a higher L value than RBSP-B. 3) The last three events occur after the spacecraft have reached apogee, with RBSP-B becoming closer to the southern lobe and higher in L than RBSP-A.

The most simplistic picture for what defines which spacecraft encounters the OCB first would be that the southernmost spacecraft would encounter the southern lobe first as it expanded upwards towards the equator. However, for this event RBSP-B encounters the lobe first for all four of the events seen by both spacecraft, even though RBSP-A is actually further southward in magnetic latitude for events 2 and 3.Another explanation is that the OCB is perturbed locally and a “bump” forms, expanding over the two spacecraft before retreating. In this scenario the spacecraft to enter the lobe first would exit it last, which is inconsistent with what is observed i.e. RBSP-B both enters and leaves the lobe first for all four events.

The diagram in Figure 12 describes a third scenario which is most consistent with the observations. These observations could be explained by a localised disturbance or expansion of the boundary, which travels from the tail, always reaching RBSP-B first. Events 1 and 6 only being seen by one of the spacecraft can be explained in this scenario by the disturbance not having sufficient extent in magnetic latitude to reach RBSP-B and RBSP-A respectively. This is further supported by the relative weakness of these events, which would be consistent with the spacecraft only just encountering the boundary. It is worth noting that the first scenario, a simple expansion of the boundary to lower negative latitudes, is believed to be occurring in combination with that described in Figure 12 to produce the observed phenomena. A global expansion of the lobe is required to bring the OCB close enough to the spacecraft to allow them to observe these smaller scale perturbations of the boundary.

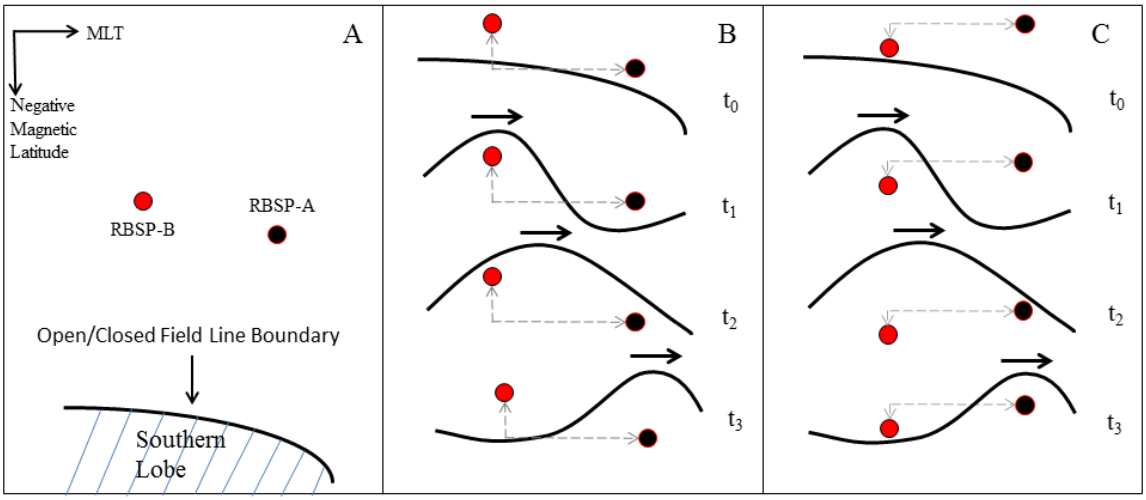

Figure 13: Diagram of possible OCB motion during lobe crossing events. A) Diagram is drawn in an MLT vs negative magnetic latitude frame. RBSP-A and RBSP-B are represented by black and red circles respectively. The southern OCB is represented by a black line with the open field lines of the southern lobe below it and the closed field lines of the equatorial region above it. Panels B and C show an expansion of the boundary moving forward in MLT from the tail, with B showing the spacecraft configuration before apogee and C the spacecraft configuration after apogee. B) RBSP-B is closer to the southern magnetic pole than RBSP-A. C) RBSP-A is closer to the southern magnetic pole. For both panels B and C, RBSP-B is always behind RBSP-A in MLT. t_0 – t_4 are four representative time steps used to illustrate the motion of the boundary: t_0 - neither spacecraft is within the lobe. t_1 – the expansion on the OCB has arrived at RBSP-B and it is not within the lobe. t_2 – the expansion of the OCB now covers both spacecraft. t_3 – the expansion of the OCB has passed RBSP-B and it is now outside the lobe, RBSP-A is still within the lobe.

Open Closed Field Line Boundary distances calculated using CRCM + BATS-R-US have shown some correlation with what is observed by the Van Allen Probes and LANL spacecraft. For the three spacecraft in the dawn sector (RBSP-A, RBSP-B and LANL-97A) periodic movements of the boundary towards the spacecraft are observed which coincide fairly well with the times of the lobe encounters. This approach and then retreat of the boundary is seen for both the northern and southern lobes simultaneously. This implies that this disturbance of the boundary is a global phenomenon where the expansion of each lobe is being driven by the same source. The model shows the polar caps widening and narrowing in concert, not as expected for the B_y effect. An alternate explanation is that reconnection across the front of the magnetosphere can remove closed flux from both hemispheres symmetrically.

There is an overlying trend in the MHD model prediction of the distance to the lobe for the dawn spacecraft where independent of the periodic motion of the boundary there is a gradual approach of the boundary, from approximately 3 R_E away at 0100 UT to only 1 R_E away by 0400 UT. The OCB then retreats suddenly at around 0430 with the distance to the lobes rising from ~1.0 to 3.5 R_E and ~0.4 to 1.8 R_E, for the northern and southern lobes respectively. The spacecraft data does not agree with this trend, observing lobe encounters while the model puts the boundary > 1 R_E and also showing no variation in the length or strength of the events which correlates with this gradual approach of the boundary. A possible explanation for this trend in the model data is the increase and then rapid decrease in solar wind proton density seen by ACE during the events which peaks around 0400 UT would cause a compression of the magnetosphere, bring the lobes down to lower latitudes, and make them more accessible to spacecraft.

The two spacecraft in the southern dusk sector observed lobe encounters of much greater length than those seen in the dawn sector, with the largest being event 8 seen by LANL-080 which lasted 50 minutes. The MHD model prediction of the distance to the lobe for these spacecraft show a very different picture to that seen in the dawn sector. For the three events that occur before 0400 UT (8, 9 and 11) the model puts the spacecraft either very close to or inside the lobe, but with no correlation between the actual lobe crossing times and when the spacecraft crosses the boundary in the model. The MHD model predictions of the distance to the lobe do show that the spacecraft would have access to the lobe during this period, even if it does not show a movement of the boundary for each event.

At approximately 0345 UT the MHD model prediction of the distance to the lobe for both spacecraft rapidly increases to 3.4 and 1.3 R_E for LANL-080 and LANL-01A respectively. This coincides with a change in direction of IMF B_y seen by ACE, which according to the model proposed by *Moldwin et al*. [1995] would reverse the direction in which the lobes are skewed and cause the southern dusk section of the magnetosphere to have less access to them. Events 10, 12, 13 and 14 all occur after this retreat of the OCB away from the spacecraft, despite the model putting LANL-080 more than 3 R_E away from the lobe. Interestingly there is a clear movement of the boundary towards

the spacecraft for the two events seen by LANL-01A which match the event times very well. There are movements of the boundary for the events seen by LANL-080 but they are not as well defined and do not correlate with the spacecraft event times.

3.5 Chapter Conclusion

Between 0200 and 0515 UT on November 14th 2012 the twin Van Allen Probes observed particle dropouts consistent with crossing the open-closed boundary from closed field lines onto open lobe field lines. The events occurred on the flank between 4 and 6.6 local time and at altitudes between 5.6 and 6.2 R_E. The events occurred during the main phase of a geomagnetic storm while Dst was less than 100nT with the IMF being strongly southward (B_z = -15nT) and eastward (B_y = 20 nT). Observations at geosynchronous orbit also show lobe encounters at the dawn and dusk flanks.

The two spacecraft configuration of the Van Allen Probes is used to constrain the spatial and temporal characteristics of each lobe encounter, allowing analysis of the OCB dynamics during this unique event. We found the lobe encounters were the result of the boundary moving over the spacecraft, with a scenario where a local expansion of [disturbance on?] the OCB propagating from the tail and travelling over the two spacecraft fitting the observations best.

These events have provided a chance to examine the global magnetic field topology in detail using multiple spacecraft and compare it to a global MHD model. The models attempt to reproduce the closed and open magnetic field line topologies at the location of the spacecraft. Qualitatively, the models show good correlation with a varying boundary location near the spacecraft during this time period. A new technique has been developed to quantitatively assess the model boundary's distance from the spacecraft, which can then be compared to the times at which they are observed entering the lobe. This technique found that the model reproduces the motion of the boundary towards and away from the spacecraft at times similar to the events but overestimates the overall distance between the OCB and the spacecraft by as much as 3 R_E, which is significant compared to the model's resolution of 0.125 R_E. This implies the model is correctly reproducing the dynamic processes which are causing

the OCB to approach and retreat from the spacecraft but does not accurately map the global topology of the magnetosphere.

The measured magnetic field signature shows significant stretching and drastic changes in orientation. The measured field vectors are also compared to the CRCM + BATS-R-US model's prediction of magnetic field strength and direction. There are often significant differences which can be roughly summarized that the model field is not flattened (in the y direction) and dynamic enough. Common tools like Tsyganenko models are built from average behavior and are not suitable for these times.

This event illustrates the complexities which should not be underestimated of understanding dynamic large scale topologies during geomagnetic storms. Such difficulties underlie our field; multipoint measurements and a systems approach are necessary to gain understanding. Such efforts are required to correctly interpret magnetosphere-ionosphere coupling and underlying mechanisms of ion outflow as well.

4. VAN ALLEN PROBES LOBE ENCOUNTER SURVEY

A survey of Van Allen Probe data was performed over a two year period from October 2012 – October 2014. During this time the twin spacecraft's orbits have precessed around the entire equatorial plane, sampling the magnetosphere at near geosynchronous orbit for all MLTs and in both the northern and southern hemispheres. This allows a survey to examine the distribution of magnetospheric lobe encounters spatially, in MLT and magnetic latitude, as well as comparing their frequency to factors such as IMF conditions and substorm occurrences.

The aim of the survey was to continue the analysis of the underlying causes and dynamics of flank lobe encounters, which began with the case study of the November 14th 2012 event. This series of quasi-periodic lobe encounters were characterised by rapid dropouts of energetic particle fluxes which recovered minutes later as the spacecraft crossed the open-closed field line boundary into the lobe and then back again. Magnetometer data from the Van Allen Probes showed a sharp increase in magnetic field strength and a flattening of the field in the x-y plane concurrent with the flux dropout, which relaxed back to its previous configuration as the flux recovered. Analysis of multiple lobe encounters allows us to discover whether the unusual characteristics of the November 14th event are specific to it or if they are endemic of lobe encounters.

Solar wind conditions prior to lobe encounters are also of great interest, with previous research indicating that both strong IMF By and strong southward IMF can produce changes in magnetospheric topology that make the lobes accessible to spacecraft near geosynchronous orbit. Analysis of data from the ACE spacecraft was performed to attempt to identify consistent trends in the solar wind behaviour. Oxygen-rich, field-aligned ion outflows were observed by the Van Allen Probes during the November 14th event and were present on both open and closed field lines. The exact nature of these outflows is currently unclear and this survey aimed to discover whether they are truly associated with lobe encounters either as symptoms of a larger process or resulting from certain combinations of solar wind conditions and other factors. The frequency of these ion outflows are

compared to that of lobe encounters in different regions of the magnetosphere and ion compositions before and after each event are examined.

Moldwin et al [1995] defined two types of lobe encounter, those occurring around local midnight and those occurring on the flanks of the magnetosphere. Those observed near midnight are associated with a thinning of the plasma sheet during the substorm growth phase, which brings the southern lobe northward and the northern lobe southward, towards the equatorial plane. This makes the lobes accessible to spacecraft in this region and can result in dropouts of varying length depending on the position of the spacecraft. Once the substorm injection has occurred the lobes relax back to higher latitudes and the spacecraft should return to the closed field lines of the inner magnetosphere. Flank lobe encounters are less well understood, with the lobes being brought down to lower latitudes, becoming accessible to spacecraft at or near geosynchronous orbit.

4.1 Survey Methodology

Medium energy (~30 keV – 4 MeV) electron data from the MagEIS instrument will be used primarily to identify flux dropouts. A plot for each day will be examined by eye using the PNGWalk functionality of the Autoplot tool, which allows you to search through a series of summary plots made by the RBSP-ECT team. Any suitable looking events are added to a "first pass" list. Days which have been selected for further examination then have a customisable plot object created in Autoplot containing MagEIS electron and proton data, as well as magnetic field strength from the EMFISIS magnetometer. This allows us to check if the dropouts are also seen for the protons and also if there is an accompanying rise in magnetic field strength mirroring the flux dropouts.

4.1.2 EXAMPLE EVENT: 2013-06-07

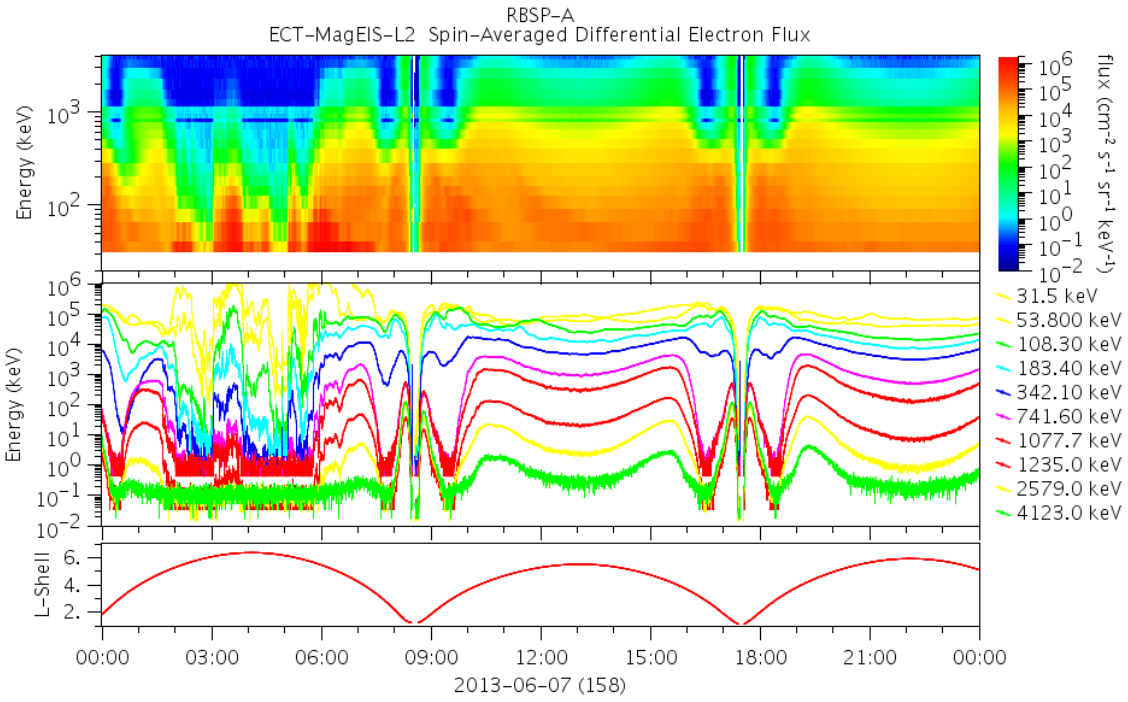

Figure 14: Spin averaged electron flux data from the MagEIS instrument aboard RBSP-A for June 7th 2013. The top and central panels show the electron fluxes as a spectrogram and as separate channels. The bottom panel describes the spacecraft's orbit in L-shell. The period of interest is between 0200 – 0600 within the first orbit of the day, where there are clear flux dropouts and particle injections.

Figure 14 shows an example of one of these lobe encounter candidates, observed by RBSP-A on 2013-06-07. It can be seen that during the first orbit there are complete dropouts of electron fluxes, partial dropouts and also some strong particle injections. Figure 15 shows continues the analysis of the example event shown above, having zoomed in to just show the period of interest. The four panels show electron fluxes, proton fluxes, magnetic field strength and electron flux for the 183.4 keV channel; chosen to give a more distinct visual of the beg inning and end of each dropout. Unfortunately the changes in magnetic field strength are small compared to the parabola trend caused by the spacecraft's orbit so it becomes necessary to zoom in further and examine each apparent dropout individually.

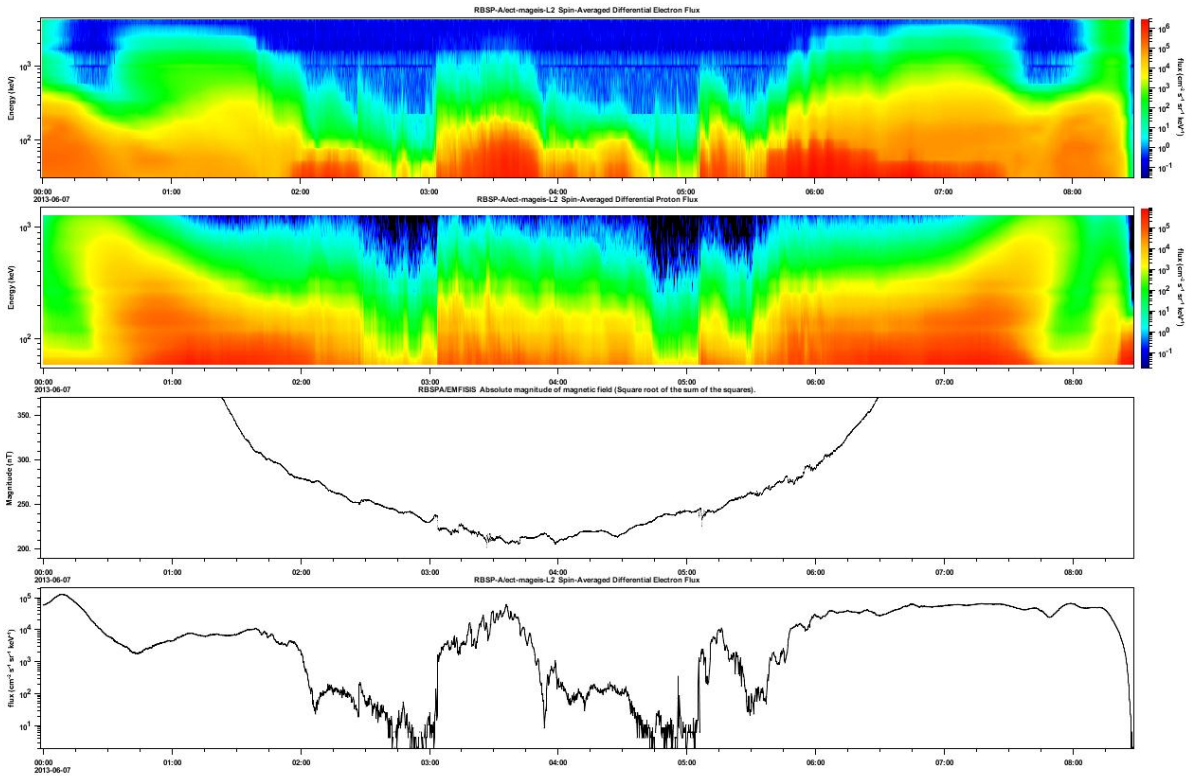

Figure 15: MagEIS and EMFISIS data for the first orbit on June 7th 2013. Panels 1 and 2 show electron and proton fluxes from MagEIS. Panel 3 shows magnetic field strength from EMFISIS and Panel 4 the 183.4 keV electron channel for MagEIS. There are two clear periods of complete flux dropout beginning at approximately 0230 and 0445, as well as longer partial flux dropouts, which are accompanied by corresponding increases in magnetic field strength.

Figure 6 shows the period containing the first dropout between 0220 and 0310, where the flux begins to drop out at about 0230, reaching a minimum at 0243 before recovering briefly and then decreasing back to background levels before a sharp increase in flux occurs, most likely a substorm injection. It can be seem in the third panel that the magnetic field strength increases as the flux drops out, though the overlying downward trend of the magnetic field strength as the spacecraft reaches apogee can make it hard to discern. In this example the dropout is considered to have started from the point where the magnetic field strength sharply increases and the electrons begin to drop out to where the magnetic field relaxes and the injection occurs.

This example raises a few interesting points regarding the classification of events in this study and how their characteristics are recorded. The gradual decrease in flux is very different to the sharp dropout seen for the November 14th event. This is most likely a result of the lobe slowly expanding

towards the equatorial region as the plasma sheet is compressed during a substorm growth phase. Once the expansion phase begins and energetic particles are injected into the inner magnetosphere the lobe retreats rapidly, with the OCB passing over the spacecraft and in-situ observations returning to those typical to a region of closed field. The intensification of magnetic field strength just prior to the end of the dropout is also consistent with the onset of a substorm injection. The increase of particle fluxes and reduction in magnetic field strength between approximately 0245 and 0250 raises a question of whether a brief recovery should be defined as the end of the first dropout and the start of a new one or if the whole period of contact with the lobe should be taken as a single event. The length of the recovery compared to that of the entire event is important here, being around 15% of the total event duration. This is justification to consider the whole event as a single dropout, with the brief recovery just a consequence of the OCB being non-static and subject to localised turbulence. For an event where for example there were two dropouts lasting ten minutes each separated by a "recovery" of thirty minutes, they would be considered as two separate events, which was the case for November 14th where the dropouts were typically less than ten minutes long and occurred roughly every forty-five minutes.

Using this methodology a total of one hundred lobe encounters were identified by the two spacecraft, over a total of forty-four different days. Lobe encounter events were observed in both hemispheres, across the entire night side of the magnetosphere, and in varied solar wind and geomagnetic conditions.

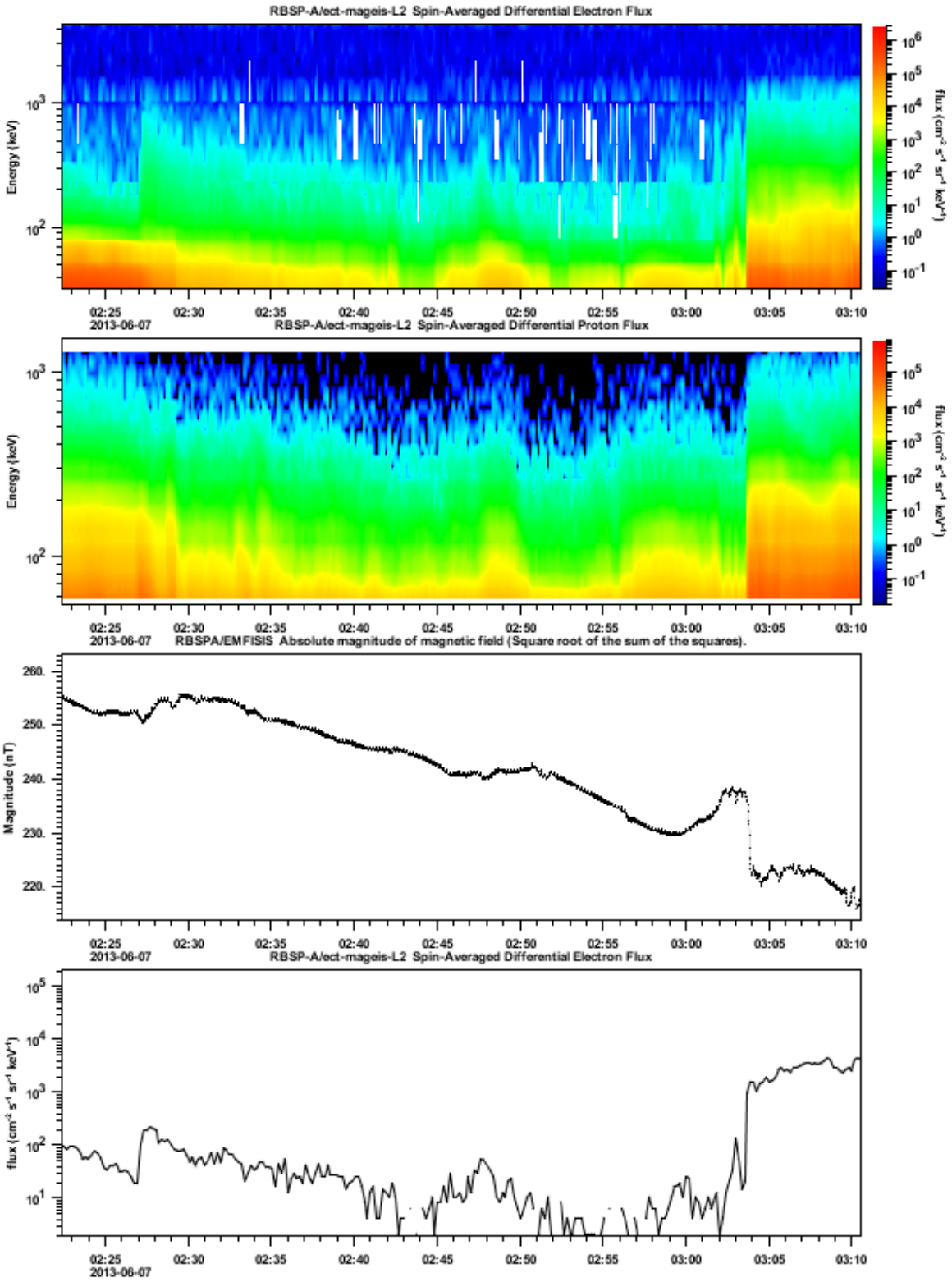

Figure 16: RBSP-A MagEIS and EMFISIS data for the first flux dropout event on the 7th June 2013. The flux begins to drop out just before 0230, dropping to near background levels until 0304 where there is a sharp recovery in flux. The magnetic field strength (Panel 3) shows a corresponding increase, intensifying at 0300 before dropping sharply at 0304 as the spacecraft re-enters the lobe

4.2 Lobe Encounter Survey Results

4.2.1 Unfiltered distribution of events in MLT and magnetic latitude

Figure 17 shows the distribution of the events in MLT for both spacecraft. The centre of the plot shows the orbits on which the lobe was encountered, with the period of lobe entry marked by a solid box. The outer plot is a histogram binning the events by which 6 hour MLT sector (0-6, 6-12, 12-18 and 18-24) their mid-point occurs in. At first glance it is clear that the vast majority (94%) of the events happen on the night-side of the magnetosphere with a slight preference for the

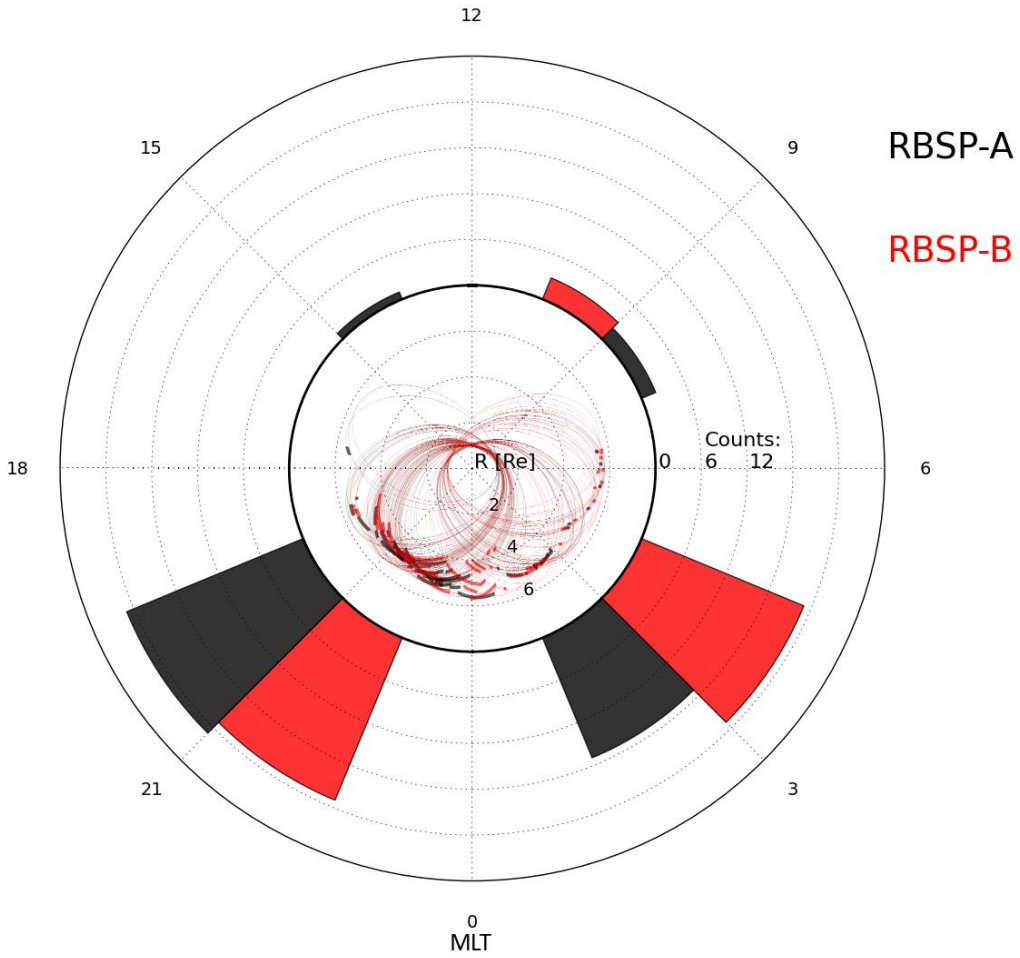

Figure 17: The inner circle is a polar plot of MLT vs altitude (R_E) displaying the orbits (thin lines) and lobe encounters (thick boxes) for RBSP-A and RBSP-B over a two year period from October 2012 – 2014. The outer circle is a histogram binning the events based on which region of the magnetosphere they began in. There is a slight preference for events in the pre-midnight sector (51%) compared to post midnight (43%), with six of the events occurring just inside the dayside.

dusk/pre-midnight sector (51%), over the dawn/post-midnight sector (43%) . The thicker clustering of event boxes in this region is also a result of events occurring in this sector appearing to have longer durations, giving larger boxes and giving the impression of a much greater number of events than in the morning sector when the difference is only 8%.

Figure 18 shows the one-hundred events distributed in MLT and magnetic latitude – derived using the TS04 model and obtained from RBSP-ECT ephemeris files. On the left hand side of the figure a histogram has been overlaid, binning the events in twenty degree intervals (0-20, 20-40 etc.). Similarly to the polar plot above the orbits on which events occurred are plotted with the actual times of lobe entry highlighted by shaded boxes. The x-axis has been shifted so that midnight – the region around which most of the events are clustered – is in the centre of the plot. The first thing to note from this figure is that none of the events occur at magnetic latitudes lower than $\pm 20^{\circ}$, which is consistent with the OCB expanding down to lower latitudes and encountering the spacecraft. It is also likely a product of the orbital configuration of the spacecraft; their tilted orbital path means they move to higher magnetic latitudes as they reach apogee, making them more likely to encounter the lobe. It is also apparent from this figure that the majority of events occurred in the south-dawn and north-dusk regions of the magnetosphere and were mostly clustered fairly close to midnight. It is possible that this preference for south-dawn and north-dusk is the result of there being increased geomagnetic activity when the spacecraft are in certain regions of the magnetosphere. For example, the majority of the events happened in either winter 2012/2013 or summer 2013, periods where the spacecraft was in the south dawn and north dusk regions respectively.

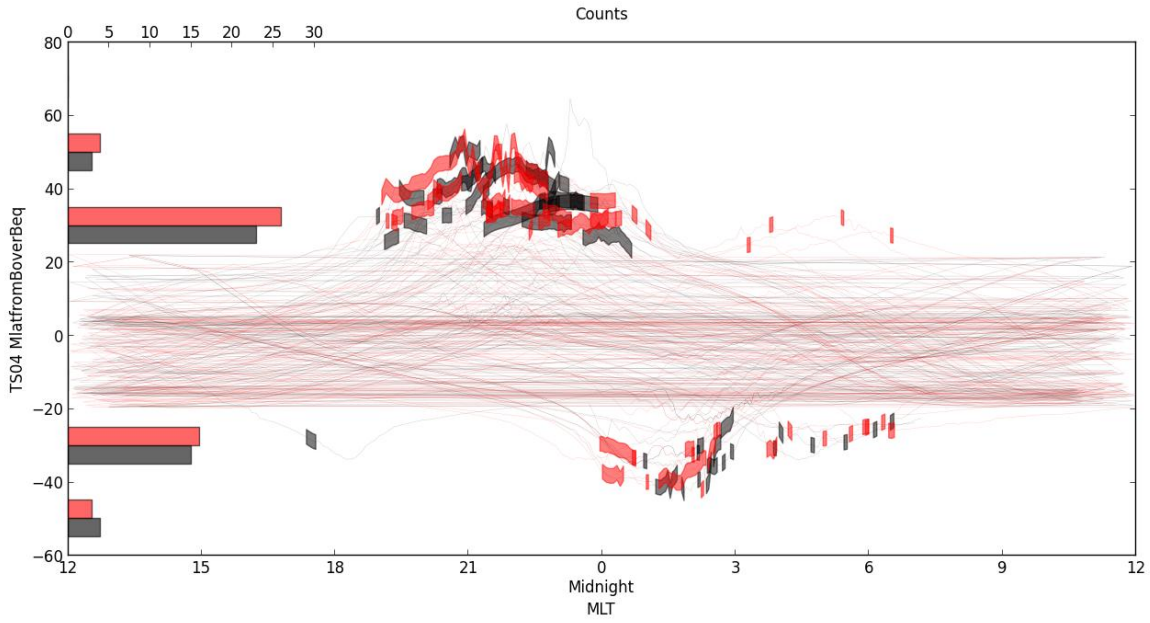

Figure 18: MLT vs Magnetic Latitude (based on TS04) for lobe encounter events. Orbits of spacecraft are displayed as thin lines, lobe encounter events as thick boxes. On the left hand of the plot is a histogram, binning the data in bands on 20 degrees of magnetic latitude. There is a clear preference for the northern hemisphere and also for events to occur in either the north-dusk or south-dawn regions.

A first look at the distribution in Dst of the events is given in Figure 19, which is arranged in the same manner as the previous Figure but with Dst on the y-axis. The peak of the distribution is at low Dst with 28% of events occurring in the 0 to -20 Dst band and 21% in the -20 to -40 band. If we consider all the events with Dst lower than -40, which can be considered at least a weak geomagnetic storm then we get a total of 44% of the sample occurring in these conditions. Considering the general paucity of geomagnetic storms during the period examined, having this proportion of events occurring during one agrees with previous work [*E.g. Kopanyi & Korth,*. 1995] that the likelihood of lobe encounters increases during a storm. The large number of events that occurred during periods of weak Dst also implies that even if geomagnetic activity increases the frequency of spacecraft entering the lobe, it is not a requirement.

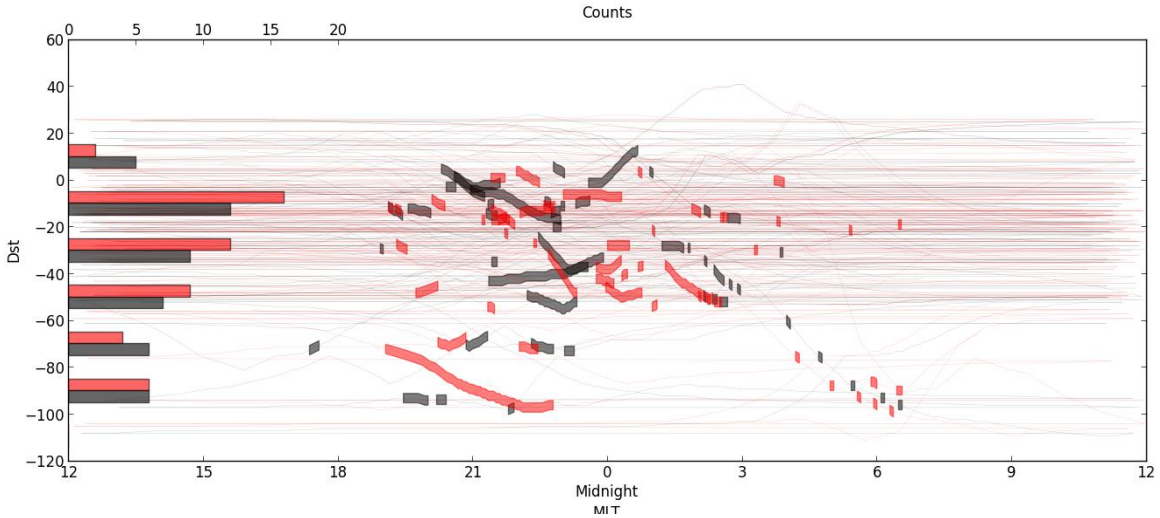

Figure 19: MLT vs D_{ST} index for lobe encounter events. Events occurring during a storm do not appear to prefer an particular region of the magnetosphere. Distribution of events peaks at low (> -40) D_{ST} but there are still a significant number of events during stormier periods.

4.2.2. Substorm Associated Events

One of the subsets recorded in the survey was of lobe encounters that were associated with injections of energetic particles. This includes events that were ended by an injection – similarly to the 2013-06-07 example shown previously – and also those which had particle injections occurring within the same orbit. The aim here is to see if there is a preference for substorm related events in certain regions and to see if this explains any of the trends seen in the unfiltered results.

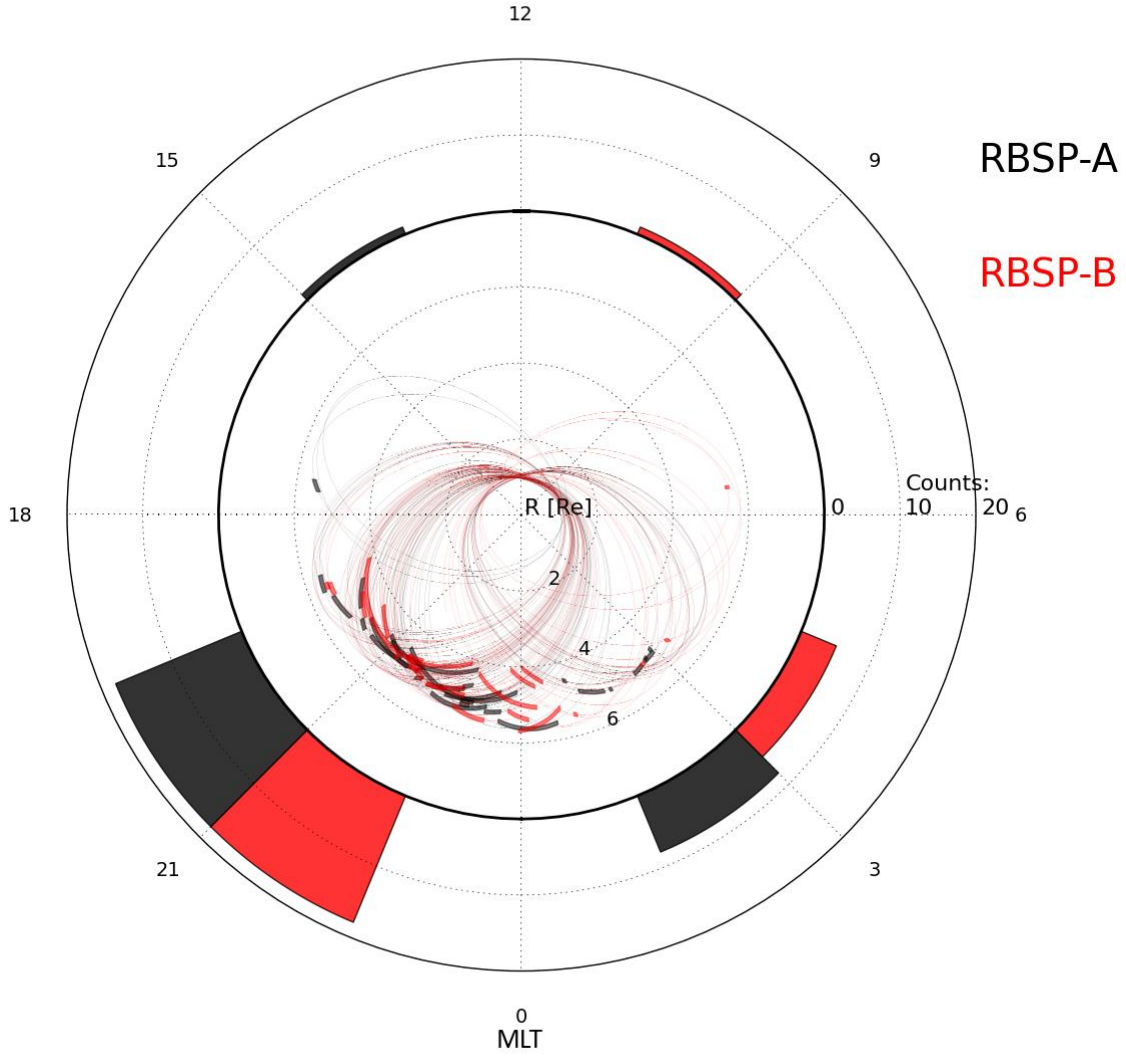

Figure 20: MLT vs altitude for the lobe encounter subset where the events were associated with an energetic particle injection. There is a clear preference for the post-midnight sector with thirty six of the events (71%) of occurring in this region.

In total 51 of the lobe encounter events were associated with a particle injection, with the majority (36) occurring in dusk (18-00) sector. There were thirteen events observed in the dawn (00-06) sector and just two on the dayside of the magnetosphere, both of which occurred within one hour of MLT from the day/night line. The lobe encounters in the dusk sector were significantly longer in duration than those occurring elsewhere. These long flux drop outs mostly occur with a gradual decrease in flux, accompanied by an increase in magnetic field strength mirroring the flux signal. The events then usually end with a very sharp increase in flux and relaxation of the magnetic field as the spacecraft observes an injection of energetic particles. These types of lobe encounters are associated

with stretching of the near-Earth magnetic field, leading to thinning of the plasma sheet, during a substorm growth phase. This brings the lobes down to lower latitudes, into the range of the Van Allen Probes orbits and causing it to enter the lobe for relatively long periods compared to those seen for the November 14th 2012 events, which occurred on the flank.

4.2.3 Dependence of events on IMF B_Y

Geosynchronous lobe encounters have been previously linked to extreme IMF conditions, which lead to large scale reconfigurations of magnetosphere geometries [*Thomsen et al*., 1994]. Using the Tsyganenko T87 model, the occurrence of these events during very strong IMF By has been previously simulated [*Moldwin et al*., 1995] to show what the expected magnetic field topology should be during these conditions. An asymmetry was found in the magnetic field configuration which predicts that regions of open field lines should be brought closer to geosynchronous orbit for northern dawn and southern dusk sectors for positive B_y, and southern dawn and northern dusk for negative B_y.

Table 2: Distribution of lobe encounter events for IMF By positive and negative subsets.

	MLT Sector				**Magnetic Latitude**	
IMF By Polarity	**0-6 (Dawn)**	**6-12 (Morning)**	**12-18 (Afternoon)**	**18-24 (Dusk)**	**Southern Hemisphere**	**Northern Hemisphere**
Negative	31 (52%)	5 (9%)	0 (0%)	23 (39%)	31 (53%)	28 (47%)
Positive	12 (29%)	0 (0%)	1 (2%)	28 (68%)	12 (29%)	29 (71%)

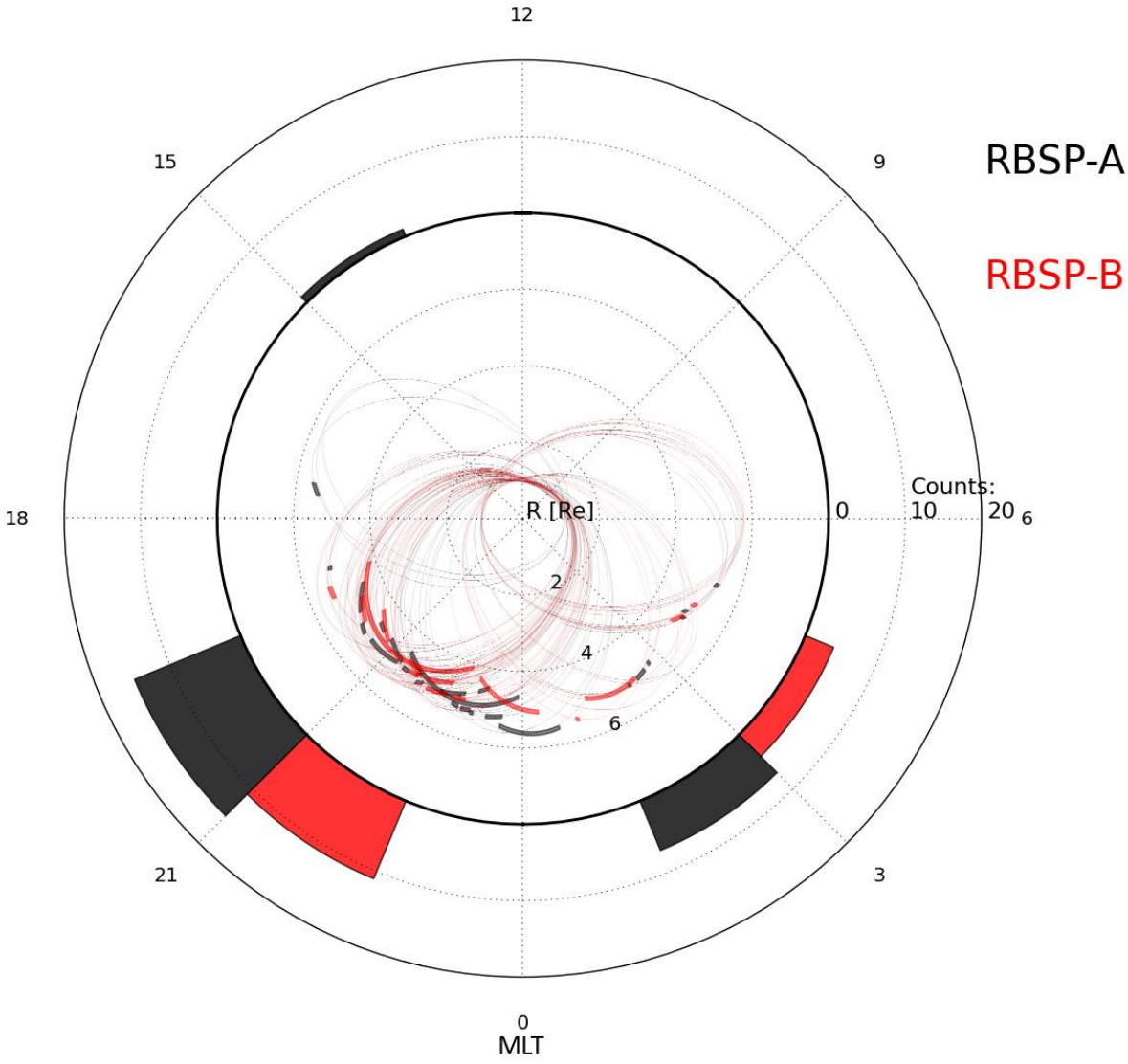

Figure 21: MLT vs altitude for the lobe encounter subset where the events occurred during positive IMF By. The majority of events (68%) occurred in the dusk/pre-midnight region.

To examine this link, the survey events have been split into two subsets depending on whether they occurred during positive or negative IMF By, with a total of 41 and 59 events for each subset respectively. Figures 21 and 22 show the distributions in MLT and magnetic latitude for the positive By events, and Figures 23 and 24 show those for the negative By events. Table 2 summarizes the distributions in terms of MLT sector and magnetic latitude hemisphere.

The positive IMF By subset appears to show a clear preference for events occurring in the dusk/pre-midnight sector, with 68% of events occurring in the 18-24 MLT range. The majority of the remaining events (29%) took place in the morning/post-midnight sector, between 0 and 6 MLT, with a single event observed just inside the afternoon (12 – 18 MLT) sector at about 17.5 MLT. Examination

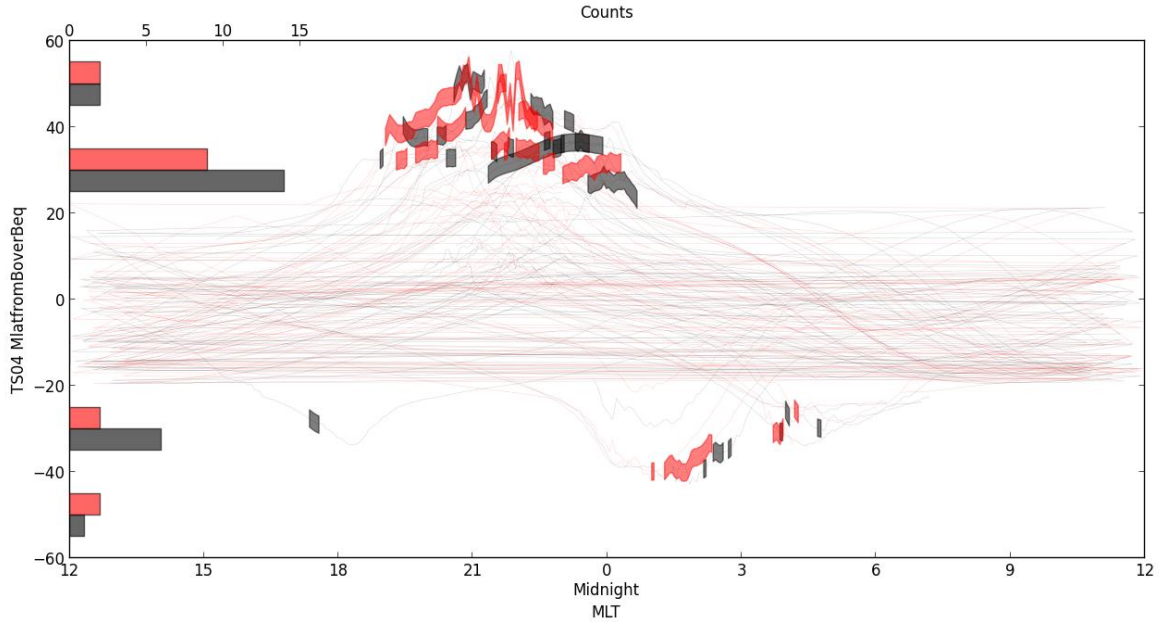

Figure 22: MLT vs Magnetic Latitude plot for the lobe encounter subset where the events occurred during positive IMF By. Majority of events observed in the north-dusk region of the magnetosphere.

of the magnetic latitude data shows an even stronger preference for events in the northern hemisphere, with 71% occurring north of the magnetic equator. The negative IMF By subset has a majority of events (52%) occurring in the dawn/post-midnight sector with a smaller but significant proportion (39%) observed in the dusk/post-midnight section. There were also five events (9%) in the morning (6 - 12 MLT) sector, but it can be seen in Figure 23 that these events all occur between 6 and 7 MLT, just inside the range. There is a slight preference towards encountering the lobe in the southern hemisphere (53%), which does not at first seem significant.

It is worth considering the overall distribution of the whole, non By-filtered sample at this point, where 43% of events occurred in dawn sector, 51%% in the dusk sector, 43% in the southern hemisphere and 57% in the northern hemisphere. This allows us to look at the distributions from a different viewpoint, calculating what proportion of the total number of events in a sector happened in

IMF By positive or negative. From this we can calculate that for the southern hemisphere, 72% of events occurring during negative IMF By and only 28% during positive By. For the northern hemisphere the split is effectively 50/50, with 28 events for negative By and 29 for positive By.

These results do not fully agree with the predictions made in by *Moldwin et al.* [1995], with positive By appearing to prefer northern dusk, rather than northern dawn or southern dusk, as predicted in the Tsyganenko T87 model. The negative By results seem to have better agreement with the prediction, showing a slight preference for southern dawn. When we consider the greater number of northern hemisphere events in total, the tendency towards the southern hemisphere in the negative By subset becomes more significant, representing 72% of the total number of southern events. This also weakens the result for the positive subset where the seemingly large number of northern hemisphere observations (71%) is inflated by there being a higher number of such observations overall. This leaves us with a relatively good agreement between the prediction and the survey results for By negative, which preferred south/dawn and an some disagreement for By positive, which shows a weak preference for north dusk.

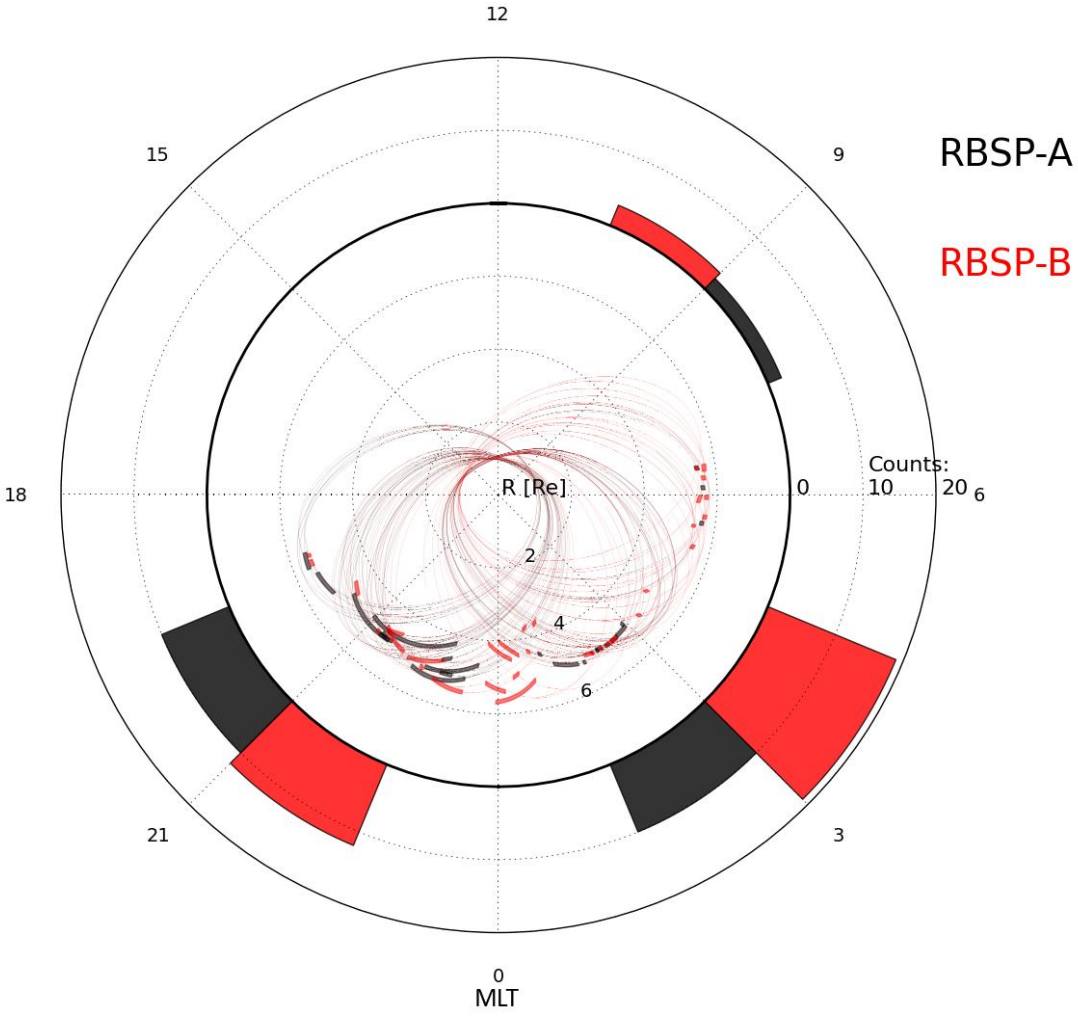

Figure 23: MLT vs altitude for the lobe encounter subset where the events occurred during negative IMF By. The majority of events (52%) occurred in the dawn/post-midnight region.

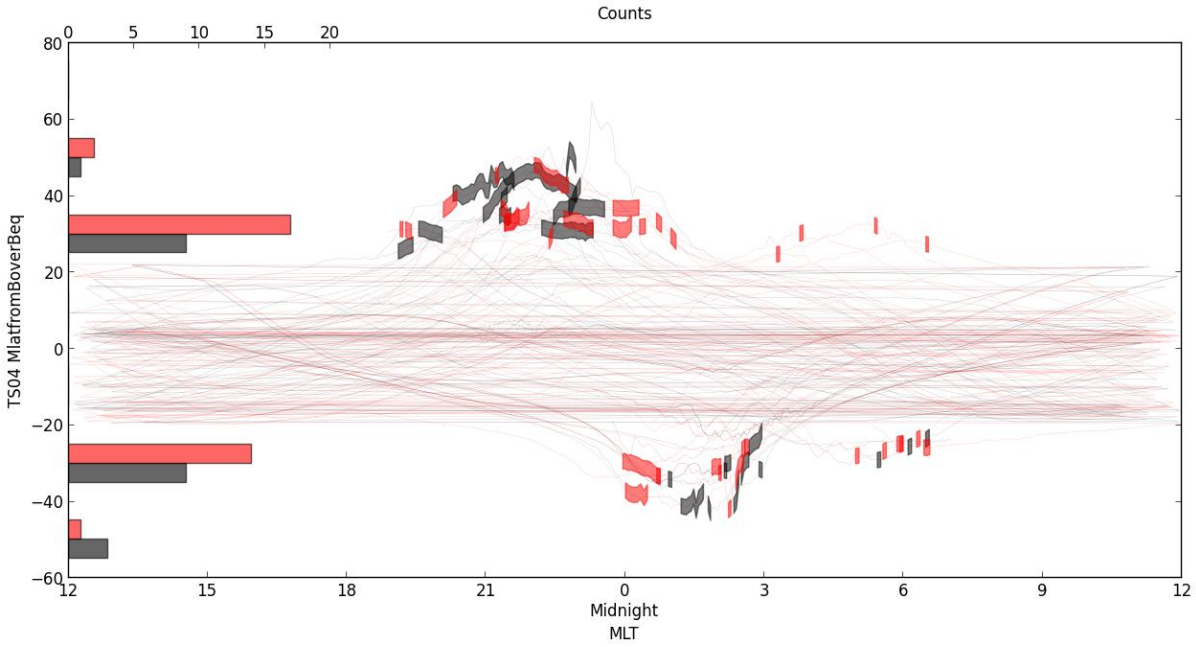

Figure 24: MLT vs Magnetic Latitude plot for the lobe encounter subset where the events occurred during negative IMF By. Very slight preference for events in the south-dawn region, though these events appear to be of relatively short duration.

4.3 SUPERPOSED EPOCH ANALYSIS (SEA) OF LOBE ENCOUNTERS

The case study of the November 14th 2012 events highlighted certain characteristics in the behavior of the Interplanetary Magnetic Field (IMF) and the local field observed by the EMFISIS instruments aboard the Van Allen Probes. To what extent these observations are unique; either to this set of events or flank lobe encounters as a whole is worthy of further analysis. To do this Superposed Epoch Analysis will be used to try and identify common signatures associated with the IMF conditions preceding these events and the magnetic field topology observed by the Van Allen Probes as they cross the OCB into and out of the magnetospheric lobe.

This technique can also be used to examine the ion composition observed by the spacecraft as they move between the inner magnetosphere and lobe populations. The November 14th 2012 events showed sharp changes in ion composition as the Van Allen Probes moved in and out of the lobes, with fluxes falling to near background levels very rapidly before recovering equally quickly as the

spacecraft reentered the inner magnetosphere. This was typical of the spacecraft moving back and forth between two distinct particle populations, separated by the open-closed field line boundary and should not have resulted in a net change in ion composition. While both inside and outside the lobe the spacecraft observed oxygen rich, energy dispersed ion structures which were most likely accelerated along both the open and closed field lines from an ionospheric source. These ion flows cause an increase in ion fluxes - particularly oxygen - after some of the lobe encounters and it is of interest to see if similar structures are observed during the survey. To examine this SEA will be performed on the number density of particle populations observed by the Van Allen Probes.

These events occurred during the main phase of a moderate geomagnetic storm (minimum D_{st} = -108 nT) and during a period of highly disturbed IMF. Prior to the commencement of the storm ACE detected a C-type CME followed by rapidly fluctuating IMF conditions before a period of very strong, persistent IMF B_y (+20 nT) and a rotation of IMF B_z from northward to southward beginning approximately fifteen hours before the events and remaining southward until a few hours after the lobe encounters ended. Both the strength and orientation of the IMF are of note, with IMF By being at its highest value of 2012 and there being previous work indicating that the direction of IMF By can skew the magnetosphere eastward or westward, increasing the likelihood of lobe encounters in certain regions.

4.3.1 Interplanetary Magnetic Field Analysis

Data from the magnetometer aboard the ACE spacecraft is used here to analyse the orientation of the IMF prior to the lobe encounter events. A window of 24 hours either side of the onset of each event is used for the SEA. Data from both Van Allen Probes spacecraft have been combined into one dataset as there was no clear benefit to analysing them separately.

Initially no filtering of the events was used but this caused two problems for the SEA analysis:

1. For days where there were multiple lobe encounters (e.g. November 14th 2012, which had 10 events across both spacecraft or 10% of the total sample size) their signals were being artificially boosted. Where there was a gap of minutes between events compared to the 48 hour window size of the SEA, the same signal with a small shift in time was being included in the analysis multiple times. To combat this, only the first event from each day was used in the analysis.

2. Events with IMF vectors of opposite polarities cancelled each other out in the SEA, which weakened the overall signal and gave an inaccurate representation of the IMF's behaviour. One option would have been to just take the absolute values but as the direction of each IMF vector was important this was avoided and instead events were split for each B direction into positive and negative subsets depending on their polarity at the epoch.

Removing the repeat data for each day left forty-three datasets to be used across the two spacecraft. Splitting the remaining datasets by IMF vector polarity varied for each direction and the distribution is shown in Table 3.

Table 3: Distribution of lobe encounters based on in-situ magnetic field polarity.

	Negative (%)	**Positive (%)**
Bx	23 (54%)	20 (46%)
By	17 (40%)	26 (60%)
Bz	33 (77%)	10 (33%)

4.3.1.1 IMF Bx

IMF Bx had the most even split of the three directions, being roughly equal in distribution. The SEA for both the positive and negative subsets shows a highly disturbed field, with the signal appearing noisy even after being averaged in the SEA. Only the negative results show anything of interest, with a sharp decrease in Bx just after the epoch, lasting for a couple of hours. This signal appears in both the mean and median, implying that it is not just the result of a strong outlier. Previous surveys of lobe encounters did not show a link between the behaviour of IMF Bx and their frequency, which alongside the general noisiness of the signal and approximately half of the events showing no such signature, implies that it may not be significant.

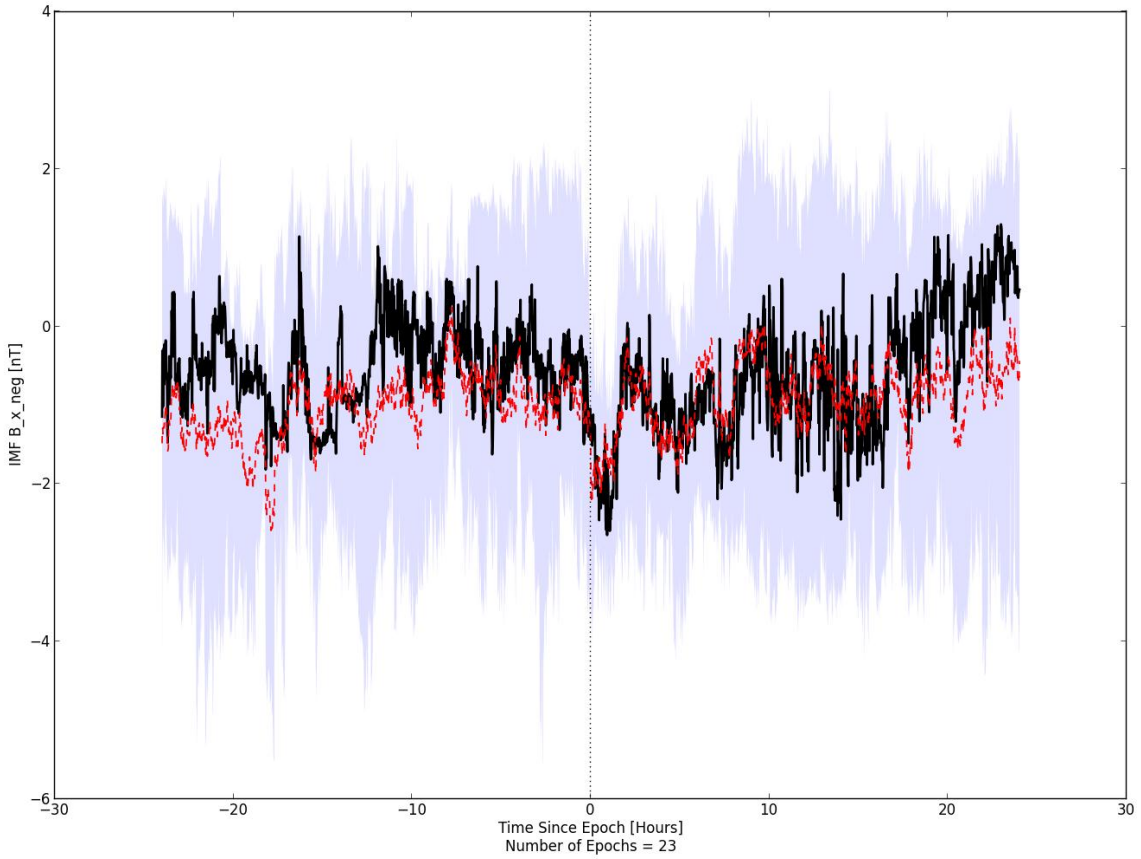

Figure 25: Superposed Epoch Analysis results for the subset of events where IMF B_x was negative at the epoch. SEA window size = 48 hours and epoch defined as the onset of the lobe encounters. Median shown by solid black line, mean by dashed red line and shaded area defines the upper and lower quartiles. The signal in the median and mean noticeably dips by a couple of nT just after the epoch, lasting for a couple of hours.

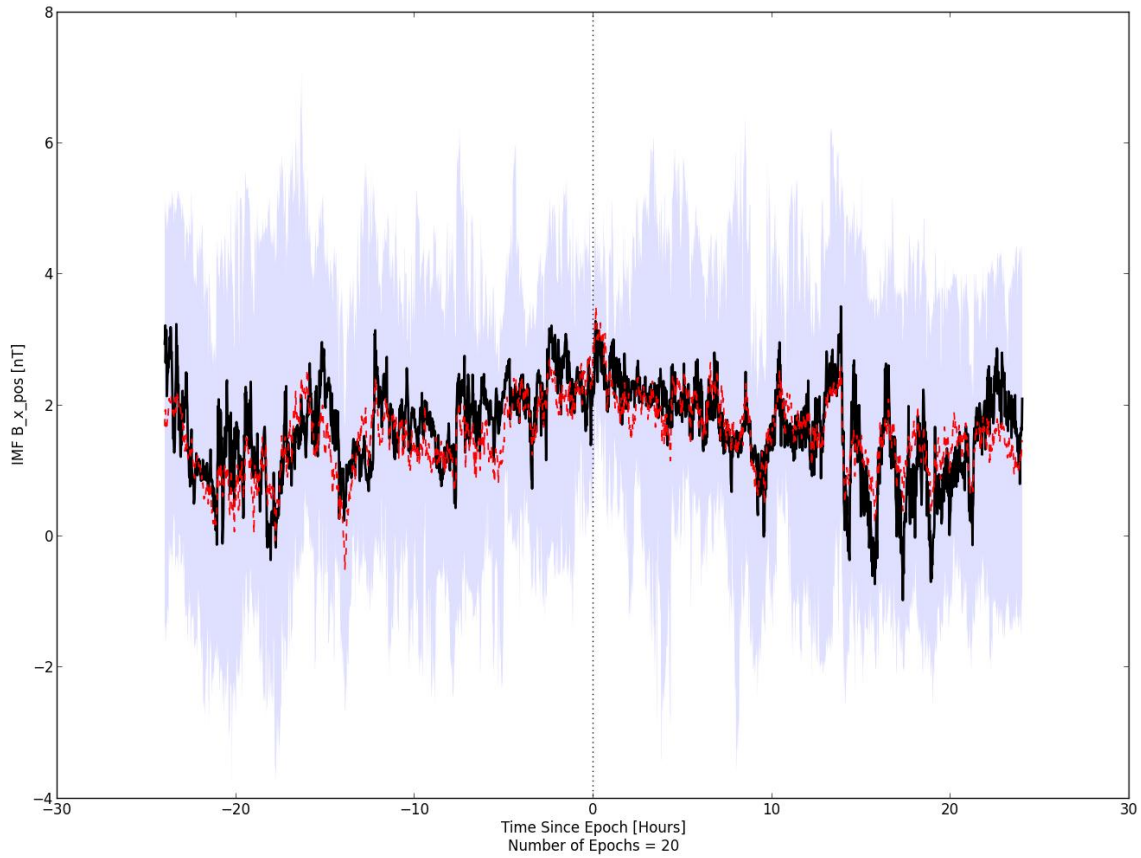

Figure 26: Superposed Epoch Analysis results for the subset of events where IMF B_x was positive at the epoch. SEA window size = 48 hours and epoch defined as the onset of the lobe encounters. Median shown by solid black line, mean by dashed red line and shaded area defines the upper and lower quartiles. There is no clear signal associated with the epoch, though IMF B_x is clearly disturbed during the period surrounding the events.

4.3.1.2 IMF By

Simulations of the magnetosphere model [*Moldwin.*, 1995] during strong IMF B_y found an asymmetry in the magnetic field configuration which predicts that regions of open field lines should be brought closer to geosynchronous orbit during these conditions. Positive IMF By was believed to increase the likelihood of a spacecraft crossing the OCB by bringing the lobe down to lower latitudes in the south/dawn and north/dusk regions and similarly, negative By would have the same effect in the north/dawn and south/dusk regions.

There is a slight preference for events occurring during a period of positive IMF By (60%), though the signal in the SEA does seem to fluctuate between positive and negative prior to the event. This change in direction is less pronounced in the mean than the median, implying that this is at least partially the result of a few events with very strong signatures. For example, the November 14th 2012 events had IMF By as high as +20 nT prior to their commencement. Both the positive and negative subsets seem to show a rotation of the IMF in the y-direction in the day leading up to the epoch, which is consistent with what was seen for November 14th 2012. The field for both subsets is highly disturbed, fluctuating by as much as 4 nT in a relatively short amount of time.

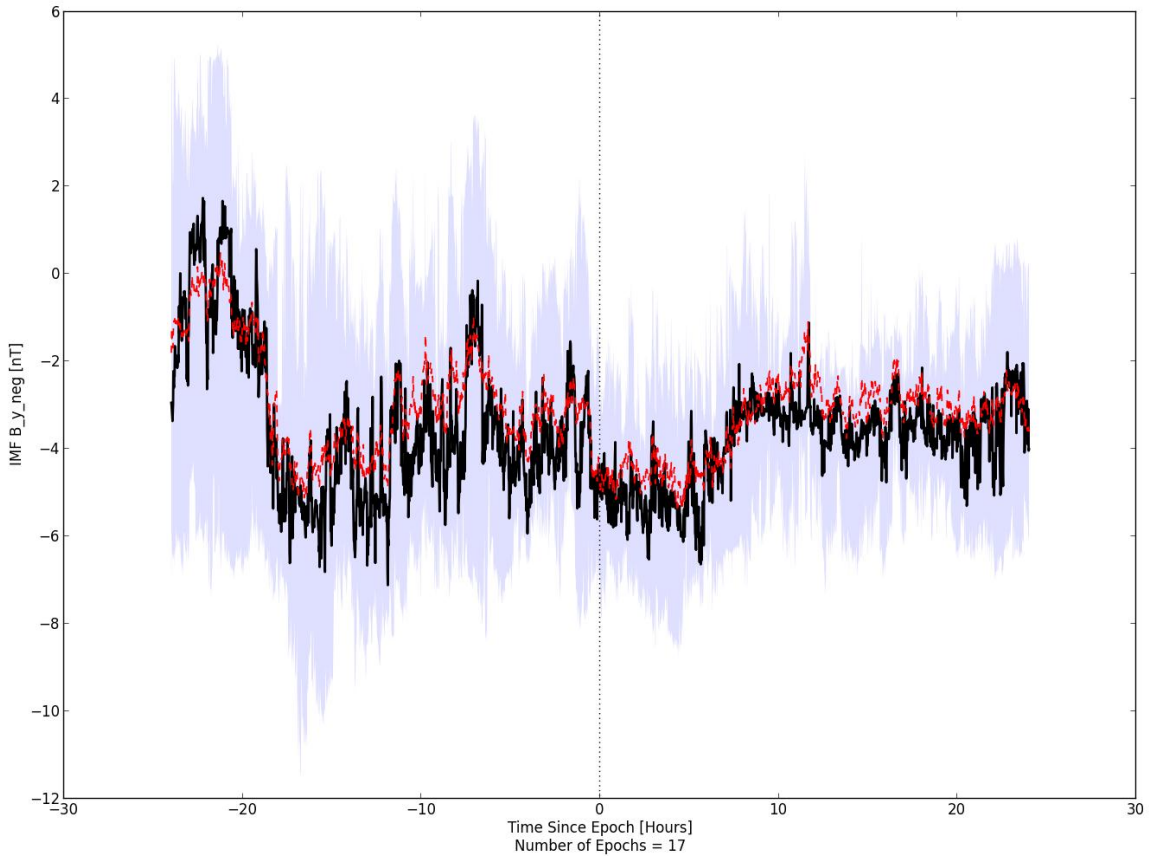

Figure 27: Superposed Epoch Analysis results for the subset of events where IMF B_y was negative at the epoch. SEA window size = 48 hours and epoch defined as the onset of the lobe encounters. Median shown by solid black line, mean by dashed red line and shaded area defines the upper and lower quartiles. There is a clear increase in negative IMF B_y twemty hours before the epoch, remaining negative until the end of the window examined.

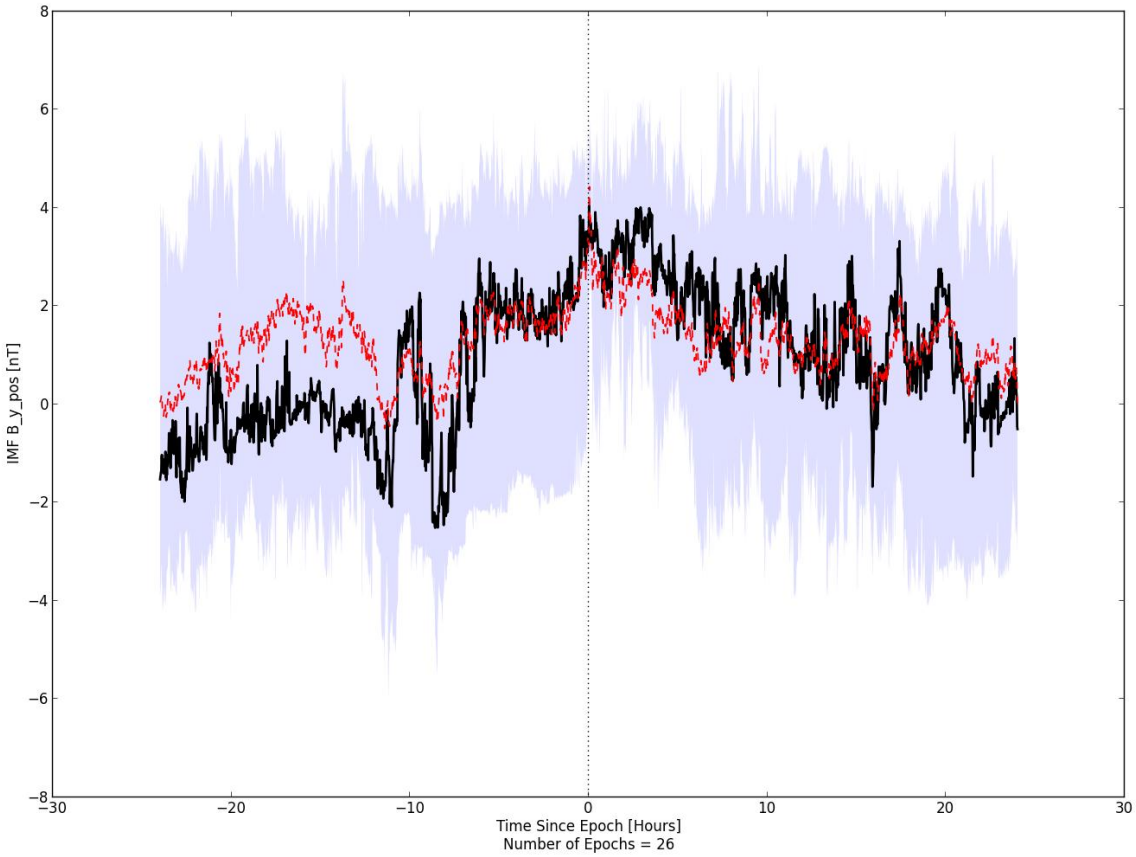

Figure 28: Superposed Epoch Analysis results for the subset of events where IMF B_y was positive at the epoch. SEA window size = 48 hours and epoch defined as the onset of the lobe encounters. Median shown by solid black line, mean by dashed red line and shaded area defines the upper and lower quartiles. IMF B_y is highly disturbed in the twenty hours prior to the epoch, fluctuating between positive and negative. Approximately eight hours before the epoch the B_y component becomes positive and remains that way until fifteen hours after the epoch.

4.3.1.3 IMF Bz

The vast majority of the events occurred during southward IMF Bz (77%), with only a small amount happening during northward IMF Bz (23%). Despite this the two subsets actually show a very similar signature, just with a shift in time. For both there is a period of southward turned By, with the field increasing in strength as it approaches the epoch and then a northward turning of the IMF. For the negative Bz subset this turning appears more gradual and begins just after the epoch, whereas for the positive subset turns much more sharply and a few hours prior to the epoch.

This prolonged southward turning of the IMF is consistent with the growth phase of a geomagnetic storm [ref] before the onset of the expansion phase when the field turns northward. Approximately half of the lobe encounter events occurred within the same orbit as a substorm injection, which came at the end of the lobe encounter and brought the spacecraft back into the inner magnetosphere. This is the result of the plasma sheet thinning and the tail lobe coming down to lower latitudes as reconnection transports flux to the night side of the magnetosphere. When the energy is released in a substorm, the lobes relax back to higher latitudes and the OCB passes over the spacecraft, leaving it in the plasma sheet. This is consistent with the MagEIS flux data for many of the events, which show a substorm injection coinciding with the end of the lobe encounter.

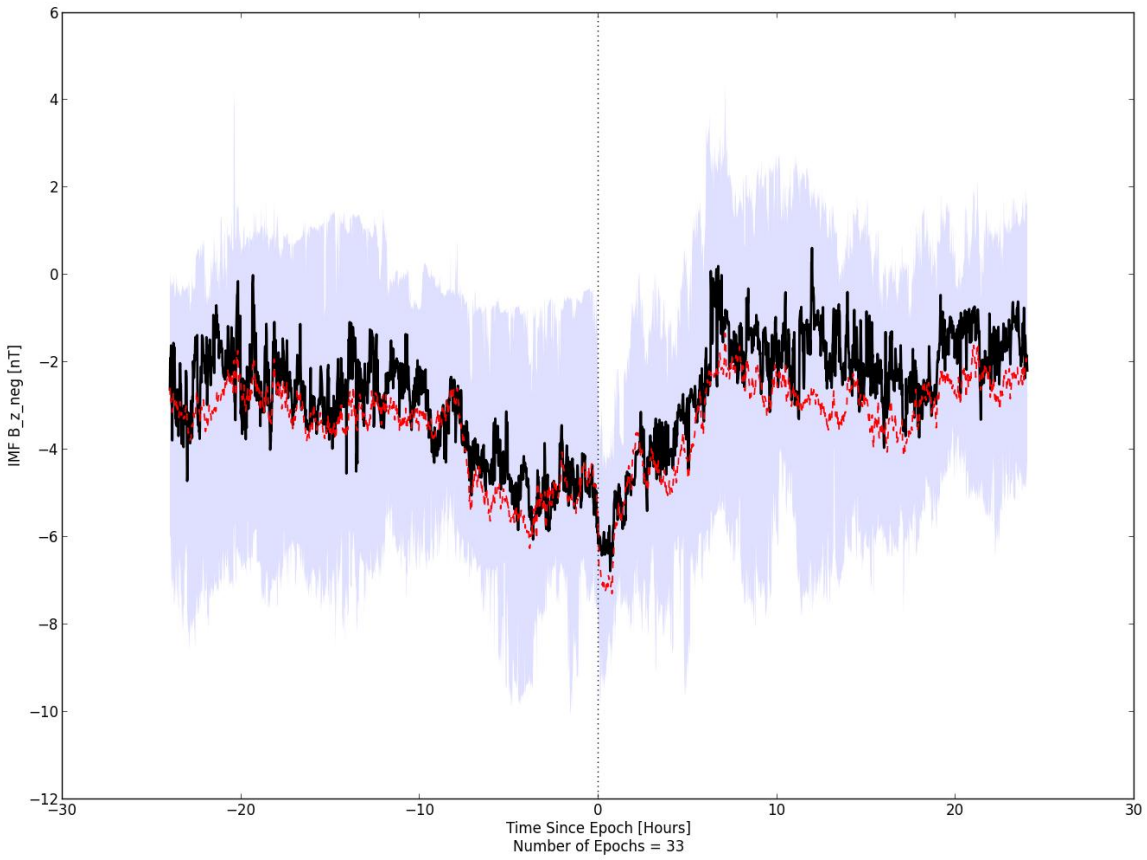

Figure 29: Superposed Epoch Analysis results for the subset of events where IMF B_z was negative at the epoch. SEA window size = 48 hours and epoch defined as the onset of the lobe encounters. Median shown by solid black line, mean by dashed red line and shaded area defines the upper and lower quartiles. IMF B_z is consistently southward before the epoch, intensifying at the epoch and then steadily turning northward afterwards.

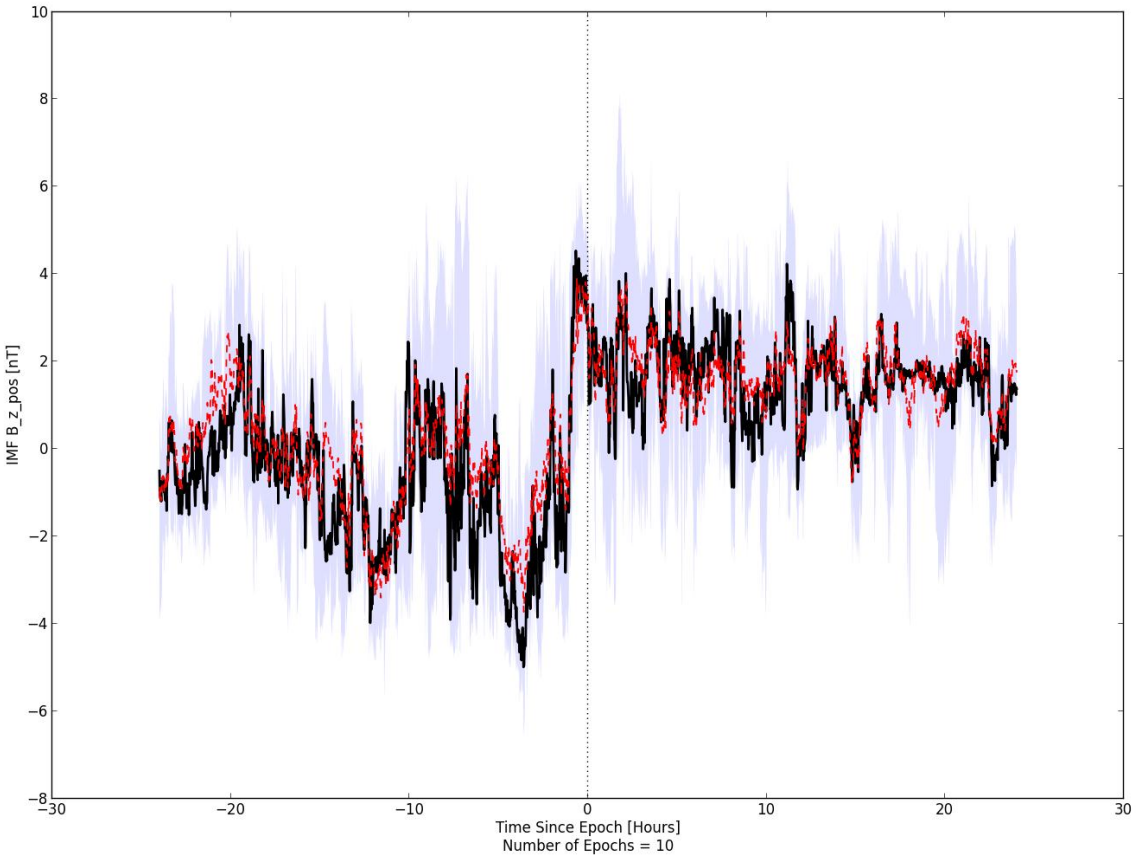

Figure 30: Superposed Epoch Analysis results for the subset of events where IMF B_z was positive at the epoch. SEA window size = 48 hours and epoch defined as the onset of the lobe encounters. Median shown by solid black line, mean by dashed red line and shaded area defines the upper and lower quartiles. IMF B_z is highly disturbed, fluctuating between positive and negative prior to epoch. The signal becomes strongly southward approximately five hours before the epoch before turning sharply northward just before it.

4.3.2 IN-SITU EMFISIS MAGNETOMETER ANALYSIS

The November 14th 2012 events encountered a distinct and consistent magnetic field topology as the spacecraft moved in and out of the lobes. The field inside the lobe was significantly stronger and highly stretched in the positive-x and negative-y direction. The SEA performed here aims to examine if these signatures are consistent across the whole set of lobe encounters surveyed here.

Before the magnetometer data can be used the background field must be removed to account for the orbital effects and isolate the changes associated with the lobe encounters. Similarly to the method used for the November 14th 2012, the expected magnetic field characteristics, which are derived from

the TS04 model and contained in the HOPE ephemeris data, are removed from the EMFISIS magnetometer data for both absolute magnitude and magnetic field vectors.

Because the length of time the spacecraft spend in the lobe can vary greatly for each event, it is necessary to perform SEA twice, with the epoch defined as either the start or the end of the event. This gives a clear signature for the onset and end of the events, regardless of their length. A third plot is created for each magnetic field variable which combines the start and end SEAs together by removing the period of time when the spacecraft is actually inside the lobe to allow us to examine whether there is a net change in the magnetic field topology as the spacecraft enters and exits.

4.3.2.1 Bm (Magnitude)

The November 14th 2012 lobe encounters were characterised by a sharp increase in magnetic field strength as the spacecraft entered the lobes, followed by an equally sharp decrease as they exited. This criteria was used to identify the start and end of each event for the survey, so it is expected that these signatures will be clear in the SEA.

Figure 31 (top panel) shows the SEA for the onset of the lobe encounters, with the epoch defined as the start of the event. It clearly shows the rise and in magnetic field strength expected and with the end of the event obscured in the analysis by the varying durations of each lobe encounter. The mean shows the sharp increase best and is most likely dominated by events similar to November 14th 2012, where the spacecraft moved into the lobe very quickly. The median signal shows a more gradual increase in field strength, taking roughly ten minutes to reach a peak and representative of events where the entry into the lobe was more gradual.

Figure 31 (centre panel) is the SEA where the epoch is the exit from the lobe, where the magnetic field strength has returned to previous levels. As expected it shows a sharp decline in magnitude and unlike the start of the event there is little difference between the mean and median. This is consistent with the spacecraft exiting the lobe swiftly for the majority of the events, often as the result of a substorm injection.

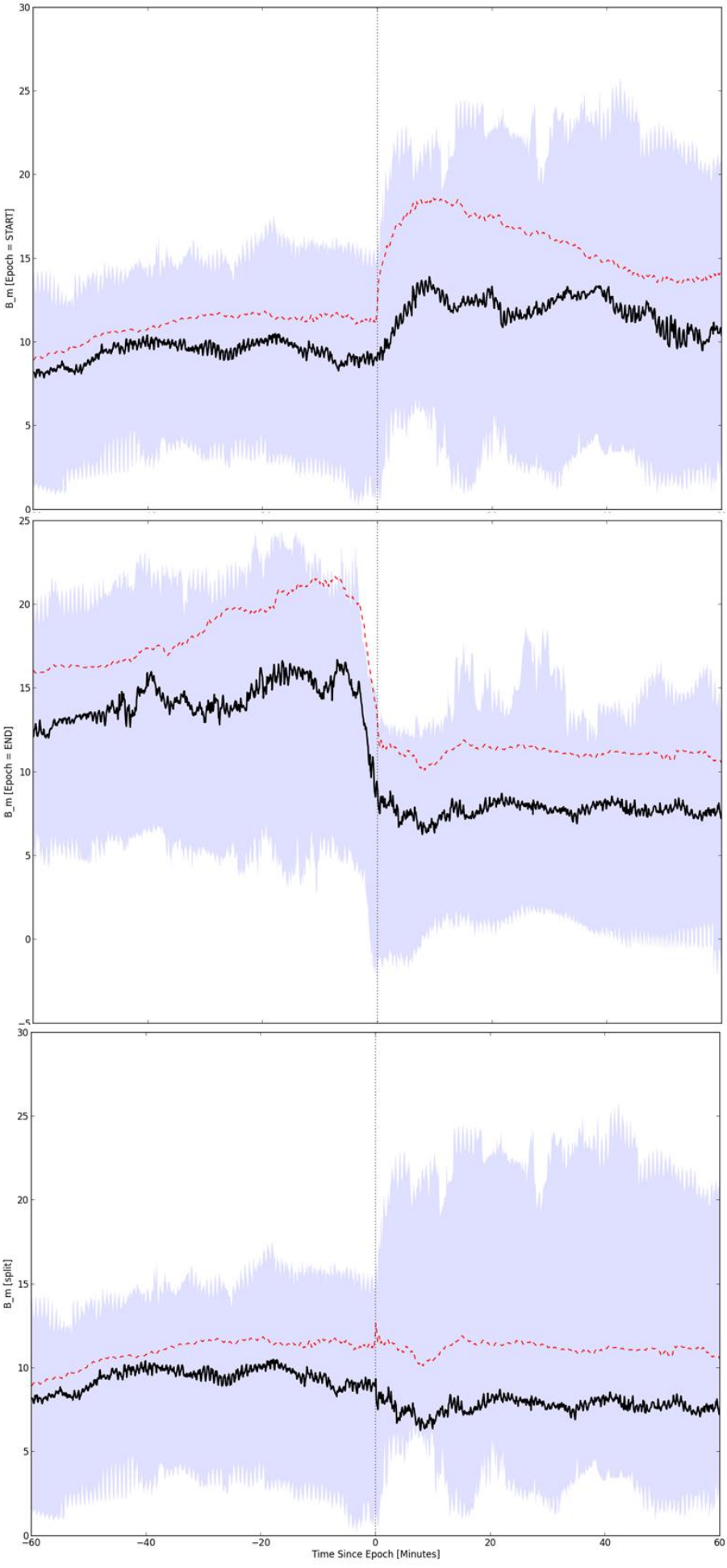

Figure 31: Superposed Epoch Analysis of in-situ magnetic field strength data from the Van Allen Probes EMFISIS instrument.

The top panel uses the onset of the lobe encounters as the epoch and shows a clear increase in B_m, which is sharper in the mean.

The centre panel uses the end of the events as the epoch and shows the decrease in field strength associated with exiting the lobe.

The bottom panel combines the two to show the net change in magnetic field strength across the lobe encounter. There is arguably a small reduction in field strength just after the events but the change is not significant compared to the changes seen for the start and end of the events.

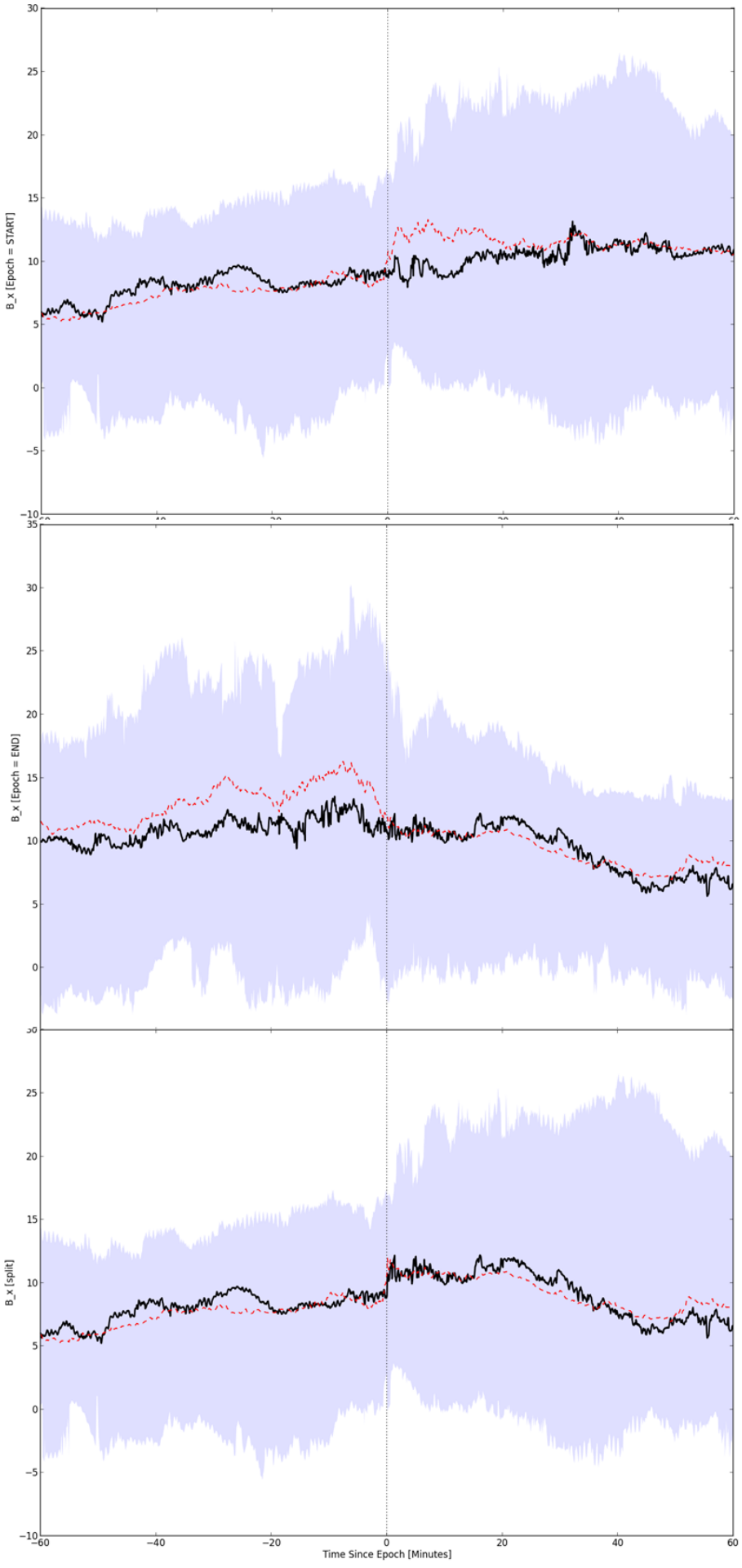

Figure 32: Superposed Epoch Analysis of in-situ magnetic field x-component data from the Van Allen Probes EMFISIS instrument.

The top panel uses the onset of the lobe encounters as the epoch and shows a small increase in the mean but not the median.

The centre panel uses the end of the events as the epoch and shows a decrease in the mean but not the median, mirroring the signal seen for the onset epoch,

The bottom panel combines the two to show the net change in magnetic field strength across the lobe encounter. There is a net increase in B_x of ~3 nT, seen in both the median and the mean.

The panel is a combination of the SEAs for the start and end of the events, which allows us to examine the net change in magnetic field strength before and after the spacecraft enter the lobes. There is arguably a small decrease in field strength after the event but it is not much greater than other variations in the signal and is not seen prominently in the mean.

4.3.2.2 Bx

Both the start and end SEAs for the x-component of the magnetic field show little change in the median around the epoch, but a clearer signature in the mean (Figure 32, top and centre panels). For the start of the events there is an increase in positive Bx and conversely, a decrease at the end of the events. This is consistent with some of the November 14th 2012 events, where the spacecraft encountered a strong positive Bx field when entering the lobe. The lack of consistency for those events implies that many of the events in the survey did not seen such a signal and that it is a minority of events with a strong Bx signal that are represented in the mean.

Interestingly there seems to be a clear increase in Bx between the start and end of the events (Figure 32, bottom panel), which is consistent between the mean and median. The increase is small but implies a slight net increase in Bx, though the significance of this is unknown.

4.3.2.3 By

Figure 33 (top panel) shows the y-component SEA for the start of the lobe encounters and gives a very clear signal, consistent with that seen for the November 14 2012 events. As the spacecraft enters the lobe it encounters a highly stretched magnetic field structure with a strong negative By component. The mean shows a very sharp change in the field, whereas the median changes more gradually, taking less than ten minutes to reach a minimum. Similarly to the signatures seen for the magnetic field strength, this is the result of some of the stronger events with much faster entries into the lobe dominating the mean and the slower, more gradual entries being better represented in the median.

The exit from the lobe, shown in Figure 33 (centre panel), has the magnetic field y-component returning to its previous state over a period of roughly ten minutes and is consistent for both the mean and median. This seems to imply that the magnetic field structure inside the lobe may be relaxing prior to the spacecraft reentering the inner magnetosphere. The combined start and end SEA (Figure 33, bottom panel) shows no net change in By as the spacecraft moves into and out of the lobe, though there is a sharp change in the mean which is most likely the result of a strong, anomalous result.

4.3.2.4 Bz

The start SEA for the z-component of the magnetic field seems to show a small drop in Bz after the spacecraft enters the lobe but the weakness of the signal in the median implies that this may be influenced by a strong drop seen in just a few events. It is also interesting that unlike for other signatures seen at the start of the events, the field seems to recover within ten minutes, which is shorter than the duration of most of the events. This implies changes in the magnetic field topology while the spacecraft are still inside the lobes.

Figure 34 (bottom panel) shows a very strong signal for the end of the events with a strong, northward turning of the magnetic field prior to the exit from the lobe. Starting around twenty minutes before the event ends, this increase in positive Bz reaches a peak at the epoch before levelling off. Also of interest is the large difference in Bz seen between the start and end of the events, with the median and mean rising by approximately 4 and 8 nT, respectively.

4.3.2.5 Magnetic Topology Discussion

These Superposed Epoch Analysis results show some clear signatures which can be taken as fairly representative of the sample of one hundred lobe encounter events. As the spacecraft move into the lobe they enter a strong, flat magnetic field structure, dominated by a negative y-component and with a smaller, but significant positive x-component. This is consistent with the spacecraft having encountered the tail field and also with what was seen for the November 14th 2012 event, where all of

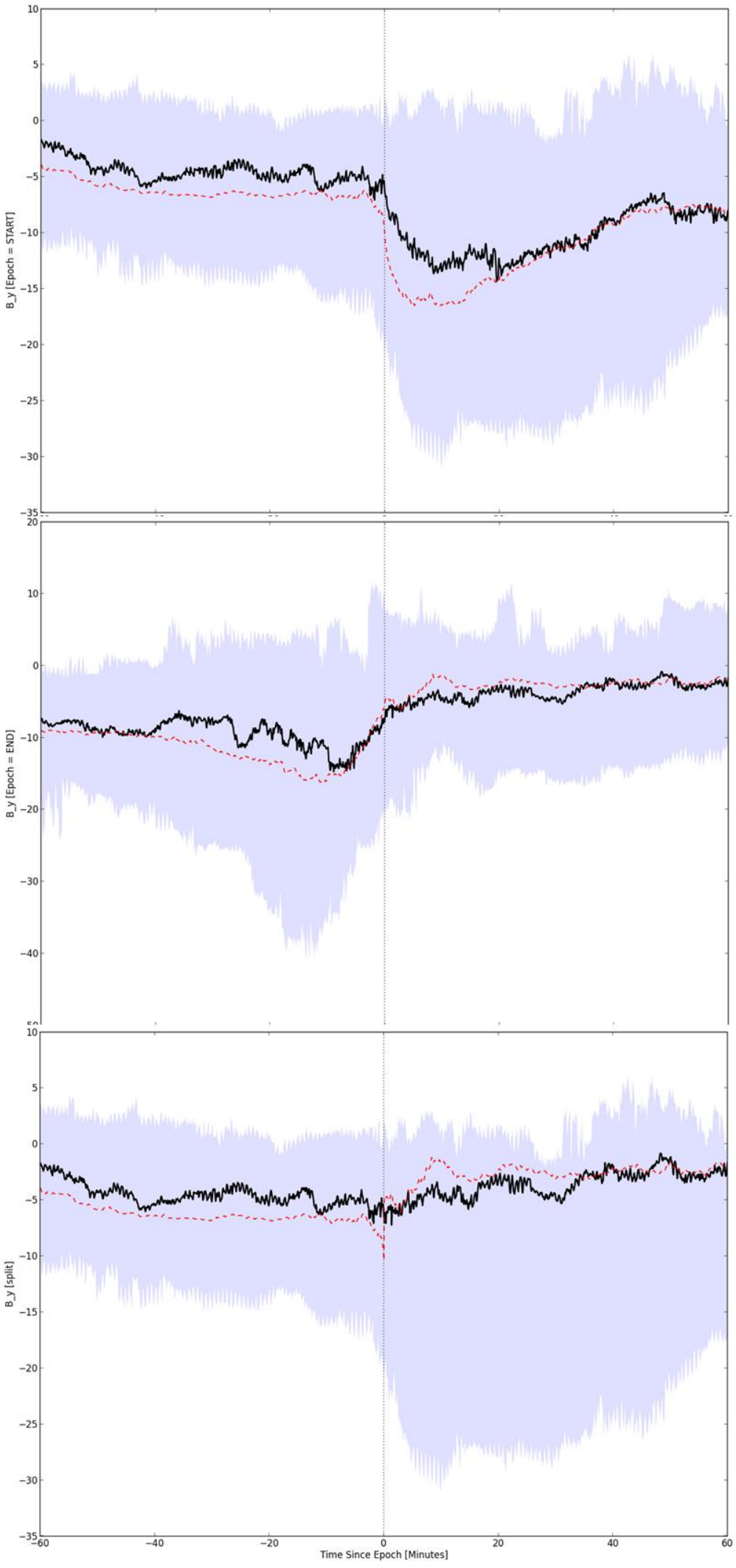

Figure 33: Superposed Epoch Analysis of in-situ magnetic field y-component data from the Van Allen Probes EMFISIS instrument.

The top panel uses the onset of the lobe encounters as the epoch and shows a clear increase in negative B_y in both the median and the mean, thought the mean signal drops more sharply.

The centre panel uses the end of the events as the epoch and shows a gradual decrease in negative B_y in both the mean and median as the spacecraft exits the lobe.

The bottom panel combines the two to show the net change in magnetic field strength across the lobe encounter. There is a no net change in By in the median but there is a small increase seen in the mean at the epoch, as well as a steady rise for ten minutes afterwards.

the lobe encounters were characterized by this flat, highly stretched field. The lack of a strong signal in the x-component also matches what was seen for the November 14th event, where not all of the events showed significant changes in Bx as they spacecraft moved in and out of the lobe.

The SEAs for the end of the events showed a weakening of the stretched, By dominated field inside the lobe which seemed to occur over a period of around ten minutes. There was an accompanying increase in Bz, with the field turning strongly northward prior to the spacecraft reentering the lobe. These signatures are typical of the onset of a substorm, as the tail field dipolarizes and the tail lobes relax and retreat back to higher latitudes. Though only 51% of the events were associated with a substorm injection, it is possible that the strong, consistent magnetic field behavior typical of a substorm has been able to dominate the SEA results. It is also a possibility that although a substorm injection was not apparent in the Van Allen Probe data, one still occurred and produced similar magnetic field behavior to that seen for the substorm associated events.

In theory, as the spacecraft is moving between two distinct and separate regions of open and closed field lines, we would expect for there to be no net change in magnetic field topology between the start and end of the events. Any unrelated fluctuations in the field should be cancelled out in the SEA and the combination plots show a fairly flat curve across the epoch. This is observed in the SEA for the magnitude and y-component, with a small decrease in Bm just after the epoch but nothing of significance. For Bx there is a net increase of ~3 nT, which is seen in both the median and the mean. This implies there is a minor change in the topology of the closed field lines over the course of the events. The biggest net change comes in the Bz SEA, where the median and mean rose by approximately 4 and 8 nT, respectively. The reason for this seems clear, with the massive increase in Bz seen in the twenty minutes prior to the end of the events occurring on both sides of the OCB and the spacecraft continuing to observe it once it has exited the lobe.

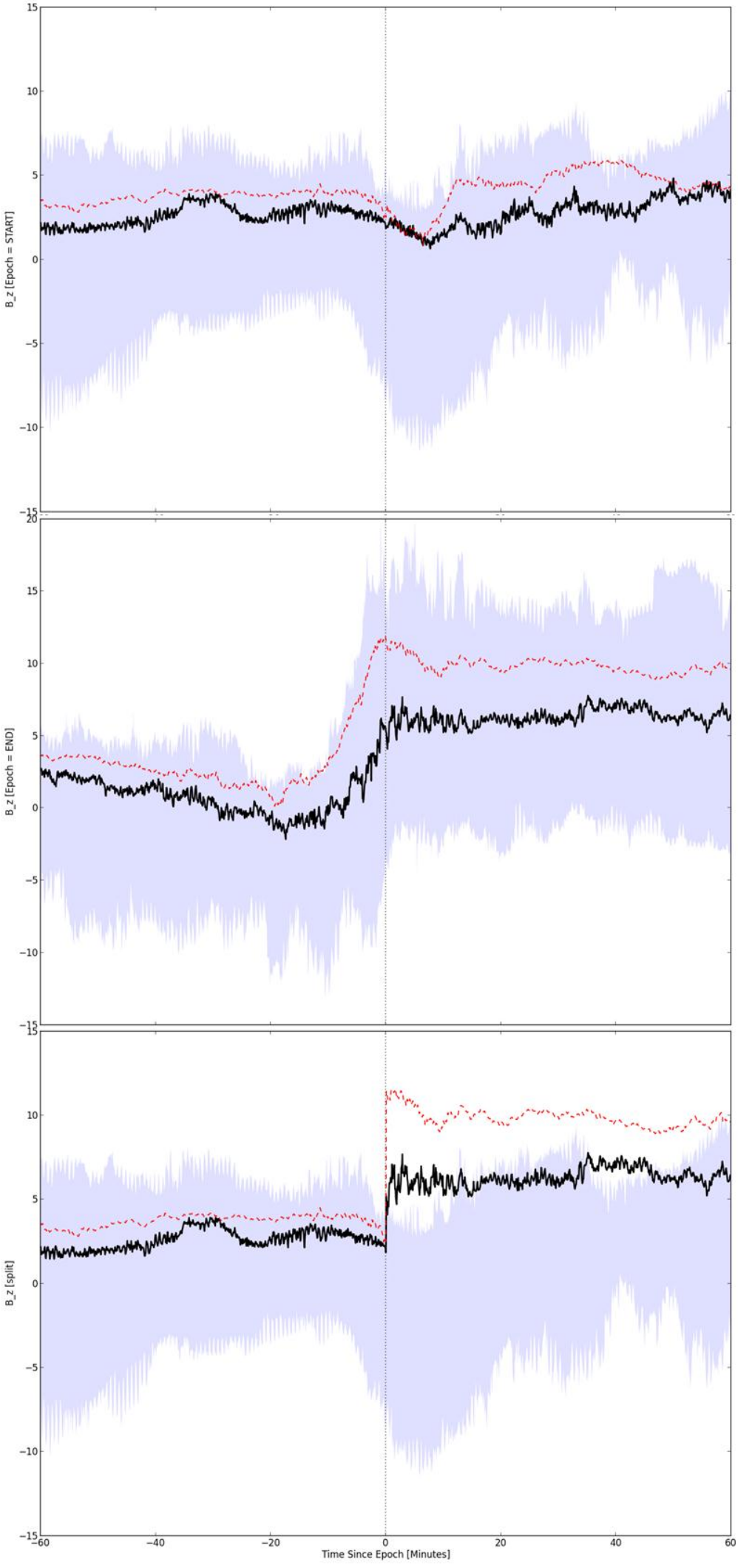

Figure 34: Superposed Epoch Analysis of in-situ magnetic field z-component data from the Van Allen Probes EMFISIS instrument.

The top panel uses the onset of the lobe encounters as the epoch and shows a small, temporary decrease in B_z which is more apparent in the mean.

The centre panel uses the end of the events as the epoch and shows a large increase in B_z which begins around twenty minutes before the epoch.

The bottom panel combines the two to show the net change in magnetic field strength across the lobe encounter. There is a large net increase in B_z, seen in both the median and mean.

4.2 CONCLUSIONS

The aim of this survey was to try and establish if there were general characteristics that could be identified for magnetospheric lobe encounters and how these compared to previous studies. Also of interest was how the behaviour of the interplanetary magnetic field affected the likelihood of lobe encounters, both in general and in particular regions of the magnetosphere. These findings could also then be compared to what was observed for the November 14th 2012 event to discover whether those observations were indicative of lobe encounters as a whole, just flank encounters, or unique to that event.

The survey found one hundred lobe encounter, seen over a total of forty-four different days, in both the north and south hemispheres, and across the whole of the night side of the magnetosphere. There was a preference for lobe encounters to occur in the north-dusk and south-dawn regions, though this is most likely the a result of there being increased geomagnetic activity when the Van Allen Probes apogee was in these regions, increasing the likelihood of the spacecraft entering the lobe. All of the events occurred either 20 degrees above or below the magnetic equator, as they would have easier access to the lobes at higher latitudes and would also be nearer apogee at these latitudes, placing them nearer to geosynchronous orbit.

Analysis of the D_{ST} at the onset of each event showed that geomagnetic activity increased the likelihood of a spacecraft encountering the lobe, but was not a necessity. The SEA of the IMF showed strong IMF B_y before the events, which agrees with previous studies [*Thomsen et al.*, 1994 of lobe encounters and also matches what was seen for November 14th 2012. There was also strong southward IMF B_z which turned northward at a similar time to the lobe encounters, typical of the onset of a storm.

For fifty-one of the events the Van Allen Probes also detected a substorm injection within the same orbit, usually coinciding with the end of the lobe encounters. This is consistent with the current sheet thinning prior to a substorm injection, bringing the lobes to lower latitudes and making them

accessible to the Van Allen Probes. It is also possible that many of the lobe encounters that occurred around midnight where no substorm injection was observed did in fact coincide with one but the Van Allen Probes did not detect it. The stretched field, flattened in the x-y plane which was prevalent in the SEA results is consistent with what is expected in the tail lobe [*Fennell et al*., 1996] and also with what was observed for November 14th 2012. The dipolarization seen in the SEA for the end of the events is also consistent with the onset of a substorm and the strength of this signal in the analysis implies that for many of the events the Van Allen Probes may have seen the magnetic field signature of a substorm, even if they did not observe the injection.

It was disappointing that the survey failed to find any flank lobe encounters similar to the November 14th 2012 event, where the spacecraft is moving back and forth into the lobe in a consistent manner over a relatively short period of time. Part of the reason that this study saw relatively few flank encounters compared to earlier studies is that the GOES satellites were at geosynchronous orbit and CRRES had an apogee of 7 - 8 R_E compared to that of the Van Allen Probes, which is only 5.8 R_E. This means the lobe would have to be brought down to much lower latitudes for the Van Allen Probes to access, explaining why the type of event seen on November 14th 2012 only happened during a large geomagnetic storm and extreme IMF B_y. This does imply that near-midnight lobe encounters associated with substorms do not require as extreme conditions to reach the orbit of the Van Allen Probes, demonstrated by their relative abundance.

5. THESIS CONCLUSIONS

5.1 SUMMARY OF WORK PERFORMED

A study into the tail lobe encounter events has been performed, consisting of a case study of a unique series of lobe encounters observed by the Van Allen Probes on November 14th 2012 and a survey of one-hundred lobe encounter events observed over a period of two years.

On November 14th 2012 between 0200 and 0515 UT the twin Van Allen Probes observed particle dropouts consistent with crossing the open-closed boundary from closed field lines onto open lobe field lines. The events occurred on the flank between 4 and 6.6 local time and at altitudes between 5.6 and 6.2 R_E. The events occurred during the main phase of a geomagnetic storm while D_{ST} was less than 100nT with the IMF being strongly southward (B_z = -15nT) and eastward (B_y = 20 nT). Observations at geosynchronous orbit also show lobe encounters at the dawn and dusk flanks.

The two spacecraft configuration of the Van Allen Probes was used to constrain the spatial and temporal characteristics of each lobe encounter, allowing analysis of the OCB dynamics during this unique event. The lobe encounters were found to be the result of the boundary moving over the spacecraft, with a scenario where a local expansion of the OCB propagating from the tail and travelling over the two spacecraft fitting the observations best.

The global magnetic field topology was examined in detail using multiple spacecraft, allowing the position of the OCB to be constrained in multiple points around the magnetosphere at similar times. This was then compared to a global MHD model and the differences between the observed and predicted boundary behaviour were analysed. A scenario was then proposed to explain the motion of the boundary of the spacecraft in terms of a local disturbance which propagated from the tail.

The survey found one hundred lobe encounter, seen over a total of forty-four different days, in both the north and south hemispheres, and across the whole of the night side of the magnetosphere. The distribution of these events was analysed in three dimensions and preferences for certain regions were identified and explained. Subsets based on substorm occurrence and IMF B_y polarity were also separated and then analysed. Then Superposed Epoch Analysis was used on the IMF conditions surrounding the event and also on in-situ magnetometer data obtained by the Van Allen Probes to try and identify common drivers and behaviours associated with the lobe encounters.

5.2 Conclusions

The characteristics and drivers of near-geosynchronous lobe encounters have been explored by looking very closely at a single, unique event and also on a larger scale by performing a long term study of events observed by the Van Allen Probes.

The observed behaviour of the open/closed field line boundary was shown to disagree with that predicted by the BATS-R-US + CRCM model, which successfully reproduced the large scale motion of the lobes down to lower latitudes at times similar to the events but underestimated its extent. The model failed to produce the smaller scale disturbances that moved over the spacecraft but considering the resolution of the model this was unsurprising.

A scenario was suggested for the behaviour of the OCB that explained the timings of the spacecraft crossing the boundary based on their relative positioning. A local disturbance on the OCB which propagated from the tail, enveloping each of the spacecraft fitted the observed behaviour best.

The survey of lobe encounters observed by the Van Allen Probes highlighted how unusual it was to see a strong series of flank events - like that seen for November 14th 2012 - at a relatively low apogee (5.8 R_E) compared to previous studies. The predominance of substorm associated near-midnight encounters implies that these events are able to bring the lobe closer in to the Earth, making it more likely for spacecraft with lower orbits to encounter them.

Analysis of the Interplanetary Magnetic Field drivers of these events shows strong IMF B_Y and B_Z in the day preceding the event. Negative IMF By, was shown to prefer the south/dawn region of the magnetosphere, in agreement with *Moldwin et al*. [1995]. In-situ magnetometer data was analyzed and showed the spacecraft encountering a highly stretched field typical of the lobe, as well as a strong dipolarization of the field prior to exiting the lobe, which can be associated with a substorm injection.

5.3 FURTHER WORK

There is much opportunity for further work in this area, with the causes of flank encounters still not being completely understood. Extending the study to include the rest of the Van Allen Probes lifetime with the hope of finding more strong, flank events like November 14th 2012 to support the findings of this work.

Further use of supporting data from other spacecraft would be incredibly useful as well, for example a survey of similar scope but using the data from the LANL GEO spacecraft. There greater number and higher orbit would hopefully lead to the observation of more flank events, though their lack of an on board magnetometer might limit the insight that could be gained.

WORKS CITED

Aikio, A.T., Pitkänen, T., Fontaine, D., Dandouras, I., Amm, O., Kozlovsky, A., Vaivdas, A. and Fazakerley, A. (2008) 'EISCAT and Cluster observations in the vicinity of the dynamical polar cap boundary', *Ann. Geophys.*, vol. 26, pp. 87-105, Available: doi:10.5194/angeo-26-87-2008.

Aikio, A.T., Pitkänen, T., Kozlovsky, A. and Amm, O. (2006) 'Method to locate the polar cap boundary in the nightside ionosphere and application to a substorm event', *Ann. Geophys.*, vol. 24.

Amm, O. (1997) 'Ionospheric elementary current systems in spherical coordinates and their application', *J. Geomag. Geoelectr.*, vol. 49, pp. 947–955.

Amm, O. (1998) 'Method of characteristics in spherical geometry applied to a Harang discontinuity situation', *Ann. Geophys.*, vol. 16, pp. 413–424.

Belian , R.D., Gisler, G.R., Cayton, T. and Christensen, R. (1992) 'High Z energetic particles at geosynchronous orbit during the great solar proton event of October, 1989', *Geophys. Res.*, no. 97(A11), pp. 16897–16906, Available: doi:10.1029/92JA01139.

Blake, J.B., Carranza, P.A., Claudepierre, S.G., Clemmons, J.H., Crain Jr., W.R., Dotan, Y., Fennell, J.F., Fuentes, F.H., Galvan, R.M., George, J.S., Henderson, M.G., Lalic, M., Lin, A.Y., Looper, M.D., Mabry, D.J., Mazur, J.E., McCarthy, B., Nguyen, C.Q., O'Brien, T.P., Perez, M.A. et al. (2013) 'The Magnetic Electron Ion Spectrometer (MagEIS) Instruments Aboard the Radiation Belt Storm Probes (RBSP) Spacecraft', vol. 179, no. 1-4, pp. 383-421, Available: doi: 10.1007/s11214-013-9991-8.

Chisham, G., Freeman, M.P., Sotirelis, T., Greenwald, R.A., Lester, M. and Villain, J.-P. (2005) 'A statistical comparison of SuperDARN spectral width boundaries and DMSP particle precipitation boundaries in the morning sector ionosphere', *Ann. Geophys.*, vol. 23, pp. 733-743, Available: doi:10.5194/angeo-23-733-2005.

Clausen, L.B.N., Baker, J.B.H., Ruohoniemi, J.M., Milan, S.E., Coxon, J.C., Wing, S., Ohtani, S. and Anderson, B.J. (2013) 'Temporal and spatial dynamics of the regions 1 and 2 Birkeland currents during substorms', *J. Geophys. Res. Space Physics*, vol. 118, Available: doi:10.1002/jgra.50288.

Cully, C.M., Donovan, E.F., Yau, A.W. and Arkos, G.G. (2003) 'Akebono/Suprathermal Mass Spectrometer observations of low-energy ion outflow: Dependence on magnetic activity and solar wind conditions', *J. Geophys. Res.*, vol. 108, Available: doi:10.1029/2001JA009200.

De Zeeuw, D.L., Sazykin, S., Wolf, R.A., Gombosi, T.I., Ridley, A.J. and Toth, G. (2004) 'Coupling of a global MHD code and an inner magnetospheric model: Initial results', *J. Geophys. Res.*, vol. 109, no. A12, Available: doi:10.1029/2003JA010366.

Fennell, J.F., Blake, J.B., Roeder, J.L., Sheldon, R. and Spence, H.E. (1997) 'Tail lobe and open field line region entries at mid to high latitudes', *Advances in Space Research*, vol. 20, no. 3, pp. 431-435, Available: doi:10.1016/S0273-1177(97)00705-9.

Fennell, J., Roeder, J., Spence, H., Singer, H., Korth, A., Grande, M. and Vampola, A. (1996) 'CRRES observations of particle flux dropout events', *Advances in Space Research*, vol. 18, no. 8, pp. 217-228, Available: doi:10.1016/0273-1177(95)00991-4.

Fok, M., Moore, T.E., Kozyra, J.U., Ho, G.C. and Hamilton, D.C. (1995) 'Three-dimensional ring current decay model', *J. Geophys. Res.*, vol. 100, pp. 9619-9632.

Glocer, A., Fok, M., Meng, X., Toth, G., Buzulukova, N., Chen, S. and Lin, K. (2013) 'CRCM + BATS–R–US two–way coupling', *J. Geophys. Res. Space Physics*, no. 118, pp. 1635–1650, Available: doi:10.1002/jgra.50221.

Glocer, A., Tóth, G., Gombosi, T. and Welling, D. (2009) 'Modeling ionospheric outflows and their impact on the magnetosphere, initial results', *J. Geophys. Res*, vol. 114, no. A05216, Available: doi:10.1029/2009JA014053.

Hwang, K.-J., Sibeck, D.G., Fok, M.-C., Zheng, Y., Nishimura, Y., Lee, J.-J., Glocer, A., Partamies, N., Mitchell, D.G., Singer, H.J., Reeves, G.D., Kletzing, C.A. and Onsager, T. (2014 (submitted)) 'The global context of the 14 November, 2012 storm event', *J. Geophys. Res.*

Johnson, M. H., Kierein, J., Combined Release and Radiation Effects Satellite (CRRES) – Spacecraft and Mission, Journal of Spacecraft and Rockets, Volume 29, No. 4, 556-563, 1992

Kabin, K., Rankin, R., Rostoker, G., Marchand, R., Rae, I.J., Ridley, A.J., Gombosi, T.I., Clauer, C.R. and De Zeeuw, D.L. (2004) 'Open-closed field line boundary position: A parametric study using an MHD model', *J. Geophys. Res.*, vol. 109, no. A05222, Available: doi:10.1029/2003JA010168.

Kessel , R.L., Fox, N.J. and Weiss, M. (2013) 'The Radiation Belt Storm Probes (RBSP) and Space Weather', *Space Science Reviews*, vol. 179, no. 1-4, pp. 531-543, Available: doi:10.1007/s11214-012-9953-6.

Kletzing, C.A., Kurth , W.S., Acuna, M., MacDowall, R.J., Torbert, R.B., Averkamp, T., Bodet, D., Bounds , S.R., Chutter, M., Connerney, J., Crawford, D., Dolan, J.S., Dvorsky, R., Hospodarsky, G.B., Howard, J., Jordanova, V., Johnson, R.A., Kirchner, D.L., Mokrzycki, B., Needell, G. et al. (2013) 'The Electric and Magnetic Field Instrument Suite and Integrated Science (EMFISIS) on RBSP', *Space Science Review*, vol. 179, no. 1-4, pp. 127-181, Available: doi:10.1007/s11214-013-9993-6.

Kopányi, V. and Korth, A. (1995) 'Energetic Particle Dropouts Observed in the Morning Sector by the Geostationary Satellite GEOS-2', *Geophysical Research Letters*, no. 22, pp. 73-76, Available: DOI: 10.1029/94GL02910.

Mauk, B.H., Fox, N.J., Kanekal, S.G., Kessel, R.L., Sibeck, D.G. and Ukhorskiy, A. (2013) 'Science Objectives and Rationale for the Radiation Belt Storm Probes Mission', *Space Science Reviews*, vol. 179, no. 1-4, pp. 3-27, Available: doi:10.1007/s11214-012-9908-y.

McComas, D.J., Bame, S.J., Barraclough, B.L., Donart, J.R., Elphic, R.C., Gosling, J.T., Moldwin, M.B., Moore, K.R. and Thomsen, M.F. (1993) 'Magnetospheric plasma analyzer: Initial three-spacecraft observations from geosynchronous orbit', *J. Geophys. Res.*, no. 98(A8), pp. 13453–13465.

McComas, D.J., Elphic, R.C., Moldwin, M.B. and Thomsen, M.F. (1994) 'Plasma observations of magnetopause crossings at geosynchronous orbit', *J. Geophys. Res.*, no. 99(A11), pp. 21249–21255, Available: doi:10.1029/94JA01094.

McComas, D.J., S.J. Bame, P. Barker, W.C. Feldman, J.L. Phillips, P. Riley, J.W. Griffee, Solar Wind Electron Proton Alpha Monitor (SWEPAM) for the Advanced Composition Explorer, Space Science Reviews, Volume 86, 563-612, 1998

Meng, X., Toth, G., Glocer, A., Fok, M.-C. and Gombosi, T. (2013) 'Pressure anisotropy in global magnetospheric simulations: Coupling with ring current models', *J. Geophys. Res*, vol. 118, no. 9, pp. 5639–5658, Available: doi:10.1002/jgra.50539.

Mitchell, D.G., Lanzerotti, L.J., Kim, C.K., Stokes, M., Ho, G., Cooper, S., Ukhorskiy, A., Manweiler, J.W., Jaskulek, S., Haggerty, D.K., Brandt, P., Sitnov, M., Keika, K., Hayes, J.R., Brown, L.E., Gurnee, R.S., Hutcheson, J.C., Nelson, K.S., Paschalidis, N., Rossano, E. et al. (2013) 'Radiation Belt Storm Probes Ion Composition Experiment (RBSPICE)', *Space Science Review*, vol. 179, no. 1-4, pp. 263-308, Available: doi: 10.1007/s11214-013-9965-x.

Moldwin, M.B., Thomsen, M.F., Bame, S.J., McComas, D.J., Birn, J., Reeves, G.D., Nemzek, R. and Belian, R.D. (1995) 'Flux dropouts of plasma and energetic particles at geosynchronous orbit during large geomagnetic storms: Entry into the lobes.', *J. Geophys. Res*, no. 100(A5), pp. 8031-8043, Available: doi:10.1029/94JA03025.

Moya, P.S., Pinto, V.A., Viñas, A.F., Sibeck, D.G., Kletzing, C.A., Kurth, W.S., Hospodarsky, G.B. and Wygant, J.R. (2014 (under review)) 'Weak Kinetic Alfv´en Waves turbulence on the November 14th 2012 geomagnetic storm from Van Allen Probes observations', *J. Geophys. Res.*

Paschmann, G., Haaland, S. and Treumann, R. (ed.) (2003) *Auroral Plasma Physics, Space Science Series of ISSI.*

Rae, I.J., Kabin, K., Rankin, R., Fenrich, F.R., Liu, W., Wanliss, J.A., Ridley, A.J., Gombosi, T.I. and De Zeeuw, D.L. (2004) 'Comparison of photometer and global MHD determination of the open-closed field line boundary', *J. Geophys. Res.*, vol. 109, no. A01204, Available: doi:10.1029/2003JA009968.

Ridley, A.J., Gombosi, T.I. and De Zeeuw, D.L. (2004) 'Ionospheric control of the magnetosphere: conductance', *Ann. Geophys.*, no. 22, pp. 567-584, Available: doi:10.5194/angeo-22-567-2004.

Sauvaud, J.A. and Winckler, J. (1980) 'Dynamics of plasma, energetic particles, and fields near synchronous orbit in the nighttime sector during magnetospheric substorms', *J. Geophys. Res.*, no. 85(A5), pp. 2043–2056, Available: doi:10.1029/JA085iA05p02043.

Seki, K., Elphic, R.C., Hirahara, M., Terasawa, T. and Mukai, T. (2001) 'On Atmospheric Loss of Oxygen Ions from Earth Through Magnetospheric Processes', *Science*, vol. 291, no. 5510, pp. 1939-1941.

Shue, J.-H., Chao, J.K., Fu, H.C., Russell, C.T., Song, P., Khurana, K.K. and Singer, H.J. (1997) 'A new functional form to study the solar wind control of the magnetopause size and shape', *J. Geophys. Res.*, vol. 102.

Spence, H.E., Reeves, G.D., Baker, D.N., Blake, J.B., Bolton, M., Bourdarie, S., Chan, A.A., Claudepierre, S.G., Clemmons, J.H., Cravens , J.P., Elkington, S.R., Fennell, J.F., Friedel, R.H.W., Funsten, H.O., Goldstein , J., Green, J.C., Guthrie, A., Henderson, M.G., Horne, R.B., Hudson, M.K. et al. (2013) 'Science Goals and Overview of the Radiation Belt Storm Probes (RBSP) Energetic Particle, Composition, and Thermal Plasma (ECT) Suite on NASA's Van Allen Probes Mission', *Space Science Review*, vol. 179, no. 1-4, pp. 311-336, Available: doi:10.1007/s11214-013-0007-5.

Thomsen, M.F., Bame, S.J., McComas, D.J., Moldwin, M.B. and Moore, K.R. (1994) 'The magnetospheric lobe at geosynchronous orbit', *J. Geophys. Res.*, no. 99(A9), pp. 17283-17293, Available: doi:10.1029/94JA00423.

Tsyganenko, N.A. and Sitnov , M.I. (2005) 'Modeling the dynamics of the inner magnetosphere during strong geomagnetic storms', *Journal of Geophysical Research*, vol. 110, no. A03208, Available: doi:10.1029/2004JA010798, 2005.

Urban, K.D., Gerrard, A.J., Bhattacharya, Y., Ridley, A.J., Lanzerotti, L.J. and Weatherwax, A.T. (2011) 'Quiet time observations of the open-closed boundary prior to the CIR-induced storm of 9 August 2008', *Space Weather*, vol. 9, no. 11, Available: doi:10.1029/2011SW000688.

Van Allen, J. A., G. H. Ludwig, E. C. Ray, and C. E. McIlwain, Observations of high intensity radiation by satellites 1958 Alpha and Gamma, Jet Propul., 28, 588-592, 1958

Walsh, B.M., Foster, J.C., Erickson, P.J. and Sibeck, D.G. (2014) 'Simultaneous Ground- and Space-Based Observations of the Plasmaspheric Plume and Reconnection', *Science*, vol. 343, no. 6175, pp. 1122-1125, Available: doi: 10.1126/science.1247212.

Wrenn , G.L., Johnson, J.F.E., Norris, A.J. and Smith, M.F. (1981) 'Geos-2 magnetopause encounters: Low energy (